INFORMATION TO USERS

This manuscript has been reproduced from the microfilm master. UMI films the text directly from the original or copy submitted. Thus, some thesis and dissertation copies are in typewriter face, while others may be from any type of computer printer.

The quality of this reproduction is dependent upon the quality of the copy submitted. Broken or indistinct print, colored or poor quality illustrations and photographs, print bleedthrough, substandard margins, and improper alignment can adversely affect reproduction.

In the unlikely event that the author did not send UMI a complete manuscript and there are missing pages, these will be noted. Also, if unauthorized copyright material had to be removed, a note will indicate the deletion.

Oversize materials (e.g., maps, drawings, charts) are reproduced by sectioning the original, beginning at the upper left-hand corner and continuing from left to right in equal sections with small overlaps.

ProQuest Information and Learning
300 North Zeeb Road, Ann Arbor, MI 48106-1346 USA
800-521-0600

DISSERTATION

EVOLUTION OF DRAINAGE NETWORKS AND HILLSLOPES

Submitted by
David A. Raff
Department of Civil Engineering

In partial fulfillment of the requirements
for the Degree of Doctor of Philosophy
Colorado State University
Fort Collins, Colorado
Fall 2002

ProQuest Information and Learning Company
300 North Zeeb Road
P.O. Box 1346
Ann Arbor, MI 48106-1346

Colorado State University

August 30, 2002

WE HEREBY RECOMMEND THAT THE DISSERTATION PREPARED UNDER OUR SUPERVISION BY DAVID A. RAFF ENTITLED EVOLUTION OF DRAINAGE NETWORKS AND HILLSLOPES BE ACCEPTED AS FULFILLING IN PART REQUIREMENTS FOR THE DEGREE OF DOCTOR OF PHILOSOPHY.

Committee on Graduate Work

Adviser

Co-Adviser

Department Head

ABSTRACT OF DISSERTATION

EVOLUTION OF DRAINAGE NETWORKS AND HILLSLOPES

Drainage networks are an integral part of the dynamics of almost every hydrologic system. We, as scientists, are currently in an extremely exciting period in the study of drainage networks. Over the past decade we have seen a dramatic paradigm shift from a largely empirical to a more fundamental understanding and quantitative descriptions of the inherent forms and processes that create drainage networks. During this period of time, much of the work has focused on river networks and has generally only considered changes in length scales. This dissertation focuses on the influence of time scales in drainage network development.

One of the more prominent current theories of drainage network development is that the three-dimensional form of the drainage networks is largely dominated by optimality in energy dissipation. A relationship between a characteristic discharge or drainage area and elevation gradient has been presented in the literature, $S = gQ^z \approx S = gA^z$. Originally it was suggested that z = -0.5 for optimality in the above sense; however, more recently some real world systems have been shown to be near optimal while deviating from this value of z. Field data shows that this relationship varies dramatically from z = -0.5. An explanation for this deviation is presented using a simulation approach by accounting for differences in flow distributions based on drainage area and accounting for the relative effectiveness of each flow.

There is very little quantitative data in the literature on how networks grow with time. A physical experiment was conducted in an experimental hillslope facility 10 [m] x 3 [m] on two different slopes, 9° and 5°, to study the structure of drainage networks on a slope void of vegetation as they develop through time under constant rainfall. Two new quantitative measures are proposed and tested as a means to describe the network growth as a function of time and slope. Space filling characteristics of the networks, specifically the fractal dimension D_f, are calculated at 1-hour intervals for 4- to 5-hour rainfall simulations. Statistical analysis shows that the network becomes more space filling with time and that this occurs more rapidly on the steeper slope. Fourier series fits to width functions at 1-hour intervals over the duration of the rainfall simulation are shown to be very accurate describing the frequency characteristics of the networks. The signal strength associated with each frequency in the Fourier series is analyzed statistically. The analysis shows that low frequencies become relatively more important with time and that the bifurcation characteristics remain constant through time. Results are also presented which show that while the geomorphic characteristics of the networks, like Horton's bifurcation and length ratios, do not vary for the two different slopes, the width, depth, and width-to-depth ratio do depend on slope.

A two-dimensional hillslope model is presented which solves the coupled full hydrodynamic equations for overland flow, Richards equation for infiltration in one-dimension, and a physically based sediment detachment and transport equation. This is the most advanced hillslope model yet to be developed. The use of Richards equation allows continuous simulations of discontinuous rainfall events, and the coupling of the sediment detachment and transport algorithm with the overland flow algorithm allows the

modeling of hillslope topographic evolution. The energy expenditure characteristics of an evolving hillslope are found to possess attributes, which have been characterized as optimal in the past and are subject to the scales at which the measurements are made.

David A. Raff
Department of Civil Engineering
Colorado State University
Fort Collins, CO 80523
Fall 2002

ACKNOWLEDGEMENTS

I have had the pleasure of working with many incredible people during my doctoral studies and it would be impossible to mention them all in a reasonable space. However, there are a few people whom I would be truly remiss not to name. Among them are the members of my dissertation committee: my advisor Dr. Jorge A. Ramírez, my co-adviser Dr. Chester C. Watson, and committee members Dr. Brian Bledsoe and Dr. Jim Smith. They have permitted me intellectual freedom, perhaps the most important aid to growth anyone could provide. While I have not even begun to develop the scientific maturity that they possess, the example they have set and the guidance they have offered have put me on the right path. My future aspirations have been strongly influenced by these men; because of them, I know that I want to do science for the sake of increasing mankind's store of knowledge, and helping and encouraging others to do the same.

In addition, I would like to thank the staff and students at the Engineering Research Center, especially Michael Robeson and Dr. Christopher Thornton. I would also like to thank my assistant Kelly Brom, whose diligent work cannot be assigned proper value.

Finally, I would like to say to all those whom I cannot mention specifically that your contributions are not and will never be forgotten. To all of you, thank you.

DEDICATION

I would like to dedicate this dissertation to my family: my grandmother Ruth Rosenstein, my parents Barry and Marsha Raff, my sister and brother Melissa and Richard Goldberg and my niece and nephew Rebecca and Adam Goldberg. I would also like to dedicate this to anyone whose interests lead him or her to reading a part or the whole of this work; and I would like to say that if I may ever be of any assistance in your work please do not hesitate to contact me.

TABLE OF CONTENTS

LIST OF TABLES AND FIGURES

Chapter 1: Introduction

1.1. Introduction

R.H. MacArthur said "To do science is the search for repeated patterns." The work presented in this dissertation is the search for patterns and explanations of water and sediment interactions that lead to the formation of drainage networks and occur at all scales at which water moves and sediment substrate is readily available and transportable.

1.2. Background

Drainage networks develop through the interplay between probability, physics, and geometry, which has long been the driving focus of hydrologic theories and practice. Fundamental knowledge of drainage structures holds almost limitless possibilities for river management and hillslope erosion prediction. However, there are still large gaps in our scientific knowledge before applications can achieve their full potential.

Drainage networks develop in space with time. Most scientific work previously done on drainage networks has concentrated on river networks. The length scale is much more important than the time scale as the river networks studied are relatively static in mean values. The time scale becomes increasingly important at very small length scales (hillslopes) and when considering some of the variability which has been displayed for geometric characteristics of river systems. Application of hillslope drainage network theories into hillslope erosion models, as is currently being suggested, requires more

studies on how drainage networks develop with respect to time. Scientific predictions of river network response under anthropogenic changes will also be improved with greater understanding of drainage network develop with time.

1.3. Research Objectives

The objectives of this research are:

- Objective 1: To describe the characteristics of drainage network longitudinal profiles under conditions where the flow responsible for network form may not be of equal frequency of occurrence throughout the network domain.
- Objective 2: Create a physical model of a hillslope and use quantitative measures to describe drainage network evolution with time.
- Objective 3: Continue development of a distributed hillslope hydrology model by incorporating erosion and sediment transport processes and by improving the description of infiltration.
- Objective 4: Use the theoretical model to examine hillslope evolution with respect to energy expenditure and drainage network formation.

1.4. Approach

The approach to objective 1 will be a simulation of daily discharges along a river profile. Each cross-section along this profile is subjected to a distribution of flows defined by the contributing area to that cross-section. Each flow from the distribution has a different ability to affect the morphology of the link, and this ability is assumed to be proportional to a power of the flow magnitude. With respect to energy expenditure, the overall slope-area relationship, $S \propto A^{z}$, will be studied to find the optimal z value such

that the local rate of energy expenditure throughout the network is constant. Results will be compared to data from actual drainage networks.

Objective 2 will be accomplished through the creation of an artificial hillslope with a rainfall simulation system. Evolution of drainage networks will be studied in terms of their fractal dimension, D_f, and how the space filling qualities of the network change with time. The fractal dimension will be measured through a functional box counting method. The inherent structure of the system will be measured through the frequency characteristics of the width functions and trends in these frequencies will be examined with respect to time. Width functions will be determined for each rainfall simulation at multiple times and a Fourier series will be fit to the width functions with fixed frequencies. The high frequencies within the width function represent the bifurcation characteristics of the system, and the low frequencies represent the space filling structure of the system (Rodríguez-Iturbe and Rinaldo 1997).

Objective 3 will be accomplished by enhancing an existing model of hillslope hydrologic response based on the full two-dimensional hydrodynamic equations. A physically based erosion and sediment transport algorithm will be implemented in two-dimensions as well as Richards equation for infiltration in one-dimension. Coupling these equations will create the most advanced model of this type developed to date. Model verification will consist of comparisons of individual algorithms with analytical solutions as well as a comparison with a physical experiment.

In order to examine the energy expenditure characteristics of a hillslope using this theoretical model, Objective 4, the model will be executed under a variety of initial conditions as well as spatially varied rainfall rates and soil hydraulic conductivities. In

addition, a one-dimensional model will be considered, for simplicity, and the rates of energy expenditure will be examined under a variety of rainfall and erosion rates. The longitudinal profile described as $S \propto Q^z$ will be examined. Two-dimensional model runs will also be studied with respect to the characteristics of the governing equations modeled and energy expenditure analyses.

1.5. Expected Results

Expected results pertaining to Objective 1 are as follows. The value for z as defined in the downstream hydraulic geometry relationship $S \propto A^z$ should reflect the dominant flow within the distribution of flows throughout the drainage network. The dominant flow is a function of the recurrence interval of the flow and the amount of sediment the flow is capable of moving. Under these conditions, it is expected that the network as a whole can still possess the quality that the energy per unit flow area approaches a constant everywhere within the network. The variability within the equilibrium values of z under different sediment properties and flow distributions should reflect real world variability such as differences observed between longitudinal profiles of gravel bed and sand bed rivers.

The characteristics of an evolving drainage network as they pertain to objective 2 are expected to be quantifiable through their fractal dimension and width functions. The properties of network evolution that have most often been described qualitatively with terms such as elongation, micro-piracy, and increased sinuosity should be describable quantitatively through mathematical tools originally developed for river systems. The fractal dimension D_f, which describes how much space is filled by the network, should increase with time. The low frequencies contained within width functions, which

represent the space filling characteristics of the network, should become more dominant with time when compared to high frequencies that represent the bifurcation characteristics of the network.

Expected results as they pertain to objectives 3 and 4 are as follows. It should be possible to develop a physically based hillslope model that implements the fundamental equations governing water movement over and through the soil as well as sediment transport. The foreseen model is partially hyperbolic in nature and highly non-linear and therefore subject to instabilities. The use of Richards equation on a moveable boundary is a problem that has yet been considered and new methods will probably be required to accomplish this task. It is unknown *a priori* how these equations will behave in this framework and how well they will truly model the evolution of a hillslope. What is expected is that for a one-dimensional case, an initially smooth straight slope should progress to a longitudinal profile capable of being described through $S \propto Q^{z}$, and z should approach a value where the energy per unit area anywhere along the slope is constant. The actual value of z should reflect the sediment transport properties defined within the model transport capacity algorithm. The rate at which the slope approaches a steady state longitudinal profile should be related to the rate at which potential energy is added to the system through rainfall and also to how efficient the water is at transporting sediment. The evolution of a slope subject to spatial variability in two-dimensions should show characteristics of concentration of flows that lead to drainage network development and should also show a decrease in global energy expenditure and tend towards constant distribution of energy expenditure per unit area anywhere where flow is concentrated.

1.6. Contributions

The contributions of this research to the field of Hydrologic Science and Engineering are:

- Verification that the slope-area relationship can vary with respect to geomorphic and hydrologic conditions and still reflect principles of optimality in energy expenditure.
- Quantitative descriptions of drainage network development on a physical hillslope that progresses from an initially smooth surface to a steady state drainage network. Hillslope scale slope is positively correlated with the rate at which a channel network fills space. The width, depth, and width-to-depth ratio characteristics of individual channels within the network are also dependent on the hillslope scale slope.
- A theoretical model, the most mathematically complete, process-based to date, capable of modeling the fine scale interactions of water, sediment and infiltration, processes which may lead to drainage network development.
- The theoretical model produces drainage systems that exhibit simple scaling relationships reflective of river networks and that also minimize total global energy expenditure throughout hillslope evolution.

Chapter 2: Literature Review

2.1. Introduction

As is presented in Chapter 1 specific research objectives are:

- Objective 1: To describe the characteristics of drainage network longitudinal profiles under conditions where the flow responsible for network form may not be of equal frequency of occurrence throughout the network domain.
- Objective 2: Create a physical model of a hillslope and use quantitative measures to describe drainage network evolution with time.
- Objective 3: Continue development of a distributed hillslope hydrology model by incorporating erosion and sediment transport processes and by improving the description of infiltration.
- Objective 4: Use the theoretical model to examine hillslope evolution with respect to energy expenditure and drainage network formation.

It is prudent to develop the history and background of this research to place it into context of what has been done before and how it is a contribution. Below is a discussion of some of the most important work on the structure of drainage networks as it pertains to the research objectives.

The first section is related to river networks. The literature is replete with work on the statistical nature of river networks. A reasonable assumption is that the geometric characteristics of a river system hold information on the underlying physics that causes

those characteristics. A series of scaling relationships based on power laws have been observed and river networks have been shown to possess many attributes that are scale invariant. This self-similar behavior has been tied to optimality in energy dissipation. One important scaling law from the so-called downstream hydraulic geometry relationships is that the slope of a river section is proportional to the inverse of a power of the area that that section drains, $S = gA^z$ (*e.g.*, Gupta and Waymire 1989), where S is slope, A is drainage area, g is a constant and z is the exponent (a negative number between 0 and −1). This relationship has been shown, theoretically, to produce an optimal distribution of local energy dissipation per unit flow area (*i.e.*, equal energy expenditure per unit flow area) when $z = -0.5$ (*e.g.*, Rodríguez-Iturbe and Rinaldo 1997). Molnár and Ramírez, (1998b) have shown that, when $z <> -0.5$ as is often observed in nature, the above scaling law also leads to optimal distribution of local energy dissipation per unit flow area when considering channel width and depth (Molnár and Ramírez 1998b). Physically there is a wide range of values that occur in nature, does this mean that natural river networks are not optimal? A review of the literature as it pertains to river networks, their geometric characteristics and optimality in energy expenditure, specifically the slope-area relationship, is discussed below and the research is presented in Chapter 3.

A separate section is presented on mathematical tools developed to analyze river networks. This section is presented separate from the section on river networks as well as the section on hillslope evolution, described below, as it pertains to both.

The second section discusses hillslope evolution. The spatial heterogeneity that develops on a hill is the result of many different processes operating at many different

scales. Rain, geologic uplift, soil properties and vegetation growth and decay are just a few of the dominant processes that influence the evolution of a hillslope. Evolution requires a movement of substrate either to or from the hill. This movement, in essence hillslope erosion, is of particular importance to agriculturalists whose tools have largely been shown to be inadequate for hillslope erosion prediction. If there exists predictable spatial patterns on hillslopes as they evolve, this would be a very useful tool in the development of new hillslope erosion prediction models. Objective 2 is to quantitatively describe the drainage structure development on a hillslope subject to rainfall and void of vegetation. Very little work has been done on drainage structure analysis for hillslopes per se, however, there have been many physical experiments on slopes treated as scaled versions of catchments that will be discussed in the context of hillslopes.

Part of this work is the development of a theoretical model capable of modeling the fine scale interactions that occur on a hillslope. This hillslope hydrology model describes the movement of water and sediment on a hillslope and is inherently an erosion prediction tool. A review of previous hillslope erosion models is therefore presented.

2.2. River Networks

As stated earlier, river networks possess a wide variety of characteristics that are largely scale invariant. This subsection presents a review of some of the quantitative descriptions of this scale invariance and its implications as it pertains to this dissertation. These describe the characteristics of the link structure while a series of downstream hydraulic geometry (DHG) relationships have been observed which describe actual river cross-sections as a function of their position within the network. One of these DHG relationships is the so-called slope scaling relationship, $S = gA^z$, which becomes

particularly interesting when considered with respect to the energy expenditure characteristics of a network.

Leopold and Maddock (1953) expressed channel form in a series of DHG relationships:

$$w = aQ^b \quad \textbf{2.1}$$

$$d = cQ^f \quad \textbf{2.2}$$

$$v = kQ^m \quad \textbf{2.3}$$

$$S = gQ^z \quad \textbf{2.4}$$

where w, d, v, and S are width, depth, velocity, and slope respectively, and Q is stream flow of equal frequency of occurrence throughout the river network. As is presented elsewhere in this dissertation a common substitution is made as drainage area has been shown to be close to directly proportional to Q thus $S = gA^z$.

One particular explanation for the statistical nature of river networks is optimality in energy expenditure. The idea that optimality in energy expenditure may play a role in formation of natural river patterns has been developed by many researchers throughout the latter half of the last century (*e.g.*, Howard 1971, Leopold and Langbein 1962, Rodríguez-Iturbe et al. 1992) and has led to a theory based on a set of local and global energy optimality principles relating energy expenditure characteristics of river networks to their geomorphologic characteristics. Restated from Rodríguez-Iturbe et al. (1992), an optimal network observes three principles:

- the principle of minimum energy expenditure in any link of the network for the transportation of a given discharge;

- the principle of equal energy expenditure per unit area of a channel anywhere in the network; and
- the principle of minimum energy expenditure in the network as a whole.

The rate that energy is expended in a network as a whole is defined as

$$P = k\sum_i \frac{Q_i L_i}{d_i} \qquad 2.5$$

where i is the link in the network summed over all links, L_i is link length, d_i is flow depth, Q_i is flow and the proportionality factor k is assumed constant throughout the network for a given flow. The above relationship, restated from Rodríguez-Iturbe and Rinaldo (1997) is valid for a rectangular channel of width w, length L, and slope S. If the flow in the channel is not accelerating, the force due to the weight of the water, F_1, and the force resisting water movement, F_2, must be equal,

$$F_1 = \rho g d L w S = F_2 = \tau L(2d + w). \qquad 2.6$$

Simplifying, the shear stress in the flow, assumed constant along the wetting perimeter, can be written as:

$$\tau = \rho g S R \qquad 2.7$$

where τ is the shear stress, ρ is the density of the water and R is the hydraulic radius. Noting that for incompressible flow

$$\tau = C_f \rho v^2 \qquad 2.8$$

where v is cross-section averaged velocity and C_f is a dimensionless resistance coefficient, S can be written as

$$S = \frac{C_f v^2}{Rg} \qquad 2.9$$

the loss due to friction per unit weight of flow per unit length of channel. The loss of energy due to channel maintenance for any link in the network, P_m, the energy necessary to transport the incoming sediment load, can be written as (Rodríguez – Iturbe and Rinaldo 1997)

$$P_m = K\tau^m W_p L \qquad \textbf{2.10}$$

where K is a constant related to the sediment and bank properties, and W_p is the wetted perimeter. Thus, the total rate of energy expended in a channel link can be written as

$$P = \frac{QL}{d} k_f \qquad \textbf{2.11}$$

where k_f is assumed constant throughout the network, which implicitly assumes a network equilibrium. For energy optimality as defined above ΣP must approach a minimum during network evolution and the distribution of P per unit flow area must also approach a constant value throughout the network.

Based on these principles of optimality of energy expenditure Rodríguez-Iturbe and Rinaldo (1997) were able to explain observed characteristics in terms of downstream hydraulic geometry. The dissertation considers the relationship between the value of the exponent z in the slope scaling function and optimality. In particular, whether a value of z = -0.5 is a necessary condition for optimality. In nature, while the observed exponents of the DHG relationships vary within very narrow ranges, such as velocity remaining relatively constant ($m \rightarrow 0$, from equation **2.3**) (Carlston 1969), the exponent z varies quite dramatically from values near –0.25 to –0.75 (Carlston 1968). Molnár and Ramírez (1998 a, b) relaxed the downstream channel geometry requirements within the development of the energy dissipation definitions and showed that some real world networks are close to optimal in terms of local energy dissipation distribution even for

values of z different from –0.5. In Chapter 2 an explanation for the variability in z values is proposed, which includes flow effectiveness into the definition of Q for the DHG relationships. The distribution of discharges is affected by drainage area (Andrews 1980) and different discharges do different amounts of work within the channel based on flow frequency, magnitude and river characteristics (Wolman and Miller 1960). Therefore, one given flow of a constant recurrence interval throughout a network may not be the best predictor of DHG.

2.3. Network Measures

Quantitative measurements of network development have largely been concentrated on drainage density and individual network link scaling relationships such as Horton's, Melton's and Hack's laws, which will be discussed below for equilibrium channel river networks. Drainage density, stream or link frequency, mean link length, hillslope length and texture are all related to the same measure, the fundamental horizontal length scale associated with how the channel network dissects the landscape (Rodríguez-Iturbe and Rinaldo, 1997). The processes that control this fundamental length scale are of great importance. How many channels, how they dissect the landscape, and their transport capabilities largely define a system's water and sediment input-output response. Measures developed to describe the drainage network at the river systems scale, would also help characterize the input-output response of hillslope erosion networks.

Drainage density is by definition the ratio of total length of stream channels to the total area drained:

$$D = \frac{L_t}{A}. \qquad 2.12$$

The drainage density can also be described as a function of the fractal dimension, D_f of the drainage network. A network with $D_f = 2$ is space filling, on a two-dimensional plane; this is to say that there is a channel everywhere on the landscape. $D_f = 1$ represents a linear drainage system on a two-dimensional plane. The intermediate conditions corresponds to "fractal" dimensions such that $0 < D_f < 2$. The fractal dimension of a drainage network has generally been computed using either the Richardson method (Richardson 1961), the Lovejoy functional box counting method (Lovejoy 1987), or the Horton ratios (*e.g.*, La Barbera and Rosso 1989, Wilson and Storm 1993). Current research indicates that $1.5 < D_f < 2$ with values closer to 2 most likely to occur, but these results are highly dependent on the scale of the map used to determine the river network (Tarboton 1990).

As mentioned previously, quantitative measurements of drainage networks have been concentrated on scaling relationships, which are largely based on the Strahler stream ordering scheme (Strahler 1957) defined as follows:

- channels that originate at a source are defined as first-order channels;
- when two channels of order ω join together, a channel of order ω+1 is created;
- when two channels of different order join, the channel segment immediately downstream has the higher order of the two combined channels.

Horton's laws describe the scaling relationships between average properties of stream segments of different stream orders and stream order. Horton's law of stream lengths is:

$$\overline{L_\omega} = \overline{L_1} R_L^{\omega-1} \qquad \textbf{2.13}$$

where $\overline{L_\omega}$ is the (arithmetic) average of the length of streams of order ω. The parameter R_L is the *length ratio*. Horton's law of stream numbers is:

$$N_\omega = R_B^{\Omega-\omega} \quad \textbf{2.14}$$

where N_ω is the number of streams of order ω. The parameter R_B is the *bifurcation ratio*. R_B has a mean of 4 and ranges between 3 and 5 while R_L has a mean of 2 and ranges between 1.5 and 3.5 for river networks (Rodríguez-Iturbe and Rinaldo 1997). Horton also introduced stream frequency (F_s) as a description of stream systems:

$$F_s = \frac{N_s}{A} \quad \textbf{2.15}$$

where N_s is the total number of Strahler channels. Melton's law states that F_s is strongly correlated with D throughout stream systems by the constant relationship:

$$F_s = 0.694D^2 \quad \textbf{2.16}$$

Hack established a scaling relationship for mainstream length and drainage area

$$L_M \propto A^z \quad \textbf{2.17}$$

where L_M is mainstream length and A is drainage area. Horton's, Hack's and Melton's laws represent power law scaling relationships for drainage networks. It has been shown that these power law scaling relationships are in essence statistically inevitable for dendritic structures such as river networks (Kirchner 1993). These relationships were developed from data for large-scale river networks where changes to network structure occur at very long time scales; therefore, on a short time scale, networks are considered steady state. In Chapter 4 many of the tools described above are used to characterize developing drainage networks on a hillslope.

2.4. Hillslopes

There have been multiple theories (*e.g.*, elongation, Glockian, and Hortonian) of the development of drainage networks (Schumm 1956, Morisawa 1964, Ruhe 1952).

Theories developed were based on field observations of different landforms or scaling experiments conducted in a laboratory setting. Schumm conducted many physical experiments in the Rainfall Experimental Facility (REF) at Colorado State University and measured drainage basin development with regard to fixed and lowered base levels. Other investigations, including those done by Wilson and Storm (1993), have studied drainage network development on small upland areas. The elongation theory notes that network elongation and the addition of tributaries tend to occur simultaneously with a concurrent loss of tributaries near the major streams (Rodríguez-Iturbe and Rinaldo 1997). The Glockian theory is characterized by growth of the first order streams followed by the addition of tributaries (Glock 1931). This is in direct contrast to the Hortonian view of network growth that is characterized by parallel rills, first, and a dendritic pattern that follows after headward growth, micro-piracy, and branching (Schumm et al. 1987). The method of growth of the drainage network has been linked experimentally with changes in slope and base elevation (Schumm et al. 1987).

The above theories are largely qualitative descriptions of network growth, although there are resources to describe landform development quantitatively. Ouchi (2001) described the fractal nature of the topography change for a small drainage basin using a rainfall simulator experiment. He showed how the Hurst parameter, H related to Brownian motion, changes with time and also with restrictive forces, in this case grain size. This approach was able to capture some of the characteristics of the landform as a whole during a rainfall simulation experiment, but did not link the landform to the flow paths of water movement nor the characteristics of the erosion pattern. In Chapter 4 the results of a physical experiment are presented, designed to quantitatively describe the

erosion channel network development in terms of the network descriptors introduced above. The focus being that the time scale is very important when considering drainage network development at the hillslope scale because the network is in constant response to the changing environmental conditions. The point is made that while Horton's bifurcation and length ratios are statistically inevitable, other characteristics of drainage networks, specifically drainage density and width functions, vary with time in a predictable manner.

2.5. Hillslope Erosion Models

Soil erosion modeling in the past century has largely consisted of spatially and time lumped models that attempt to characterize the erosion potential of a site by the water input to the system and the erosion preventive properties of the site. Upland erosion has long been predicted by the Universal Soil Loss Equation, USLE, developed by the United States Department of Agriculture, USDA, Agricultural Research Service in cooperation with the USDA Soil Conservation Service (Wischmeier and Smith 1978). The USLE was originally developed as a tool to develop management plans for agricultural lands maintaining soil productivity and reducing total soil loss. The USLE is written as,

$$A = RKLSCP \qquad \textbf{2.18}$$

where A is annual soil loss per hillslope area, R is the rainfall, K is the erodability index, LS is the hillslope length-slope factor, C is a crop management adjustment factor, and P is the conservation practice adjustment factor. There have been multiple improvements to the USLE including the Revised Universal Soil Loss Equation (RUSLE) and the Modified Universal Soil Loss Equation (MUSLE) (Williams, 1975). These are all essentially more complex models of the same type, spatially lumped and empirical.

Foster (1982) identified six advantages that models based on fundamental physics have over empirical models such as the USLE: 1) fundamental models are generally more physically based; 2) they more accurately represent processes and mechanisms leading to soil erosion; 3) single storm events can more accurately be modeled; 4) they can consider more complex terrain; 5) deposition processes can be considered directly; and 6) channel erosion and deposition can be considered. Many fundamental models have been developed including AGNPS, SWAT, ANSWERS, WEPP, and CASC-2D.

The predictive tools of AGNPS and SWAT developed by the USDA are grid based computer erosion models with a water quality emphasis. Both models use modified versions of the USLE to calculate upland erosion. AGNPS uses five sediment classes and calculates runoff, sediment yield, and nutrient runoff on single storm basis but does not calculate transport between corresponding cells, as there is no sediment continuity within the USLE or its modifications. AGNPS uses the Soil Conservation Service (SCS) curve number method, lumped, to obtain flow depths. SWAT is based on the Simulator for Water Resources in Rural Basins (SWRRB). It also uses the SCS curve number approach for runoff characteristics although it adds a level of complexity by calculating peak discharge using the rational method. SWAT only uses one size class, the estimated mean sediment diameter, for erosion calculations. Grid cells for both models are generally much greater than $O(10^2)$ $[m]^2$.

The Areal Nonpoint Source Watershed Environment Response Simulation (ANSWERS) is a physically based single storm erosion prediction model. Infiltration is computed using physically based equations and runoff volume is calculated using time step increments and infiltration excess. Sediment detachment is calculated using the

Meyer and Wischmeier (1969) equations and transport capacity is calculated using the Yalin (1977) equation. ANSWERS is grid cell based and fully dynamic. This model is one-dimensional in nature; thus it is not capable of capturing the intricacies of distributed erosion and landscape development.

The Water Erosion Prediction Project (WEPP) is a physical process based erosion prediction tool. Flanagan et al. (2001) suggest that WEPP utilizes the most current technology of stochastic weather generation, infiltration theory, soil physics, plant science, erosion mechanics and hydraulics. This is not entirely true. In reality erosion is spatially distributed within the spatial scale that grid cells are generally defined within WEPP such that fine scale interactions between erosion and overland flow are lost. Thus, for extreme events where large amounts of sediment are moved and flow path development is important, much of this information is lost. CASC-2D is also a physical process based spatially distributed model capable of modeling erosion at the watershed scale. Cells are generally 30 [m] or greater on a side and therefore the interactions between flow and erosion at sub-grid scales are ignored.

In large part, all the models discussed above are limited in terms of their ability to model the fine scale mechanisms that lead to drainage network development and the patterns of soil erosion that are observable in nature. They are limited either by the fact that they are lumped in space or spatially distributed in such a manner as to not be able to capture the interactions between small flow depths, erosion and infiltration. Tayfur (2001) developed a physically based interactive model between overland flow and erosion. In his research Tayfur solved the kinematic wave equation for overland flow

$$\frac{\partial h}{\partial t}+\frac{\partial}{\partial x}\left(C_x h^{\frac{5}{3}}\right)+\frac{\partial}{\partial y}\left(C_y h^{\frac{5}{3}}\right)=(r-i) \qquad \textbf{2.19}$$

where

$$C_x = \frac{\sqrt{S_x}}{n\left[1+\left(\frac{S_y}{S_x}\right)^2\right]^{\frac{1}{4}}} \qquad 2.20$$

and

$$C_y = \frac{\sqrt{S_y}}{n\left[1+\left(\frac{S_y}{S_x}\right)^2\right]^{\frac{1}{4}}} \qquad 2.21$$

where h = overland flow depth, r = rainfall intensity, i = infiltration rate, S_x = bed slope in the x-direction, S_y = bed slope in the y-direction, and n = Manning's roughness coefficient. The erosion dynamics algorithm is modified from the 1-D formulation of Woolhiser et al. (1990) into 2-D as

$$\frac{\partial(hc)}{\partial t} + \frac{\partial}{\partial x}(q_x c) + \frac{\partial}{\partial y}(q_y c) = \frac{1}{\rho_s}(D_{rd} + D_{sf}) \qquad 2.22$$

where

$$q_x = C_x h^{\frac{5}{3}} \qquad 2.23$$

and

$$q_y = C_y h^{\frac{5}{3}} \qquad 2.24$$

where c = sediment concentration by volume, ρ_s = sediment particle density, q_x = unit flow discharge in the x-direction, q_y = unit flow discharge in the y-direction, D_{rd} = soil detachment rate by raindrops, and D_{sf} = soil detachment-deposition rate by sheet flow. Tayfur solved all equations implicitly using the Newton-Raphson iteration scheme. There is little discussion on stability, accuracy, and landform development in his paper

and it would appear that this line of research has been discontinued with the model development. The kinematic wave assumption made by Tayfur is questionable for overland flow at very small scales. The mechanisms and interactions between water and sediment movement are not kinematic waves and this approximation probably does not provide an accurate representation for hillslope evolution. Chapter 5 is a presentation of a hillslope model capable of simulating the fine scale processes of water and sediment transport. Chapter 6 is a presentation of energy expenditure characteristics of this model for hillslope topographical development.

2.6. References

Andrews ED. 1980. Effective and bankfull discharges of streams in the Yampa River Basin, Colorado and Wyoming. *J. of Hydrology* **46**: 311-330.

Carlston CW. 1968: Slope-discharge relations for eight rivers in the United States. *U.S. Geol. Survey Prof. Paper* 600-D. p. 45-47.

Carlston CW. 1969. Downstream variations in the hydraulic geometry of streams: Special emphasis in mean velocity. *Am. J. Sci.* **64**(2): 241-256.

Colorado State Soil Conservation Board, 1986. Annual Report.

Glock WS. 1931. The Development of Drainage Systems, *Geographical Review*, **21**: 475-482.

Gupta VK, Waymire E. 1989. Statistical self-similarity in river networks parameterized by elevation, Water Resources Research **25**(3): 463-476.

Howard AD. 1971. Optimal angles of stream junction: Geometric, stability to capture, and minimum power criteria, *Water Resources Research* **7**: 863-873.

Flanagan DC, Frankenberger JR, Renschler CS, Laflen JM, Engel BA. 2001. Simulating small watersheds with Water Erosion Prediction Project In (Ascough II JC, Flanagan DC eds.): Proc. Soil Erosion Research for the 21st Century, 3-5 Jan. 2001, Honolulu, HI, Amer. Soc. Agric. Engrs. St. Joseph MI. pp. 363-366.

Foster GR. 1982. Chapter Eight in *Hydrologic Modeling of Small Watersheds*, Edited by Haan CT, Johnson HP, Brakensiek DL. American Society of Agricultural Engineers.

Johnson BE. 1997. Development of a storm based two-dimensional upland erosion model, *Ph.D. Dissertation*, Colorado State University.

Kirchner JW. 1993. Statistical inevitability of Horton's laws and the apparent randomness of stream channel networks, *Geology* **21**: 591-594.

La Barbera P, Rosso R. 1989. On the fractal dimension of stream networks, *Water Resources Research* **25**(4): 735-741.

Leopold LB, Langbein WB. 1962. The concept of entropy in landscape evolution. *U.S. Geol. Surv. Prof. Paper*, 500-A.

Leopold LB, Maddock T. 1953: The hydraulic geometry of stream channels and some physiographic implications. *U.S. Geol. Survey Prof. Paper* 252, 57 p.

Lovejoy S, Schertzer D, Tsonis AA. 1987. Functional box counting and multiple elliptical dimensions in rain. *Science* **235**: 1036-1038.

Meyer LD, Wischmeier WH. 1969. Mathematical simulation of the process of soil erosion by water, *Transactions of the ASAE* **12**:754-762.

Molnar P, Ramírez JA. 1998a. Energy dissipation theories and optimal channel characteristics of river networks. *Water Resources Research* **34**(7): 189-1818.

Molnar P, Ramírez JA. 1998b. An analysis of energy expenditure in Goodwin Creek. *Water Resources Research* **34**(7): 1819-1829.

Morisawa ME. 1964. Development of Drainage Systems on an Upraised Lake Floor, *American Journal of Science* **262**: 340-354.

Ouchi S. 2001. Development of miniature erosion landforms in a small rainfall erosion facility in *Applying Geomorphology to Environmental Management*. Water Resources Publications, LLC. Highlands Ranch, CO 79 – 92.

Renard KG, Foster GR, Weesies GA, Porter JP. 1991. RUSLE: Revised universal soil loss equation, *J. Soil Water Conservation* **46**: 30-33.

Richardson LF, 1961. The problem of contiguity: An appendix of statistics of dealy quarrels, *Gen. Syst. Yearb.* **6**: 139-187.

Rodríguez-Iturbe I, Rinaldo A, Rigon R, Bras RL, Marani A, Ijjasz-Vasquez E. 1992: Energy dissipation, runoff production, and the three-dimensional structure of river basins, *Water Resources Research* **28**: 1095-1103.

Rodríguez-Iturbe I, Rinaldo A. 1997. *Fractal River Basins: Chance and Self-Organization*, Cambridge, UK, Cambridge University Press.

Ruhe RV. 1952. Topographic Discontinuities of the Des Moines Lobe, *American Journal of Science* **250**: 46-50.

Schumm SA. 1956. Evolution of Drainage Systems and Slopes in Badlands at Perth Amboy, New Jersey, *Geological Society of America Bulletin 67.*

Schumm SA, Mosley MP, Weaver WE. 1987. *Experimental Fluvial Geomorphology*, New York, New York, Wiley-Interscience.

Strahler AN. 1957. Quantitative analysis of watershed geomorphology, *Transaction of the American Geophysical Union* **38**(6): 913-920.

Tarboton DG, Bras RL, Rodríguez-Iturbe I. 1988. The Fractal Nature of River Networks, *Water Resources Research* **24**(8): 1317-1322.

Tarboton DG. 1990. Comment on 'On the Fractal Dimension of Stream Networks:' by Paolo La Barbera and Renzo Rosso, *Water Resources Research*, **26**(9): 2243-2244.

Tayfur G. 2001. Modeling two-dimensional erosion process over infiltrating surfaces, *Journal of Hydrologic Engineering*, **6**(3), 259-262.

Williams JR. 1975. Sediment-yield prediction with universal equation using runoff energy factor, *USDA-ARS Report*, Washington, D.C.

Wilson BN, Storm DE. 1993. Fractal analysis of surface drainage networks for small upland areas, *Transactions of the ASAE*, **36**(5): 1319-1326.

Wischmeier WH, Smith DD. 1978. Predicting rainfall erosion losses. *Agric. handb. 537.* USDA. Agricultural Research Service, Washington, DC.

Wolman MG, Miller JP. 1960. Magnitude and frequency forces in geomorphic processes. *J. of Geology* **68**: 54-74.

Woolhiser DA, Smith RE, Goodrich DC. 1990. KINEROS, A kinematic runoff and erosion model: Documentation and User Manual. U.S. Department of Agriculture, Agricultural Research Service, ARS-77, 130 pp.

Yalin MS. 1977. *Mechanics of sediment transport*, 2nd edition. London, Pergamon Press.

Chapter 3: Effective Optimality for the Local Rate of Energy Dissipation

Abstract

A slope- contributing area relationship for river networks is often described as a power function (slope $\propto$ contributing area^z). The value of the exponent z is a widely discussed topic in the literature. Empirically, z lies near –0.65, which represents a convex longitudinal profile. Explanations for the degree of convexity include, but are not limited to, downstream fining of sediment, optimal energy dissipation, and tributary effects. The original theoretical research on channel networks that expend minimum energy locally and globally predicted a static value of z equal to –0.5, however more recent research has shown that real world river networks are near optimal with different values of z. In this chapter skewness, sediment transport and geomorphic effectiveness of discharge are included in a simulation approach based on theoretical minimum energy dissipation research and provide an explanation by which $z \neq -0.5$ can potentially be optimal in energy dissipation

3.1. Introduction

The causes and implications of the apparent self-organization, the tendency to spontaneously move towards a pre-defined state, of river networks are interesting questions for geomorphologists and engineers. Optimality in energy dissipation and

efficiency have, for many years, been invoked as an explanation for the spatial organization of river networks in terms of the network geometric and topological structure, as well as an explanation for the observed distribution of channel slope and hydraulic geometry (*e.g.*, Leopold and Maddock 1953, Chang 1979, Howard 1990, Rodríguez-Iturbe et al., 1992). Leopold and Maddock (1953) expressed channel form in a series of downstream hydraulic geometry (DHG) relationships:

$$w = aQ^b \tag{3.1}$$

$$d = cQ^f \tag{3.2}$$

$$v = kQ^m \tag{3.3}$$

$$S = gQ^z \tag{3.4}$$

where w [L], d [L], v [L/T], and S [L/L] are width, depth, velocity, and slope respectively, and Q [L^3/T] is stream flow of equal frequency of occurrence throughout the river network. Of particular interest to the research reported in this chapter is equation **3.4**, which describes the longitudinal slope in a river network.

The value of the exponent z in equation **3.4** is a negative value observed between –0.1 and –0.75 (Carlston 1968, Langbein and Leopold 1964). A negative value of z represents a convex longitudinal profile for the river network. A lower bound on z is imposed, because for any drainage basin the average slope must remain finite $z > -1$ (Leopold and Langbein, 1962). Various causes and explanations for longitudinal profiles have been proposed. Leopold and Langbein (1962) hypothesized that z tends towards –1 for the condition of minimum total work whereas the condition of uniform distribution of internal energy tends to lessen the convexity of the profile. Discharge, sediment load, and sediment characteristics are the most important variables that control the forms of

graded river profiles and many models have been developed to study the effects of each (Snow and Slingerland, 1987). Models that use grain size variation as the dominant control include those proposed by Shulits (1941) and Yatsu (1955). Models that use discharge as the controlling factor include those of Gilbert (1877), Leopold and Maddock (1953), and Carlston (1968). Some models use combinations as in Lane (1937) and Hack (1957). From these experiments and empirical evidence some basic general trends have been identified. Profiles where bed material size decreases downstream more rapidly have been found empirically to have more convex longitudinal profiles (*e.g.*, Hack 1957, Ikeda 1970, Cherkauer 1972). Convexity increases as discharge increases more rapidly downstream (*e.g.*, Langbein 1964, Snow and Slingerland 1987).

In their work on the structure and shape of river networks, Rodríguez -Iturbe et al. (1992) postulated three principles of optimality in energy dissipation to define the optimal network, (1) minimum energy dissipation in a river link, (2) constant energy dissipation per unit channel bed area throughout the network, and (3) minimum total energy dissipation in the whole network. These principles have been restated in terms of local and global energy dissipation hypotheses (Molnar and Ramírez 1998a). The principle of local optimality states a river network adjusts its average channel hydraulic geometry properties (*i.e.*, width, depth, velocity, and slope) towards an optimal state in which the rate of energy dissipation per unit channel area P_l is constant throughout the network. The global hypothesis states that a river network adjusts its topological structure towards a state in which the total rate of energy dissipation in the network is minimum. Synthetically simulated channel networks that follow these two principles (these networks are referred to as optimal channel networks (OCN's) possess channel

hydraulic geometry characteristics and network topological structures that exhibit many similarities with natural systems (Rodríguez -Iturbe et al. 1992, Rinaldo et al. 1992, Ijjasz-Vazquez et al. 1993, Rigon et al. 1993, Sun et al. 1994). In most of these studies, restrictions imposed on the values of downstream hydraulic geometry exponents, namely $b = f$, resulted in a value of the slope scaling exponent describing the longitudinal profile of the river network, z = -0.5. Molnar and Ramírez, (1998a, b; 2002) imposed less restrictive conditions on the scaling exponents of the DHG, namely, they allowed b and f to be different from each other, and found that some real river networks have near constant distributions of local energy dissipation with z values between –0.35 and –0.65 (Molnar and Ramírez, 1998a, b, Molnar and Ramírez 2002).

Effective discharge is the flow responsible for channel form (*e.g.*, Wolman and Leopold 1957). This flow is often well above the mean discharge and is found by determining the flow, or range of flows, that move the most sediment over time (*e.g.*, Wolman and Miller 1960). It has been shown that channels that drain smaller contributing areas tend to display a more highly skewed probability density function of daily mean discharges than channels that drain larger areas, and that the skewness coefficient γ is related to drainage area as (Andrews, 1980),

$$\gamma \propto A^{\theta} \qquad \textbf{3.5}$$

Therefore, the distribution of flows relative to the effective discharge varies as skewness in discharges vary. Original OCN theory development assumes a static flow in the network (*e.g.*, bank full discharge or mean annual discharge). Molnar and Ramirez (1998a,b, 2002) considered flows of different recurrence intervals, the same quantile everywhere, within a real world drainage basin within the framework of optimality in

energy dissipation and also accounted for the sediment transport at those flows and found varying values of optimal exponents for slope as well as for width and depth.

This section examines whether the difference in exceedance probabilities of flows affects the longitudinal profile of a river within the framework of optimality in energy dissipation. In order to do so the local slopes of 15 cross-sections of an artificial river profile are considered. A long-term sequence of daily flows is simulated and then using the local energy dissipation hypothesis the optimal value of z is found which minimizes the coefficient of variation of energy dissipation per unit area for all 15 cross-sections. The different effectiveness at the daily time scale is accounted for by assigning greater weight to the larger flows through time. This is used to account for different sediment transport regimes. For example, flows from a given quantile in a system where the sediment is always in motion (live bed system) will contribute a different relative amount of work than the same quantile flow in a system where some threshold must be exceeded to begin sediment transport (threshold system). This is an inclusion of geomorphic effectiveness, which has yet to be attempted in OCN simulations. What is shown is that skewness in daily discharge and differing flow effectiveness results in optimal z values different from –0.5.

3.2. Methods

3.2.1. Simulation

Daily flows are sampled from lognormal-2 distributions for each of the 15 cross-sections at each time step. This sampling is done by randomly selecting a single quantile

from the uniform distribution and then finding the corresponding flow at each section. No flow routing or serial correlation is included in this model.

3.2.2. Discharges

Daily mean discharges are assumed to be distributed as a log-normal 2 (LN-2) distribution whose probability density function (PDF):

$$f(Q) = \frac{1}{\sqrt{2\pi}Q\sigma_y} \exp\left[-\frac{1}{2}\left(\frac{\ln(Q) - \mu_y}{\sigma_y} \right)^2 \right] \quad 3.6$$

where $y = \ln(Q)$ is normally distributed with mean μ_y and variance σ_y^2. It may be shown that the mean and variance of Q are given, respectively, by (Yevjevich 1972)

$$\mu_Q = \exp\left(\mu_y + \frac{\sigma_y^2}{2} \right) \quad 3.7$$

and

$$\sigma_Q^2 = \left[\exp(\sigma_y^2) - 1 \right] \exp(2\mu_y + \sigma_y^2) \quad 3.8$$

Likewise, the coefficient of variation (η_Q) and the skewness coefficient (γ_Q) of the variable Q are, respectively,

$$\gamma_Q = \eta_Q^3 + 3\eta_Q \quad 3.9$$

and

$$\eta_Q = \left[\exp(\sigma_y^2) - 1 \right]^{\frac{1}{2}} \quad 3.10$$

The mean discharge for any point within a river network has been noted by many in the literature to be directly proportional to the contributing area (*e.g.*, Hack 1957, Rodríguez -Iturbe and Rinaldo 1997)

$$\overline{Q} \propto A^n. \qquad 3.11$$

The work presented here assumes n = 1 although for very large basins n is often between 0.7 and 0.9 (Knighton 1998). The initial skewness in mean daily discharge is determined from the empirical work of Andrews (1980) and can be approximated by the power function

$$\gamma_Q = 10A^{-0.391} \qquad 3.12$$

Two other skewnesses are considered in this chapter and correspond to θ = -0.197 and -0.782, from equation 3.5, half and twice the exponent reported by Andrews (1980) respectively. Also a normal distribution is considered defined by μ_Q and utilizing the same standard deviation as calculated from the LN-2 distribution when $\theta = 0.391$.

With the assumption $\mu_Q = \overline{Q}$, it is possible to solve equations 3.7 – 3.10 simultaneously, which is done here using a non-linear optimization routine to find μ_y and σ_y and checking to assure that the solution matches the analytical solution. The cumulative distribution function (CDF) for the LN-2 model is well known and the simulation at a time step is straightforward with known parameters μ_y and σ_y.

3.2.3. Geomorphic Effectiveness

Each flow observed in nature performs some amount of work on the channel. This work may be referred to as the effectiveness of each flow. Because sediment transport capacity is often expressed as a power function of the flow rate with an exponent greater than one, higher flows are more effective than lower flows in a non-linear fashion. A time component must also be considered when determining effectiveness. Channels do not adjust to equilibrium on a daily time scale but are rather

in a constant state of adjustment relative to the time and effectiveness of the discharges present. It is proposed here that the geomorphic effectiveness of a flow can be quantified as a weighting function based on a flow magnitude relative to a geomorphic threshold (Q_T) at which sediment transport begins:

$$W_Q = \begin{cases} 0, & Q < Q_T \\ \left[\dfrac{(Q - Q_T)}{\max(Q - Q_T)}\right]^a, & Q \geq Q_T \end{cases} \qquad 3.13$$

where W_Q is the weight of the flow Q on the form of the channel network and the maximum value of $Q - Q_T$ is the maximum value over the entire simulation. Values of the geomorphic effectiveness exponent, a, ranging from 0 to 2.8 are explored. When a = 0 all flows are equal in influence on channel form. When $a > 0$ flows much larger than the geomorphic threshold become more important to channel form than flows closer to, or below, the threshold. The exponent a encompasses both the sediment transport characteristics of the flow Q as well as the responsiveness, with respect to time, of the network.

3.3. Calculations

The goal of this simulation is to find the values of the exponent z in the relationship $S \propto A^z$, such that the local energy dissipation hypothesis, introduced earlier, is observed for the effective discharge. That is to say, that energy dissipation per unit area of channel is constant throughout the network for the flow responsible for channel form. Energy dissipation per unit area of a rectangular channel can be written as (Molnár and Ramírez 1998a),

$$P_l = \gamma_m \frac{SQ}{w + 2h} \qquad 3.14$$

where d and w are the flow depth and width respectively and γ_m is the submerged specific weight of the fluid sediment mixture and is calculated as (Molnár and Ramírez 1998a)

$$\gamma_m = g\rho_w[1 + C_v(G-1)]. \quad \textbf{3.15}$$

In equation **3.15** g is gravitational acceleration, ρ_w is the mass density of water, G is the specific gravity of sediment, assumed here to be 2.65 (quartz particles), and C_v is the volumetric sediment concentration. The volumetric sediment is calculated from a simple sediment transport equation where the mass flux of sediment, Q_s, is

$$Q_s \propto Q^b \quad \textbf{3.16}$$

and for these simulations b is set to 1.5, a form consistent with many real world systems (*e.g.*, Holmquist-Johnson 2002).

At each time step during the simulation there are 15 values of P_l, one for each channel link as a function of z. A value of z can then be found such that the coefficient of variation (η) among channel energy dissipation per unit width is a minimum

$$\eta = \frac{\sqrt{\dfrac{\sum_{i=1}^{N}\left(P_{l_i} - \overline{P_l}\right)^2}{N-1}}}{\dfrac{\sum_{i=1}^{N} P_{l_i}}{N}} = \text{minimum} \quad \textbf{3.17}$$

3.4. Results and Discussion

Results from this simulation predict optimal channel networks with a wide range of z values dependent on flow geomorphic effectiveness characteristics and discharge skewness. Figures 3.1 shows that when the same quantile is considered from a normal distribution regardless of the weighting factor and geomorphic threshold for sediment transport, the scaling exponent z is always equal to -0.5 for optimality. Figures 3.2 – 3.4

show the values of optimal z calculated for the three different values of skewness discussed previously. What can be seen is that all geomorphic thresholds have a monotonically increasing value of optimal z with increasing effectiveness factor regardless of skewness. Also, regardless of skewness, higher values of transport thresholds correspond to greater values of optimal z. As the rate of skewness with drainage area increases ($\theta \rightarrow -1$) the case for which all flows have equal weight increases the spread about $z = -0.5$.

While it is difficult to assign actual values of grain size to values of geomorphic effectiveness or transport thresholds, some general statements can be made. Sand bed rivers tend to have low threshold values and a wide range of effectiveness values, while cobble / gravel bed rivers tend to have higher thresholds and lower overall effectiveness values.

For sand bed systems, sediment transport occurs at virtually all flows. Larger flows have a major impact on channel form as transport regime changes from bed load to bed and suspended load. The sediment transport threshold is therefore defined as a relatively small percentage of mean discharge. This is considered a live bed regime and is represented by the blue lines in Figures 3.2 – 3.4. For cobble / gravel bed rivers the transport threshold is a higher percentage of mean discharge and it is expected that the high flows will have a higher influence on the geomorphic properties of the network. This is because at very large grain sizes it takes very large flows to transport a significant amount of sediment to shape the longitudinal profile. These systems are considered to be in a threshold regime. From Figures 3.2 – 3.4 the condition of optimality in distribution

of energy dissipation per unit area thus requires that in live bed systems z is less than for threshold systems.

Often in nature mountainous headwaters in threshold regimes exhibit z values closer to –1 than do the downstream sections with finer sediment (*e.g.*, Carlston 1968), which is inconsistent with the results presented here. There are two explanations for this discrepancy. First, the condition of a reduction in global rate of energy dissipation requires that $z \rightarrow -1$ and while at high flows $z \rightarrow 0$ for the condition of equal energy dissipation per unit area optimality in the global characteristic may become dominant. Second, in nature it is possible that rates of uplift or other forces restricting longitudinal profile development may be of equal magnitude and time scale to the processes which cause optimality in local energy dissipation. Indeed here, the individual links within the network are assumed to respond entirely by slope alteration although it is noted that the channels may respond by changes in width as well or through alterations of bed form roughness. Indeed it has been shown that with respect to energy dissipation the width, depth and slope are intricately tied together (Molnár and Ramírez 1998 a, b, Molnár and Ramírez 2002).

Not only do river network systems differ in their sediment transport threshold and sediment transport capacity *vs.* flow rate relationships, but also in the distributions of flows. Network systems represent not one flow of one quantile, as downstream hydraulic geometry (DHG) relationships assume, but rather all flows from all quantiles and thus the relative abundance of each flow. It is expected that network systems with different skewness characteristics have different optimal values of z reflective of the effective discharge and its recurrence interval. Looking from Figures 3.2 to 3.4 there is a trend of

increasing maximum convexity with increasing discharge skewness, thus as the relative frequency of higher flows decreases, relative to the mean, convexity increases (minimum z becomes more negative) for live bed systems.

Skewness is inversely related to drainage area and observations of area-slope relationships shift from more to less convex as drainage area increases. The Missouri, Arkansas, Ohio, and Holston Rivers show this trend (Carlston 1968). It is difficult to compare one river system to another as often these systems vary in their distributions of discharge and sediment transport characteristics. As skewness decreases the distribution of flows about the mean becomes more uniform and the variation in optimal z decreases.

Natural river systems exhibit many of the qualities of OCNs and as Molnár and Ramírez (1998a,b, 2002) note, systems that deviate from area-slope relationships of $z = -0.5$ can still be viewed as potentially optimal. It is proposed here that an explanation for this deviation is the distribution of flows about the mean discharge and the importance each flow has on channel longitudinal profile. If long-term average slope-area relationships in actual river networks reflect optimality in local energy dissipation then from Figures 3.1 – 3.4, it can be concluded that that these relationships are highly dependent on the recurrence intervals of flows relative to the mean, the amount of work each flow does with regard to sediment transport and the relative ability of large to small flows to adjust channel form.

This simulation study focuses solely on the local energy dissipation hypothesis but results are also relevant to the global energy dissipation hypothesis. The global energy dissipation hypothesis states that the energy expended in a network as a whole is a

minimum. Total network energy dissipation is the sum of the energy expended in each link which can be written as:

$$P_T = \sum L_N \overline{\left(\frac{P_l}{L_N}\right)_N} = \sum L_N \overline{(A^z Q)}_N, \qquad 3.16$$

where L_N is the link length. As z becomes more negative P_T approaches a minimum. Results of this study which find many possible values of $z < -0.5$ based solely on equal energy dissipation per unit area actually represent less energy expended in the network as a whole.

3.5. Conclusions

Given the sole restriction of equal energy dissipation per unit area, I predict a wide range of potential optimal channel networks, defined by their area-slope relationship, and dependent on discharge skewness and sediment transport processes. The condition of optimality in local energy dissipation requires monotonically increasing values of z for the slope - area relationship $S \propto A^z$ as higher flows are given more weight in describing longitudinal form when daily discharge skewness is considered a function of contributing area. The general trend for systems in which all flows do equal work is that as discharge skewness decreases more rapidly downstream optimal z decreases. This result is consistent with the best available empirical evidence.

3.6. References

Andrews ED. 1980. Effective and bank full discharges of streams in the Yampa River Basin, Colorado and Wyoming. *J. of Hydrology* **46**: 311-330.

Carlston CW. 1968. Slope-discharge relations for eight rivers in the United States. *U.S. Geol. Survey Prof. Paper* 600-D. p. 45-47.

Chang HH. 1979. Minimum stream power and river channel patterns. *J. of Hydrology* **41**: 303-327.

Cherkauer DS. 1972. Longitudinal profiles of ephemeral streams in southeastern Arizona. *Bulletin of the Geological Society of America* **83**: 353-366.

Gilbert GK. 1877. Report on the geology of the Henry Mountains. *U.S. Geog. Geol. Survey, Rocky Mt. Region*, 160 p.

Hack JT. 1957. Studies of longitudinal stream profiles in Virginia and Maryland. *U.S. Geol. Survey Prof. Paper 294-B*, p. 45-97.

Howard AD. 1990. Theoretical model of optimal drainage networks. *Water Resources Research* **26**: 2107-2117.

Ijjasz-Vasquez EJ, Bras RL, Rodríguez -Iturbe I, Rigon R, Rinaldo A. 1993. Are river basins optimal channel networks? *Adv. Water Resources* **16**: 69-79.

Ikeda H. 1970. On the longitudinal profiles of the Asake, Mitaki and Utsube Rivers, Mie Prefecture. *Geog. Review of Japan* **43**: 148-159.

Holmquist-Johnson CL. 2002. Computational methods for determining effective discharge in the Yazoo River Basin, Mississippi, *Masters Thesis*, Colorado State University.

Knighton D. 1998. Fluvial Forms & Processes: A New Perspective. John Wiley & Sons, New York. p. 171-177.

Lane EW. 1937. Stable channels in erodable materials. *American Soc. Civil Eng. Transactions* **102**: 123-194.

Langbein WB. 1964. Profiles of rivers of uniform discharge. *United States Geological Survey Professional Paper 501B*: 119-122.

Langbein WB, Leopold LB. 1964. Quasi-equilibrium states in channel morphology. *American J. of Science* **262**: 782-794.

Leopold LB, Langbein WB. 1962. The concept of entropy in landscape evolution. *U.S. Geol. Survey Prof. Paper* 500A.

Leopold LB, Maddock T. 1953. The hydraulic geometry of stream channels and some physiographic implications. *U.S. Geol. Survey Prof. Paper* 252, 57 p.

Molnár P, Ramírez JA. 1998a. Energy dissipation theories and optimal channel characteristics of river networks. *Water Resources Research* **34**(7): 189-1818.

Molnár P, Ramírez JA. 1998b. An analysis of energy dissipation in Goodwin Creek. *Water Resources Research* **34**(7): 1819-1829.

Molnár P, and Ramírez JA. 2002. On downstream hydraulic geometry and optimal energy dissipation: Case study of the Ashley and Taieri Rivers. *J. of Hydrology* **259**: 105-115.

Rigon R, Rinaldo A, Rodríguez -Iturbe I, Ijjasz-Vasquez E, Bras RL. 1993. Optimal channel networks: A framework for the study of river basin morphology. *Water Resources Research* **29**(6): 1635-1646.

Rinaldo A, Rodríguez -Iturbe I, Rigon R, Bras RL, Ijjasz-Vasquez E, Marani A. 1992. Minimum energy and fractal structures of drainage networks. *Water Resources Research* **28**: 2183-2195.

Rodríguez -Iturbe I, Rinaldo A, Rigon R, Bras RL, Marani A, Ijjasz-Vasquez, E. 1992. Energy dissipation, runoff production, and the three-dimensional structure of river basins. *Water Resources Research* **28**: 1095-1103.

Rodríguez -Iturbe I, Rinaldo A. 1997. Fractal River Basins: Chance and Self-Organization. Cambridge University Press, New York.

Shulits S. 1941. Rational equation of river-bed profile. *American Geophys. Union Transactions* **22**: 622-630.

Sinha SK, Parker G. 1996. Causes of concavity in longitudinal profiles of rivers. *Water Resources Research* **32**(5): 1417-1428.

Snow RS, Slingerland RL. 1987. Mathematical modeling of graded river profiles. *J. of Geology* **95**: 15-33.

Sternberg H. 1875. Untersuchungen uber langen-und querprofil geschiebefurende flusse: *Zeits. Bauwesen* **25**: 483-506.

Sun T, Meakin P, Jossang T. 1994. The topography of optimal drainage basins. *Water Resources Research* **30**: 2599-2611.

Wolman MG, Leopold LB. 1957. River flood plains: some observations on their formation. *U.S. Geological Survey Prof. Paper* 282C: 87-109.

Wolman MG, Miller JP. 1960. Magnitude and frequency of forces in geomorphic processes. *J. of Geology* **68**: 54-74.

Yatsu E. 1955. On the longitudinal profile of the graded river: *American Geophys. Union Transactions* **36**: 655-663.

Yevjevich V. 1972. Probability and statistics in hydrology. *Water Resources Publications*, Fort Collins, Colorado, 302 p.

Figure 3.1:Optimal z for Normal Distribution

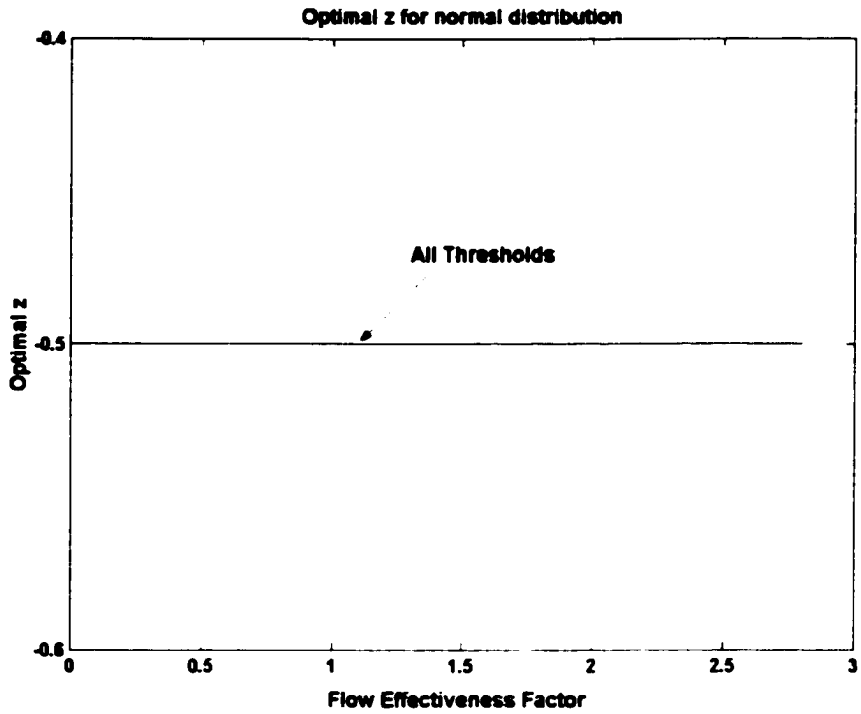

Figure 3.2: Optimal z by Skewness – Area Exponent = -0.197

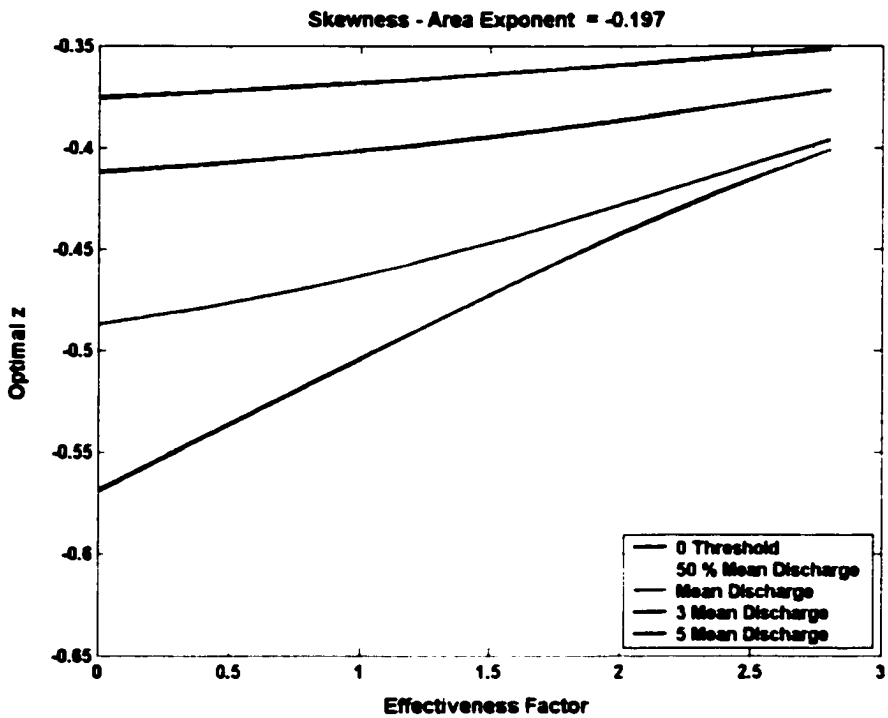

Figure 3.3: Optimal z by Skewness – Area Exponent = -0.391 (Andrews 1980)

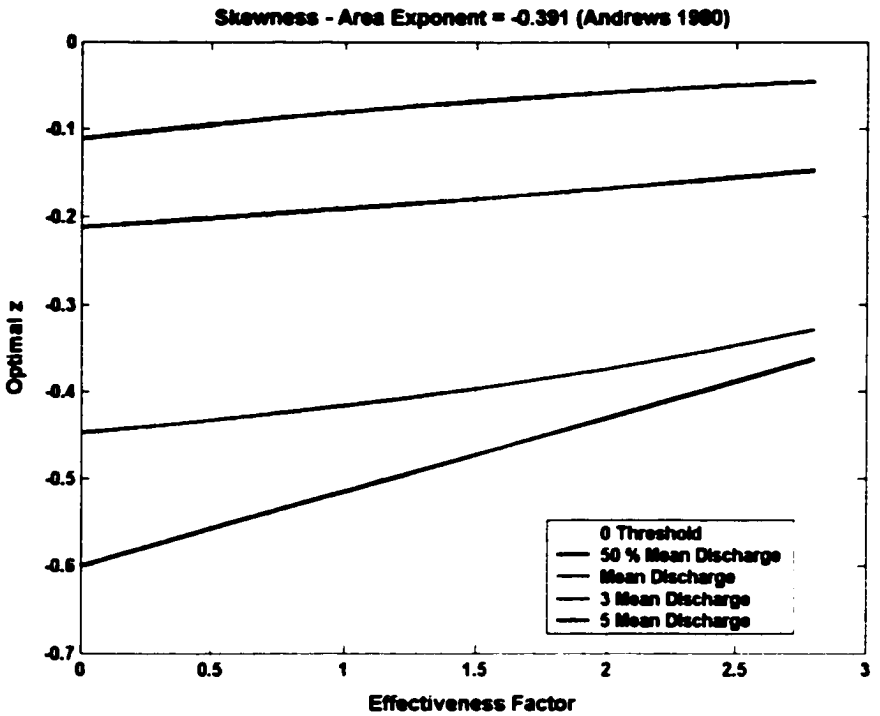

Figure 3.4: Optimal z by Skewness – Area Exponent = -0.782

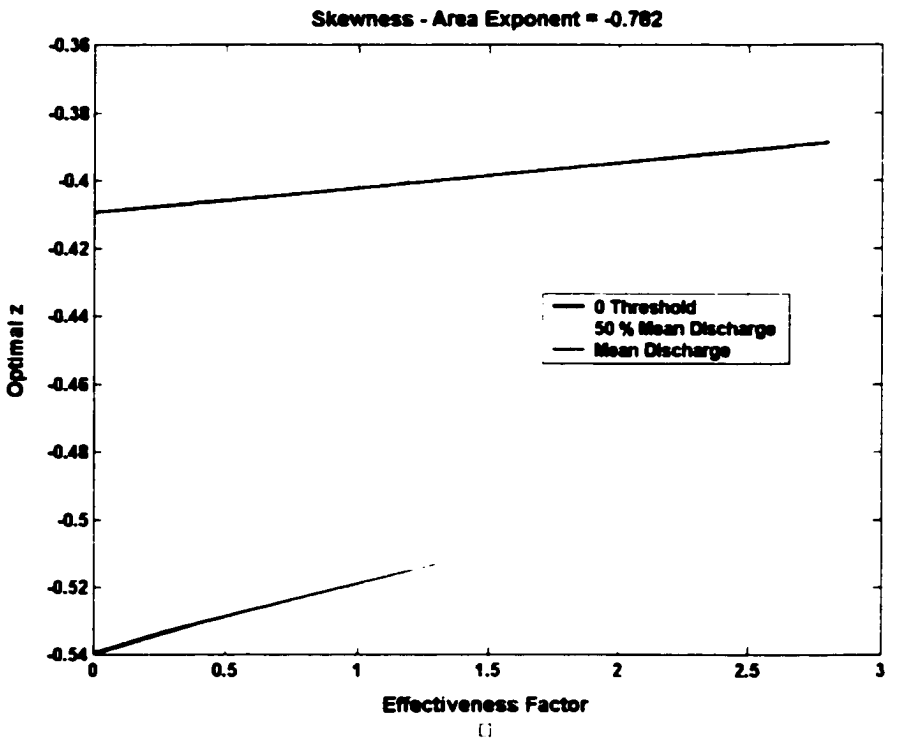

Chapter 4: Hillslope Drainage Development with Time, A Physical Experiment

Abstract

A rainfall simulator experiment is presented here in which the structure of developing erosion channel networks is studied for 9° and 5° slopes subject to constant rainfall. Quantitative measurements include some standard measurements of width, depth, and width-to-depth ratios for channels aggregated over slope, as well as fractal measures and width functions. Trends in fractal measurements and width functions with time are presented and compared to previous qualitative descriptions of network growth. Steeper slopes are shown to influence the rate at which the drainage network fills space and the properties of the width functions are shown to describe a growing network which retains bifurcation characteristics.

4.1. Introduction

This chapter presents a physical experiment, fluvial geomorphic in nature, to study hillslope evolution from a channel network point of view. The field of experimental fluvial geomorphology can be defined as the study of specific geomorphic features under closely monitored and controlled experimental conditions (Schumm et al. 1987). The advantage of the experimental approach is that it permits the study of an evolving geomorphic system rather than just differences between equilibrium and non-equilibrium

states (Rodríguez-Iturbe and Rinaldo 1997). However, the key drawback is that initial and boundary conditions, as well as natural interactions (*e.g.*, network growth rates) may not be analogous to those found in nature (Rodríguez-Iturbe and Rinaldo 1997). If, however, the scale at which the physical model exists is the same scale at which the processes are found to occur naturally, then the latter drawback can be disregarded. As conducted here, hillslope network growth as well as equilibrium states characteristics are studied from a geomorphic point of view and are an accurate representation of the physical processes that occur on non-vegetated natural slopes.

Erosion channels on hillslopes are often the dominant sediment and water transport mechanism (Nearing et al. 1997). Fundamental knowledge of erosion channel growth rates pertaining to the system of channels could be very helpful in further development of erosion prediction models. It is hypothesized that the drainage network that develops on a hillslope void of vegetation develops under the same processes and mechanisms as do larger river networks. Channel initiation mechanisms that occur at the watershed scale also exist at the hillslope scale. In the Hortonian model (1945) channel initiation occurs at the point where the shear stress exerted on the soil surface by overland flow exceeds some critical value. Shallow land sliding is another mechanism that has been suggested for channel initiation at the watershed scale (Dietrich et al. 1986, Montgomery and Dietrich 1988), and has been shown to occur in rainfall simulations at the hillslope scale similar to the type presented here (Schumm et al. 1987). As a result of the similarity in processes and mechanisms, hillslope networks should possess the same scaling relationships as river networks at equilibrium. The scaling relationships can then in turn be used as predictive tools for evolving hillslopes.

River networks have been classified as having properties which exist over a very wide range of spatial scales and these properties have led to the advancement of predictive and management tools like downstream hydraulic geometry relationships (*e.g.*, Leopold and Maddock 1953) and energy expenditure characteristics (*e.g.*, Molnár and Ramírez 1998 a, b). Landform development has also been shown to have fractal properties at scales as small as 100 m^2 (Ouchi 2001) and as large as $O(10^6)$ m^2 (Rodríguez -Iturbe and Rinaldo 1997). Recent literature suggests that water flow paths on hillslopes are fractal in nature (Ogunlela et al. 1989, Wilson 1991, Wilson and Storm 1993). From an erosion prediction viewpoint, sediment detachment and transport occurs where the water is flowing and if the water flow paths are fractal in nature, as is suggested above, then the erosion channel network that develops on a hillslope should also be fractal in nature.

The scaling structure of river networks is often described as a function of a flow of equal frequency of occurrence throughout the network. This is appropriate for perennial river systems and long time scales because the flows often chosen are close to the effective discharge, defined as the singular flow responsible for channel form (Andrews 1980). Effective discharge, *ED*, is the flow that does the most work in terms of sediment transport over time and is usually determined by the maximum of the convolution of the flow probability distribution and the sediment transport. If Q is flow rate [L^3/T], $f(Q)$ is the probability distribution function, and $Q_s(Q)$ is the sediment transport rating curve then

$$ED = \max(Q_s(Q) * f(Q)). \qquad \textbf{4.1}$$

The distribution of water fluxes on hillslopes is not as easy to describe as for perennial rivers. Generally, water only occurs on a hillslope during rainstorms, which vary in

frequency as well as in intensity and duration. However, the drainage network present on a hillslope should still be capable of transporting the water and sediment produced from a specific storm of intensity, duration, and spatial heterogeneity such that there is no local aggradation or degradation anywhere within the network. Thus at any point in time the effective storm, the storm which reflects the current structure of the drainage network present, is of a specific intensity, duration, and spatial heterogeneity whose characteristics change with the properties of the hillslope (*e.g.*, soil moisture distribution). Considering hillslope evolutionary response with respect to the effective storm, with which the current network is in equilibrium, may be a better approach to model erosion from single storm events than the current method based on lumped statistics (*e.g.*, soil types, mean rainfall intensity). In order to use this approach, descriptions of drainage network development are necessary with respect to many variables including hillslope-scale slope, rainfall intensity, duration, and spatial heterogeneity. An examination of hillslope-scale slope as it affects drainage network development is presented.

The approach utilizes mathematical tools that have been developed for the analyses of river networks (*e.g.*, functional box counting and width functions) and apply them to the analysis of the development and evolution of the erosion channel (*i.e.*, rill) network system. The goal is to show that network evolution described as a function of these mathematical tools, fluvial geomorphologic in nature, on a hillslope is predictable with respect to hillslope-scale slope.

4.2. Methods

An experiment is presented that studies the drainage network evolution on hillslopes void of vegetation. The experiment is designed to test whether techniques originally

developed for river networks can describe actively developing networks on hillslopes, and if so, how does hillslope-scale slope affect the rate of network evolution described through space filing properties and width functions.

Six rainfall simulations on an artificial hillslope of (projected) dimensions 3 x 10 [m^2] (Figure 4.1) are presented. The slope is initially smooth and compacted as uniformly as possible utilizing a roller compacter. Two slope angles are considered, 9° and 5°. In between experimental runs the soil is roto-tilled, leveled and compacted. A small amount of additional soil is mixed in with the roto-tilled soil surface in between runs to replace the sediment lost from the previous experiment and to eliminate any effects of preferential sediment transport and armoring from one experiment to the next.

Rainfall is spatially and temporally homogeneous for 4 to 5 hours, ending when the erosion channel network ceases to vary significantly over a period of 30 minutes. Eight commercial sprinkler nozzles generate the rainfall. A constant pressure input to the rainfall nozzle array was used for all experiments (207 [kPa]); this corresponds to an average rainfall intensity of 65 [mm/hr]. This rainfall intensity is used, as it is intense enough to cause the formation of channel networks and not too intense as to never occur naturally. A sample rainfall distribution is shown in Figure 4.2. The soil substrate is comprised of a sand mixture, whose grain size distribution is depicted in Figure 4.3. Photographs are taken at 1-hour intervals throughout the experiment. At the completion of the experiment the erosion channel network is mapped manually. Each erosion channel is given a stream order classification using the Strahler stream ordering system (Strahler 1957):

- erosion channels that originated at a source were defined as first-order ($\omega = 1$);

- when two erosion channels of order ω joined together, an order ω + 1 was assigned;
- when two erosion channels of different order joined, the channel segment immediately downstream had the higher order of the two combined channels
- the order of the drainage network, Ω, is equal to the order of the highest order stream in the network.

Width and depth measurements are made along each channel, same as a link, separated by a distance of 300 [mm]. Let $N_m(L)$ be the number of measurements made per channel and it is a function of the channel length. N_m has a mean of 4 and a standard deviation of 2.5. Widths and depths are then aggregated to obtain average width and depth of erosion channels for the 9° and 5° experiments, respectively.

Scaling relationships are calculated to determine whether the erosion channel networks resemble the fractal characteristics of larger river networks. These scaling relationship include Horton's law of stream lengths

$$\overline{L_\omega} = \overline{L_1} R_L^{\omega-1} \qquad 4.2$$

where R_L is the *length ratio*, and $\overline{L_\omega}$ is the (arithmetic) average of the length of streams of order ω; and Horton's law of stream numbers

$$N_\omega = R_B^{\Omega-\omega} \qquad 4.3$$

where R_B is the *bifurcation ratio*, and N_ω is the number of streams of order ω, and Ω is the system order. In river systems, R_B and R_L are typically near 4 and 2, respectively, but range between 3 and 5 for R_B and 1.5 and 3.5 for R_L (Rodríguez-Iturbe and Rinaldo, 1997).

From the photographs taken during the simulation, an estimation is made of the fractal dimension of the erosion channel network at each time using a functional box counting method as described by Lovejoy et al. (1987). Tarboton (1988) applied this method to a stream network by beginning with a set of points embedded in a *d*-dimensional space. Here the method is applied to a rill erosion network. The *d*-dimensional space (*i.e.*, here the photograph where $d = 2$) is covered by a mesh of *d*-dimensional cubes of area r^d. For any mesh let $N(r)$ be the number of cubes within the mesh that contain elements of an erosion channel. By varying the size of the cubes a relationship develops of the form

$$N(r) \propto r^{-D_f} \tag{4.4}$$

where D_f is the fractal dimension of the network defined by Hentschel and Procaccia (1983) as

$$D_f = -\lim_{r \to 0} \lim_{m \to \infty} \frac{\log N(r)}{\log r}, \tag{4.5}$$

where m is the number of points in the set. A projection of $N(r)$ vs. r on a log-log scale is a straight line of slope $-D_f$. Box sizes of $r = 4.0$, 8.5, 13.0, 17.0, and 30.0 [mm] are used. These box sizes only cover one order of magnitude, a drawback of the approach, however, smaller boxes become very difficult to work with and larger boxes become meaningless. As $D_f \to 2$ the network is said to become more space filling. An ANOVA model is used to study the dependence of the fractal dimension, D_f, on time, antecedent soil moisture and slope. Antecedent soil moisture, measured as concentration by weight, is inversely proportional to the time period since the previous rainfall experiment (Figure 4.4). Drainage densities for the erosion channel network are calculated in pixel units

from the photographs taken at the finest mesh used throughout this analysis (4 x 4 [mm^2]).

Every pair of points within a drainage network tree has a unique one-dimensional path connection. Therefore, the distance a drop of water travels from input to basin outlet is uniquely determined. Hydrologic response of a drainage system subject to rainfall input is particularly dominated by the arrangement of the concentrated flow paths (Rodríguez-Iturbe and Rinaldo 1997). The distribution of the lengths of these paths is often characterized by the width function (Shreve 1969) which gives the number of links, $N_L(x)$ in the network at a flow distance x from the outlet. Width functions are obtained from photographs taken every hour of each simulation. Width functions generally have a form dominated by a very low frequency where N_L approaches a minimum at $x = 0$ and as $x \rightarrow D_D$ (the distance to the drainage divide). N_L approaches a maximum near $D_D / 2$ and is subject to oscillations occurring at difference length scales. The dominant low frequencies describe the shape of the watershed drained by channels and the high frequencies describe the bifurcation characteristics of the network (Rodríguez and Iturbe and Rinaldo 1997). Width functions can be readily modeled by Fourier series of the form

$$S_m(x) = \frac{A_0}{2} + \sum_{n=1}^{m}\left[a_n \cos\left(\frac{nx\pi}{p}\right) + b_n \sin\left(\frac{nx\pi}{p}\right)\right] \qquad 4.6$$

where p is the period, x is distance from outlet, n is a summation index, and A_0, a_n, and b_n are constants fit to the data using a nonlinear optimization technique that reduces the total sum of square errors. Fourier fits for $n = 1$ to 3 have mean r^2 values of 0.98 and standard deviation of 0.01. An ANOVA model is used to study the dependence of the scale A_0, and signal power contained in the frequencies (n_1, n_2 and n_3) on time, antecedent soil

moisture content (specified as a time interval since last rainfall), and slope. The power contained by a single frequency $S_p(f)$ is determined here as

$$S_p\left(\frac{n\pi}{p}\right) \propto \left(a_n^2 + b_n^2\right) \qquad 4.7$$

and represents the relative importance of a given frequency in the overall power contained within the Fourier series.

4.3. Results

Mean values for Horton's bifurcation and length ratios measured at the end of rainfall simulations are 3.7 and 1.8 respectively. These are not statistically different from the expected values for river networks of 4 and 2, respectively. It is acknowledged that values at or near expected values may be statistically inevitable and thus lack validation power (Kirchner 1993). Average widths and depths for the 9° slopes are greater than those for 5° slopes (Table 4.1, Figures 4.5 and 4.6). The average width to depth ratio for 9° slopes is less than those for 5° slopes (Table 4.1, Figure 4.6). The relationship between width and depth with slope indicates a higher degree of incision on the steeper slope.

Measures of the fractal dimension D_f determined by fitting a line on the log-log plot of $N(r) \propto r$ fit to the data in Appendix A show a strong dependence with time and slope. The linear fits to the log-log plots have an average r^2 value of 0.98 and a standard deviation of 0.012. The linear ANOVA model

$$D_f = \beta_o + \beta_1 x_1 + \beta_2 x_2 \qquad 4.8$$

is fit to the values of D_f determined from each photograph where x_1 is hours since rainfall simulation began and x_2 is the hillslope scale slope at the beginning of the experiment. This ANOVA is determined to explain more than 50 % of the variability in the fractal

dimension values, D_f, and the p-values for β_1 and β_2 are $6.97(10^{-4})$ and 0.02, and have means of $4.40(10^{-3})$ and $1.86(10^{-3})$, respectively. A plot of D_f with time for all six simulations can be seen in Figure 4.8. There does not appear to be any consistent trend in these plots. Tests of width function characteristics with time, antecedent moisture, and slope show that only time is a significant variable (Table 4.2), and is only significant in determination of A_o values and the signal power contained within the n_1 frequency. A_o increases with time and the power contained within the most dominant "low" frequency also increases with time. The signal power contained within the higher frequencies does not significantly change as a function of time but is an important variable in modeling the width function.

A plot of a drainage density measurement after the first hour of rainfall versus the number of days between simulations is shown in Figure 4.9. An exponential trend is fit to the data with an exponent of –0.03 and an $r^2 = 0.80$. The high r^2 value shows the dominance of initial conditions on early network development but this dominance does not persist into hour 2.

4.4. Discussion

During these experiments the sediment flux is observed to be highly correlated with erosion channel development; however, actual sediment discharge measurements are not made. From visual inspection there is very little sediment runoff during the initial stages of simulations; although, as channels begin to develop, sediment flux increases and when the drainage networks begin to stabilize the sediment flux again becomes very low. The 9° slopes have a higher overall sediment discharge than the 5° slopes although there is

very little visual evidence of differences in terms of the inter-channel areas indicating that the higher sediment production comes largely from channelization.

The influence of channel slope on erosion potential is a highly debated topic in the literature (Nearing et al. 1997). The debate is largely based on the dependence of flow velocity on slope as velocity is often related to sediment transport capacity. Various researchers have shown that for a non-erodable bed channel velocities increased with increasing slopes (Foster et al. 1984, Rauws 1988, Abrahams et al. 1996). However Govers (1992) showed that for an erodable bed, rill velocity was not influenced by bed slope.

In a system such as the one presented in this experiment where erosion channel development is the dominant source of sediment from the hillslope, the data presented here supports the conclusion that hillslope-scale does play a significant role in the total sediment produced from an actively eroding hillslope. The transport capacity at initially larger slopes, 9°, must be greater than that at 5° as to continue the process of incisions observed visually and implied by the increased depth observed in the channels at 9° slopes (Figure 4.6). Overall it should be expected that hillslope-scale as well as local slope play a significant role in drainage network evolution under optimality principles. Optimality in energy expenditure requires that the overall energy expenditure within a drainage network approach a minimum and that the distribution of energy expenditure per unit flow area approach a constant during evolution. The drainage network that develops within a given drainage area subject to the same energy input should have the same area-slope relationship (Rodríguez -Iturbe and Rinaldo 1997, Knighton 1998) thus for $S \propto A^{z}$ to remain constant from the 5° slope to the 9° slope there would indeed require

more incision, meaning flattening of channel-scale slope, on the steeper slope. However as z approaches optimality, the hillslope-scale slope would no longer play as significant a role in sediment production.

In the real world a hillslope is not subject to a storm of spatially homogenous intensity or duration and the relationship between slopes and erosion potential becomes more complex. Let us consider this relationship with respect to an effective storm similar in conceptual development as effective discharge in a river. An effective storm is defined herein as a rainfall of constant intensity, duration and spatial heterogeneity such that the hillslope erosion channel network present is neither erosional nor depositional. For a storm less than the effective storm there will be little opportunity for erosion channel network adjustment, as there will be little sediment production; however, any adjustment would be depositional. For a storm greater than effective the channel network will be in active development adjusting to the new intensity, duration and spatial heterogeneity at a rate determined partially by the slope of the channel network in adjustment and the distribution of energy within the system. For systems in which channel development is the dominant contribution of sediment yield from the hillslope, slope may only play a significant role when the rainfall present is greater than the effective storm.

Corresponding arguments with downstream hydraulic relationships describing flow depth and width are more difficult with the data collected during this experiment as cross-section shapes are quite variable and flow depths are very small compared to the erosion channel depth. The depth and width of the erosion channels themselves may not be a good representation of the depth and width of the flow.

How drainage networks develop through time has essentially been studied qualitatively through descriptions such as Hortonian or Glockian for lack of quantitative measures (Glock 1931, Schumm et al. 1987). There have been many quantitative measures of river network characteristics as discussed in the introduction; however, these have generally been applied to equilibrium systems, not those under active development. Here quantitative tools developed for river systems are applied to describe the growth of hillslope erosion channel networks.

Horton's stream length and bifurcation ratios for the erosion channel networks have been shown to have averages similar to those for river systems. Thus, using the definition of fractal dimension from La Barbera and Rosso (1987) as

$$D_f = \max(\log R_B/\log R_L, 1) \qquad 4.9$$

the erosion channel networks retain the fractal properties of similar larger-scale counterparts. It should be noted that the derivation of the above requires that R_B and R_L hold at all scales of the network, which is not tested here. The fractal dimension, D_f, is a measure of the drainage networks space filling properties. In a 2-dimensional space, where D_f is calculated using functional box counting (Lovejoy et al. 1987) a value of $D_f =$ 2 implies that the drainage network is completely space filling and as $D_f \rightarrow 0$ there are progressively more areas not part of the drainage network. A value of $D_f = 0$ is a single point and $D_f = 1$ is a single line of no width in 2D space.

At any given point in time D_f, calculated using the functional box-counting method, represents how much space comprises the erosion channel network. That hillslope drainage (rill) networks become more space filling with time, as has been described qualitatively throughout the literature (*e.g.*, Schumm et al. 1987), has been shown

quantitatively here (Figure 4.8). From equations 4.4 and 4.8 a statistically significant $\beta_1 > 0$ implies that the drainage network is indeed becoming more space filling with time. Also statistically significant, $\beta_2 > 0$, is an indication that the erosion channel networks become more space filling quicker on steeper hillslope-scale slopes when subject to the same rainfall intensity for the same time. This is another indication that hillslope scale slope plays a significant factor in erosion potential during storms when the channel network is in active adjustment. From Figure 4.8 there does not appear to be any consistent trend distinguishable in the function $D_f(t)$, although for the first simulation at 5° slope (5° 1) there does appear to be an exponential function relating D_f and time although this relationship is not as clear in the other simulations.

For large river networks Tarboton et al. (1988) noted that there are two asymptotic trends on a log-log plot of $N(r)$ vs. r distinguished by the magnitude of r. For small-scale boxes relative to the scale of the map $D_f \rightarrow 1$ and at large scale boxes $D_f \rightarrow 2$. At very small box sizes, channels have dimension close to that of a line and $D_f \rightarrow 1$, which is generally where the experimental results in this research lie. Nor would the data fall into the transition area, as the fit of the line on the log-log chart is very capable of modeling the data. Measurements taken over a very small range of box sizes (one order of magnitude), as in this study, could play a significant role in fractal dimension D_f observed. However, the scale of the boxes used relative to the picture size is in the appropriate range to observe $D_f = 2$ if the network were space filling. Also, the ANOVA is an inappropriate model to make assertions of end state solutions as it is linear in nature and D_f must be less than or equal to 2. However, in the region of D_f values observed

herein, the linear model is able to account for more than 50% of the variability in the data.

Schumm et al. (1987) suggested that in a system with a fixed base level, networks progress through time from a very chaotic dendritic structure to a more organized network with fewer segments. While it is difficult to say exactly what is meant by chaotic, here it is interpreted as meaning that there is little structure associated with the drainage network. One description of network evolution is through a process of "slow headward growth with full elaboration of the entire texture by streams of all orders" (Rodríguez -Iturbe and Rinaldo 1997), a general view based on combinations of theories developed by Ruhe (1952), Glock (1931) and Morisawa (1964). Here I describe network development through the characteristics of a Fourier series fit to width functions. The power contained within the lowest frequency significantly grows with time. The powers in the higher frequencies do not significantly change with time; however, they are important in describing the width functions. These relative frequencies have been associated respectively with the shape of the region on which the network develops, and the bifurcation structure of the network itself (Rodríguez -Iturbe and Rinaldo 1997). These results indicate that if a "chaotic" network is one lacking inherent order, then these networks are not ever chaotic as the bifurcation structure does not significantly vary throughout evolution. Since the shape of the drainage area does not change with time the increase in power associated with the low frequency can only be associated with filling the area more fully.

Initial conditions, determined by base level position, played a large role throughout network formation during Schumm's landscape simulator experiments (Schumm 1977,

Schumm and Kahn 1971, Schumm et al. 1972). In this research, the influence of initial conditions, excluding hillslope scale slope, could not be determined to persist throughout network development although initial conditions do play an important role in early network formation. Figure 4.9 shows the drainage density, in pixel units, after one hour of rainfall at 65 [mm/hr]. The drainage density is highly dependent on the number of days that the hillslope was allowed to dry between experimental runs. This corresponds with the moisture contained within the soil at the beginning of the experiment (Figure 4.4). For drier soils more water is infiltrated during the first hour of simulation than for the wetter soils and thus network evolution is delayed. Once network evolution begins, the rate of growth between time = 0 and time = 1 hour is dominated by the initial soil moisture condition. Between hours 1 and 2 the space filling properties of the network, defined by D_f, becomes dominated by the hillslope scale slope. Therefore, even for a storm of intensity greater than effective, the duration must be greater than the time necessary to begin network evolution as defined by the initial soil moisture characteristics.

4.5. Conclusions

It has been shown that developing erosion rill networks on a slope void of vegetation and subject to constant rainfall exhibit time-varying fractal characteristics that describe the space filling properties of the networks and are a function of hillslope-scale slope. The networks have been shown to become progressively more space filling with time described through D_f as a function of slope. Steeper slope has also been shown to encourage space filling of the erosion channel network. Through an analysis of the width functions of actively developing erosion channel networks, the network appears to fill the

drainage area more completely with time while retaining its bifurcation characteristics. An inherent order is therefore contained within the erosion channel network throughout development.

Steeper hillslope-scale slope has higher overall sediment yield determined by networks that fill space more completely. It is shown that slope plays a significant role in individual erosion channel geometry, 9° slopes leading to wider and deeper erosion channels but having a smaller width to depth ratio than 5° slopes. The results that channels on a 9° slope incise more than on a 5° slope is consistent with optimality theories based on energy expenditure distribution within a channel network. A theory has also been proposed stating that, in hillslope systems where erosion channel development plays a significant role in sediment production, hillslope-scale slope alone may not be a good predictor of erosion potential without considering the effectiveness of the storm, specifically its duration, intensity and spatial heterogeneity.

Further research is warranted to find the rates of growth of hillslope channel networks under different rainfall environments and soil properties including the presence of vegetation. The purpose of which is to include the geometry characteristics of hillslope erosion channel networks into erosion prediction models, which would benefit greatly from this addition.

4.6. References

Abrahams AD, Li G, Parsons AJ. 1996. Rill hydraulics on a semi-arid hillslope, southern Arizona, *Earth Surf. Processes Landforms* **21**: 35-47.

Andrews ED. 1980. Effective and bank full discharges of streams in the Yampa River Basin, Colorado and Wyoming. *J. of Hydrology* **46**: 311-330.

Dietrich WE, Wilson CJ, Reneau SL. 1986. Hollows, colluvium and landslides in soil-mantled landscapes. In Abrahams AD (ed.). Hillslope processes. Boston: Allen & Unwin, 362-388.

Foster GR, Huggins LF, Meyer LD. 1984. A laboratory study of rill hydraulics, I, Velocity relationships, *Trans. ASAE* **27**: 790-796.

Glock WS. 1931. The development of drainage systems. *Geographical Review* **21**: 475-482.

Govers G. Relationship between discharge, velocity, and flow area for rills eroding loose, non-layered materials, *Earth Surf. Processes Landforms* **17**: 515-528.

Hentschel HE, Procaccia I. 1983. The infinite number of dimension of fractals and strange attractors. *Physica D* **8**: 435-444.

Horton RE. 1945. Erosional development of streams and their drainage basins: hydrophysical approach to quantitative morphology. *Bulletin of the Geological Society of America* **56**: 275-370.

Kirchner JW. 1993. Statistical inevitability of Horton's laws and the apparent randomness of stream channel networks. *Geology* **21**: 591-594.

Knighton D. 1998. Fluvial forms and processes: a new perspective, Arnold, London.

La Barbera P, Rosso R. The fractal geometry of river networks. *Eos Trans.* AGU **68(44)**: 1276.

Leopold LB, Maddock T. 1953. The hydraulic geometry of stream channels and some physiographic implications. *U.S. Geol. Survey Prof. Paper* 252, 57 p.

Lovejoy S, Schertzer D, Tsonis AA. 1987. Functional box counting and multiple elliptical dimensions in rain. *Science* **235**: 1036-1038.

Molnar P, Ramírez JA. 1998a. Energy dissipation theories and optimal channel characteristics of river networks. *Water Resources Research* **34**(7): 189-1818.

Molnar P, Ramírez JA. 1998b. An analysis of energy expenditure in Goodwin Creek. *Water Resources Research* **34**(7): 1819-1829.

Montgomery DR, Dietrich WE. 1988. Where do channels begin? *Nature* 336: 232-234.

Morisawa ME. 1964. Development of drainage systems on an upraised lake floor. *Am. J. Sci.* **262**: 340-354.

Nearing MA, Norton LD, Bulgakov DA, Larionov GA, West LT, Dontsova KM. 1997. Hydraulics and erosion in eroding rills. *Water Resources Research* **33**: 865-876.

Ogunlela A, Wilson BN, Rice CT, Couger G. 1989. Rill network development and analysis under simulated rainfall. *Am. Soc. Agric. Eng.* Paper no. 89-2112.

Ouchi S. 2001. Development of miniature erosion landforms in a small rainfall erosion facility in *Applying Geomorphology to Environmental Management*. Water Resources Publications, LLC. Highlands Ranch, CO 79 – 92.

Rauws G. 1988. Laboratory experiments on resistance to overland flow due to composite roughness, *J. Hydrol.* **103**: 37-52.

Rodríguez-Iturbe I, Rinaldo A. 1997. *Fractal River Basins*. Cambridge University Press, New York, NY.

Ruhe RV. 1952. Topographic discontinuities of the Des Moines lobe, *Am. J. Sci.* **250**: 46-50.

Schumm SA. 1977. The Fluvial System, J. Wiley, New York.

Schumm SA, Khan HR. 1971. Experimental study of channel patterns. *Nature* **233**: 407-411.

Schumm SA, Khan HR, Winkley BR, Robbins LG. 1972. Variability of river patterns. *Nature* **237**: 75-76.

Schumm SA, Mosley MP, Weaver WE. 1987. *Experimental Fluvial Geomorphology*. John Wiley & Sons, Inc., New York, NY.

Shreve RL. 1969. Stream lengths and basin areas in topologically random channel networks. *J. Geol.*, **77**: 397-414.

Strahler AN. 1957. Quantitative analysis of watershed geomorphology. *Trans. of the Am. Geophysical Union* **38**: 913-920.

Tarboton DG, Bras RL, Rodríguez -Iturbe I. 1988. The fractal nature of river networks. *Water Resour. Res.* **24**: 1317-1322.

Wilson BN. 1991. Topologic representation of rill networks. ASAE Paper 912005, Presented at the 1991 ASAE Summer Meeting, Albuquerque, New Mexico.

Wilson BN, Storm D. 1993. Fractal analysis of surface drainage networks for small upland areas. *Transactions of the ASAE* **36**(5): 1319-1326.

Table 4.1: Channel Geometric Characteristics by Slope

		Average	Coefficient of Variation	p-value H_o: $\mu_9 = \mu_5$	df
Widths	*9° slope*	159.65	0.65	<< 0.05	128
	5° slope	98.90	0.46		
Depths	*9° slope*	34.73	0.37	<< 0.05	128
	5° slope	14.68	0.52		
Width / Depth	*9° slope*	4.05	2.25	<< 0.05	128
	5° slope	9.27	3.95		

Table 4.2: Time Significance in signal power contained within Fourier components, fit to width functions

From ANOVA model and equation **4.6**.

		Dependent Variable			
		A_0	n_1	n_2	n_3
hour	coefficient	0.071	0.008	N/A	N/A
	significance (p-value)	0.000	0.021	> 0.05	> 0.05

Figure 4.1: 3 X 10 [m^2] artificial hillslope

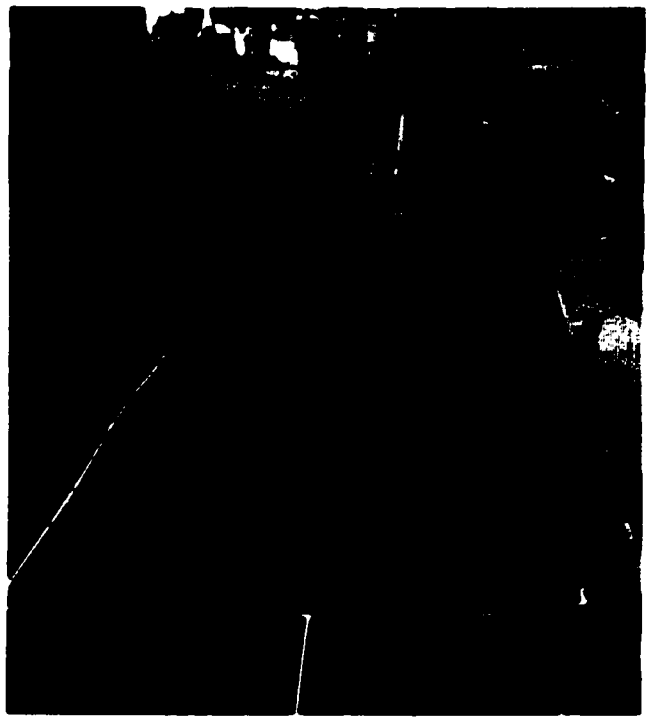

Figure 4.2: Sample rainfall distribution [mm/hr]

Axes are lengths with units [m].

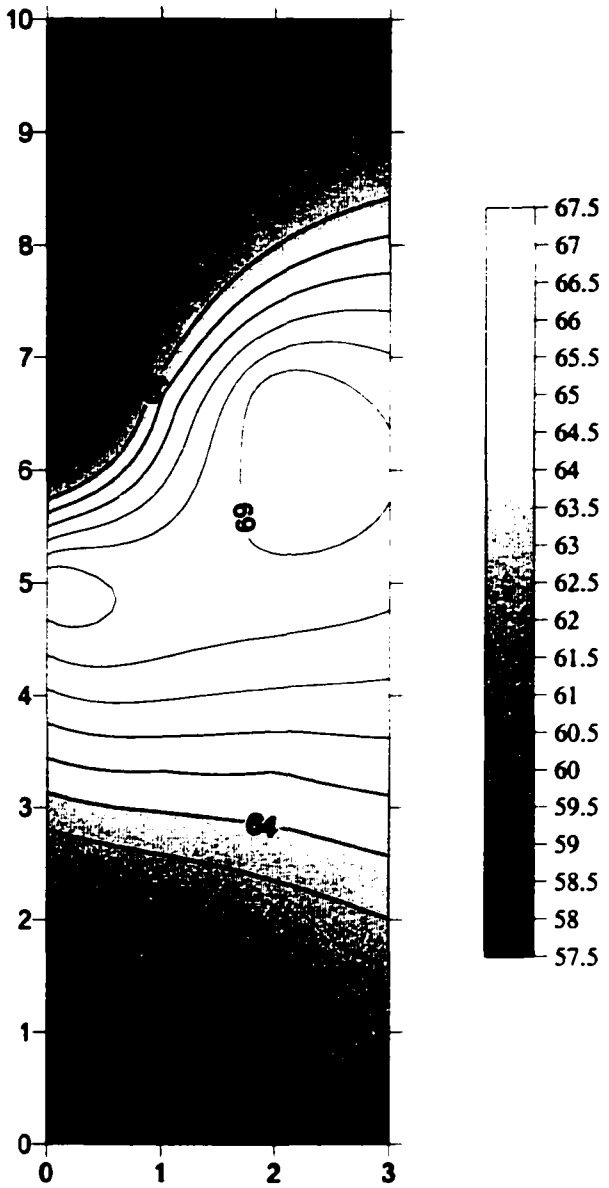

Figure 4.3: Grain Size Distribution

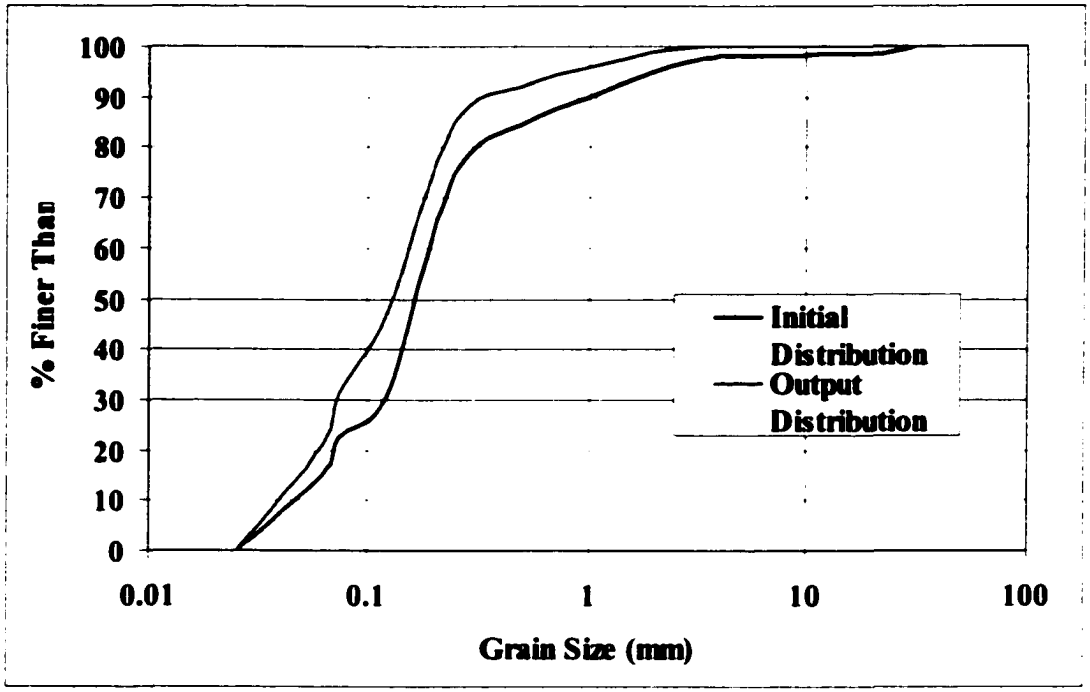

Figure 4.4: Percent soil moisture with time, sampled randomly from top 15 cm of hillslope.

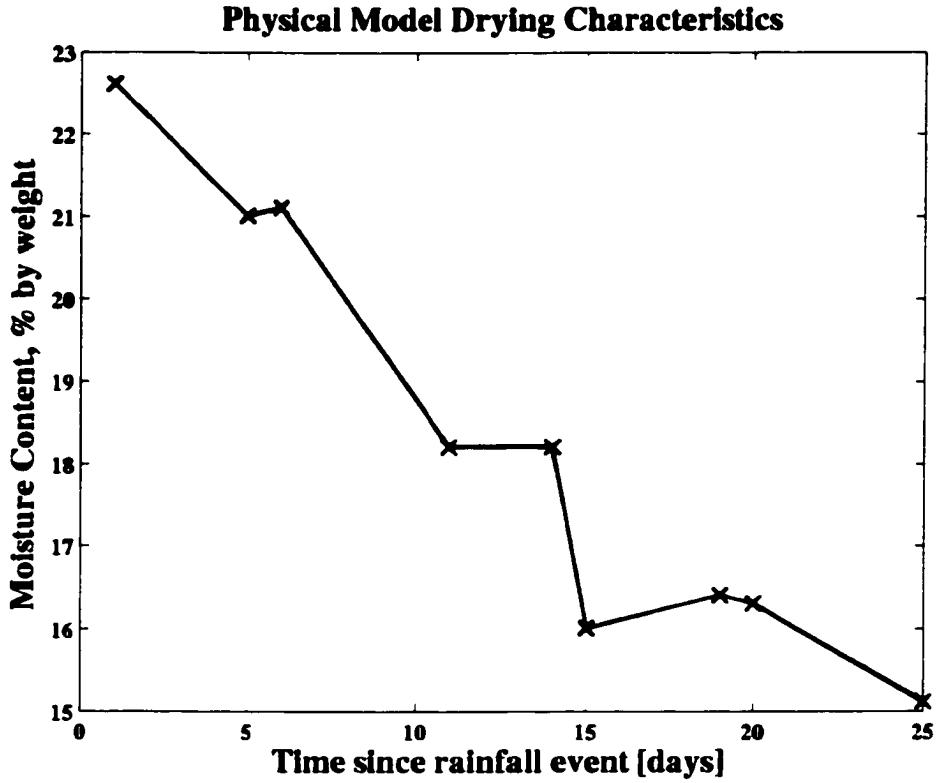

Figure 4.5: Average erosion channel widths by slope

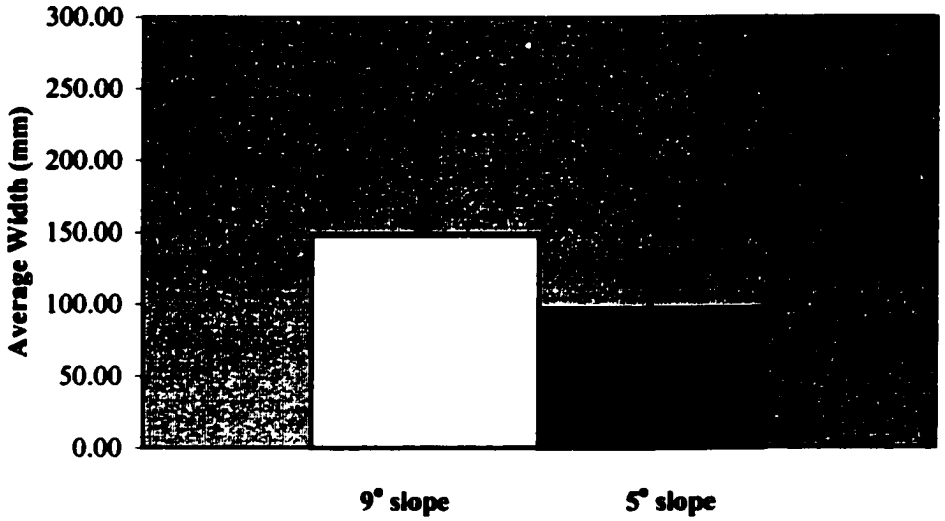

Figure 4.6: Average erosion channel depths by slope

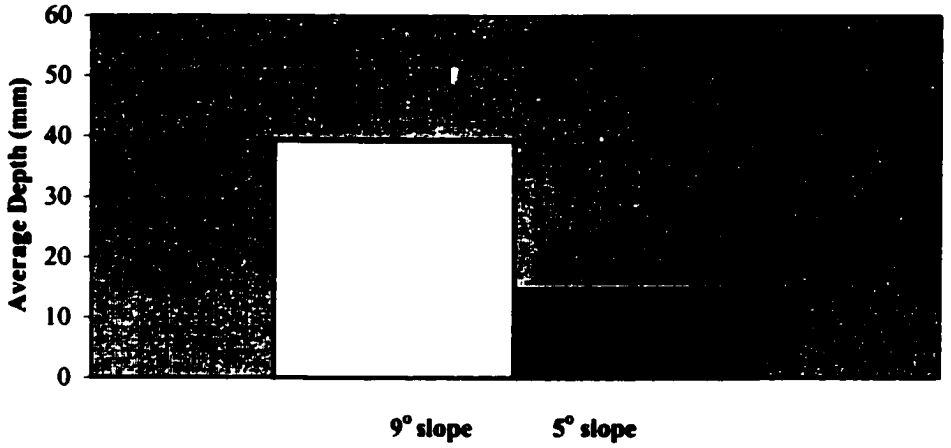

Figure 4.7: Average width / depth for erosion channels by slope

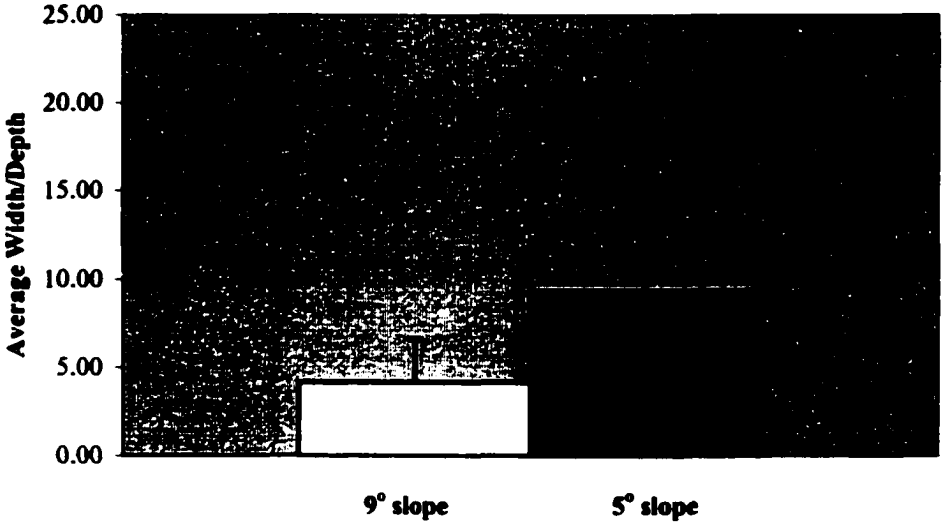

Figure 4.8: Fractal Dimension Growth with Time

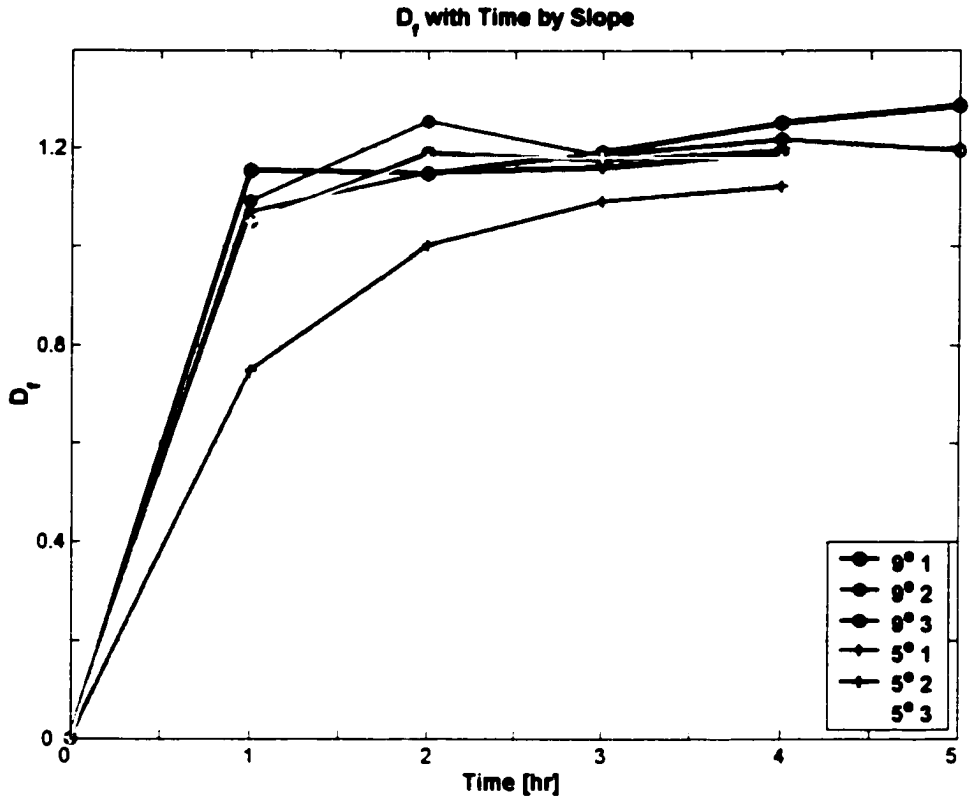

Figure 4.9: Influence of antecedent moisture on initial drainage density measurements

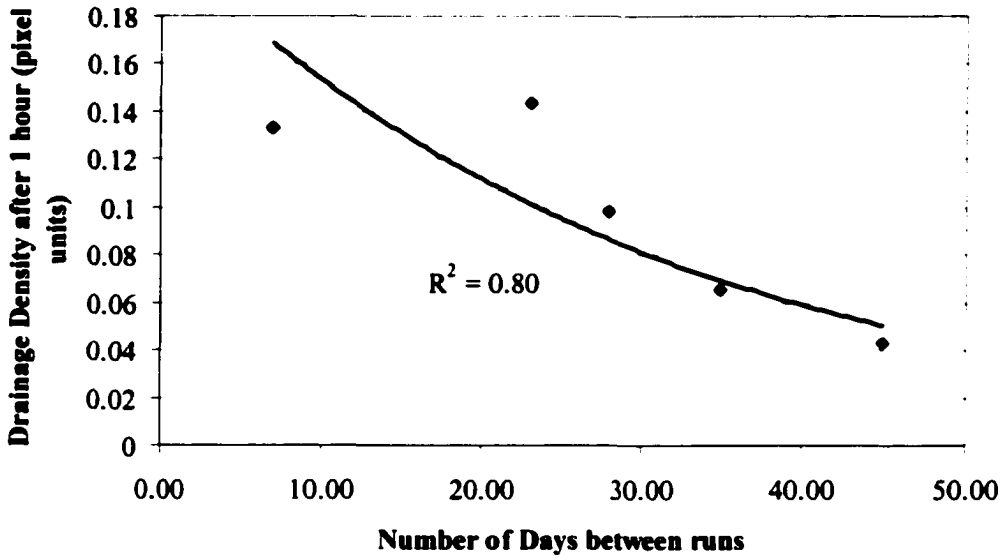

Chapter 5: Mathematical Development of a Hillslope Hydrology Model (HYDROR)

Abstract

This chapter presents the mathematical and numerical development of a distributed, physical, mechanistically based hillslope hydrology model named "HYDROR". The model couples the fully two-dimensional hydrodynamic equations for overland flow, Richards equation for infiltration, and a sediment detachment and transport model. Models based on the fundamental physics of what we believe to be the governing equations of hillslope hydrology are necessary to test our ability to fully explain the fine scale processes and mechanisms that actually occur in nature. The presented model is capable of capturing the interaction between overland flow, erosion and infiltration at very small scales. The model is also capable of modeling the evolution of hillslope caused by spatially variable erosion driven through hillslope physical variability at very fine scales.

5.1. Introduction

Hydrologists are constantly faced with problems involving predictions of rainfall-runoff response and sediment supply. These problems occur at scales from 10 [m^2] up to 10^6 [m^2]. Predictions are usually made using lumped hydrologic models, which traditionally make kinematic wave assumptions. As scientific knowledge of the micro-scale variations in soil properties, micro-topography, flow-depths and velocities increases, modelers have begun to use more complex models to describe these processes

and interactions. Fiedler and Ramírez (2000) developed a new 2-D, fully hydrodynamic, mathematical model for simulating the small scale processes associated with overland flow on an infiltrating surface capable of capturing the small-scale variations in flow-depth and velocities and of simulating interactive infiltration. Briefly, the model of Fiedler and Ramírez uses the full hydrodynamic equations (the St. Venant equations in two dimensions) with spatially variable infiltration characteristics and explicit representation of micro topographic features. The hydrodynamic equations are solved with a modified version of the explicit, second-order accurate MacCormack finite difference scheme, with special provisions for small flow depths and a discontinuous flow regime. Vertical infiltration capacity is modeled with the well-known Green-Ampt (Green and Ampt, 1911) equation, which is solved using standard methods (Newton-Raphson technique).

This paper presents the mathematical foundation for a new model for hillslope hydrological processes (HYDROR) that is largely based on the mathematical model and numerical scheme presented by Fiedler and Ramírez (2000) for two-dimensional overland flow using the full hydrodynamic equations. The new model couples Richards equation for one-dimensional infiltration to the overland flow equations. As opposed to the Green-Ampt model, Richards equation is applicable to a wide variety of situations and is easily applied to multi-storm scenarios. The new model also includes a sediment detachment and transport component, which allows examination of the interactions between overland flow, infiltration and sediment detachment and transport. Model numerical results are compared to analytical solutions when possible and a comparison is made between a numerical and a physical experiment. Results for two very different

initial soil conditions are also presented for an artificial hillslope to show the dependence of spatially variable erosion with soil conditions. Chapter 6 presents an examination of hillslope evolution using HYDROR.

5.2. Mathematical Formulation

5.2.1. Overland Flow

The overland flow component of the model is a 2-D, fully hydrodynamic, mathematical description of the small-scale processes associated with overland flow on an infiltrating surface and is based on the model of Fiedler and Ramírez (2000). This model allows for explicit representation of micro-topographic features and spatially variable infiltration characteristics.

5.2.1.1. Governing Equations

The hydrodynamic equations for overland flow in two dimensions are:

$$\frac{\partial h}{\partial t}+\frac{\partial(uh)}{\partial x}+\frac{\partial(vh)}{\partial y}-q_l=0 \tag{5.1}$$

$$\underbrace{\frac{\partial(uh)}{\partial t}+\frac{\partial\left(u^2h\right)}{\partial x}+\frac{\partial(uvh)}{\partial y}+g\overbrace{\frac{\partial\left(\frac{h^2}{2}\right)}{\partial x}}^{\text{diffusive wave}}-\overbrace{gh\left(S_{ox}-S_{fx}\right)}^{\text{kinematic wave}}}_{\text{dynamic wave}}-\overbrace{u\,q_l}^{\text{lateral}}=0 \tag{5.2}$$

$$\frac{\partial(vh)}{\partial t}+\frac{\partial\left(v^2h\right)}{\partial y}+\frac{\partial(uvh)}{\partial x}+g\frac{\partial\left(\frac{h^2}{2}\right)}{\partial y}-gh\left(S_{oy}-S_{fy}\right)-\overbrace{v\,q_l}^{\text{lateral}}=0 \tag{5.3}$$

where h [L] is flow depth, u and v are velocities [L/T] in the x and y directions respectively, S_o is bed slope [L/L] and S_f is friction slope [L/L], and q_l is lateral flux

[L^2/T] through the control boundary and is equal to the difference between precipitation and infiltration as described below, except that surface water is also allowed to infiltrate at any time it is available and the capacity exists, thus simulating fully interactive infiltration. It has been shown that the kinematic wave approximation is only appropriate in very small regions of hydraulic roughness and Froude numbers and that the diffusive and quasi-steady dynamic wave approximations are not appropriate for supercritical overland flow (Richardson and Julien, 1994). It is therefore desirable to have the full dynamic wave implementation of the momentum equations for an accurate representation of spatially variable overland flow. The bed slopes, S_{ox} and S_{oy} are computed directly from ground surface elevations values, z, as

$$S_{ox} = -\frac{\partial z}{\partial x} \text{ and } S_{oy} = -\frac{\partial z}{\partial y} \qquad \textbf{5.4}$$

respectively. The Darcy-Weisbach (D-W) formula is used to compute the friction slopes, S_{fx} and S_{fy} as

$$S_{fx} = \frac{f}{8g}\frac{p\sqrt{(p^2+q^2)}}{h^3} \text{ and } S_{fy} = \frac{f}{8g}\frac{q\sqrt{(p^2+q^2)}}{h^3} \qquad \textbf{5.5}$$

respectively, where p and q are flux [L^2/T] in the x and y directions respectively. The value f is the D-W friction factor and, assuming that the overland flow regime is laminar (Emmett 1970), it is calculated as

$$f = \frac{K_0}{R_e} \qquad \textbf{5.6}$$

a function of the Reynolds number

$$R_e = \frac{\sqrt{(p^2+q^2)}}{\nu} \qquad \textbf{5.7}$$

and K_0 a constant related to the characteristics of the ground surface (Woolhiser 1975), and ν is the kinematic viscosity of water. The kinematic viscosity is a function of the sediment concentration as:

$$\nu_m = \frac{\mu_m}{\rho_m} \tag{5.8}$$

where μ_m is the dynamic viscosity of the sediment water mixture determined from an empirical equation (Julien 1994)

$$\mu_m = \mu(1 + 2.5C_v) \tag{5.9}$$

and C_v is the sediment concentration by volume.

Equations 5.1 – 5.3 can be recast vectorially as follows

$$\frac{\partial \mathbf{U}}{\partial t} + \frac{\partial \mathbf{G(U)}}{\partial x} + \frac{\partial \mathbf{H(U)}}{\partial y} = \mathbf{S(U)} \tag{5.10}$$

where

$$\mathbf{U} = [h, p, q]^T \tag{5.11}$$

$$\mathbf{G(U)} = \left[p, \frac{p^2}{h} + \frac{gh^2}{2}, \frac{pq}{h} \right]^T \tag{5.12}$$

$$\mathbf{H(U)} = \left[q, \frac{q^2}{h} + \frac{gh^2}{2}, \frac{qp}{h} \right]^T \tag{5.13}$$

$$\mathbf{S(U)} = \left[q_l, -gh\frac{\partial z}{\partial x} - \frac{K_0 \nu p}{8h^2} + \varepsilon_l \left(\frac{\partial^2 p}{\partial x^2} + \frac{\partial^2 p}{\partial y^2} \right), -gh\frac{\partial z}{\partial y} - \frac{K_0 \nu q}{8h^2} + \varepsilon_l \left(\frac{\partial^2 q}{\partial x^2} + \frac{\partial^2 q}{\partial y^2} \right) \right]^T \tag{5.14}$$

and

$$p = uh \text{ and } q = vh \tag{5.15}$$

are the flux terms [L^2/T].

In equations **5.10** – **5.14** ***G(U)*** and ***H(U)*** are flux vectors and ***S(U)*** is the source vector. For notational convenience hereafter these vectors will be referred to as ***G***, ***H***, and ***S*** while the dependence on ***U*** is implied. The terms in equation **5.14** preceded by ε_l are viscous terms related to turbulent momentum and ε_l is a coefficient related to turbulent viscosity or eddies (Playan 1992).

5.2.1.2. Numerical Methods

Based on the work of Fiedler (1997) and Fiedler and Ramírez (2000), and for reasons of stability and accuracy, a variation of MacCormack's predictor-corrector finite difference method is used to solve the above equations. The modified MacCormack scheme implemented is a method of fractional steps (Leveque 1990). The scheme is based on splitting the two-dimensional partially hyperbolic equations (**5.1** – **5.3**) into a series of one-dimensional finite difference operators, which are explicitly solved at fractional time steps in one-dimension and then the other. The MacCormack scheme relies on a series of predictor and corrector steps. The MacCormack scheme with fractional steps is written,

$$U_{j,k}^{n+1} = L_x 2\left(\frac{\Delta t}{2}\right) L_y 2\left(\frac{\Delta t}{2}\right) L_y 1\left(\frac{\Delta t}{2}\right) L_x 1\left(\frac{\Delta t}{2}\right) U_{j,k}^{n} \qquad \textbf{5.16}$$

where L_x and L_y are one-dimensional difference operators. Each of these operators must be applied twice in a symmetrical manner. The form of the difference operators written for $Lx1$ (the others are similar) is

$$U_{j,k}^{*} = U_{j,k}^{n} - \frac{\Delta t}{2\Delta x}\left(G_{j,k}^{n} - G_{j-1,k}^{n}\right) + \frac{\Delta t}{2} S_{ox;j,k}^{n} \qquad \textbf{5.17}$$

$$U^{**}_{j,k} = 0.5\left[U^{n}_{j,k} - U^{*}_{j,k} - \frac{\Delta t}{2\Delta x}\left(G^{*}_{j+1,k} - G^{*}_{j,k}\right) + \frac{\Delta t}{2} S^{*}_{ax;j,k}\right] \qquad \textbf{5.18}$$

This method is second order accurate in time and space when predictor and corrector steps are symmetrically applied in the following manner:

L_x1: predictor, backward difference
corrector, forward difference
L_x2: predictor, backward difference
corrector, forward difference
L_y1: predictor, forward difference
corrector, backward difference
L_y2: predictor, forward difference
corrector, backward difference.

Depth appears often in the denominator throughout the finite difference scheme and therefore must be limited in its minimum value. These differential equations are also "stiff" due to the variability in the friction term with time and depth. This is handled by treating the friction term explicitly by a Taylor series expansion about the n^{th} time level at every point in the domain. In the x direction this is written as,

$$S^{n+1}_{fx} = S^{n}_{fx} + \left(\frac{\partial S_{fx}}{\partial p}\right)^{n} \Delta p + O\left(\Delta p^2\right) \qquad \textbf{5.19}$$

where $\Delta p = p^{n+1} - p^{n}$ and can be written similarly for the y direction. Combining equation **5.19** with the predictor L_x1 (equation **5.17**) through the factor

$$D_x = \frac{1}{1 - \Delta t \dfrac{\partial S_{fx}}{\partial p}} \qquad \textbf{5.20}$$

results in

$$U^{*}_{j,k} = U^{n}_{j,k} - D\frac{\Delta t}{2\Delta x}\left(G^{n}_{j,k} - G^{n}_{j-1,k}\right) + D\frac{\Delta t}{2}S^{n}_{x,j,k} \qquad \textbf{5.21}$$

where D = 1 when computing h and q, and is equal to D_x when computing p. This approach is similar for L_x2, L_y1, and L_y2. This method allows minimum flow depths on the order of 10^{-10} [m] or smaller to be used, depending on the computational environment, and time-step restrictions imposed by friction-slope stiffness are removed. The model also assigns minimum values of flux in the x and y directions on the order of 10^{-11} [m^2/s].

Hyperbolic equations are prone to oscillations and the overland flow equations are no exception (*e.g.*, Fiedler and Ramírez 2000). Oscillation control is therefore necessary and is accomplished by implementing a method developed by Jameson et al. (1981) and used by Fennema and Chaudhry (1986). The method computes a smoothing parameter, shown below for the x direction using the corrected values of flow depth, assumed below to be positive

$$\xi_{j,k} = \frac{\Delta x}{\Delta t}\frac{\left|h^{**}_{j+1,k} - 2h^{**}_{j,k} - h^{**}_{j-1,k}\right|}{h^{**}_{j+1,k} + 2h^{**}_{j,k} + h^{**}_{j-1,k}} \qquad \textbf{5.22}$$

$$\xi_{j+\frac{1}{2},k} = \varepsilon_2 \max\left(\xi_{j+1,k}, \xi_{j,k}\right) \qquad \textbf{5.23}$$

where ε_2 is a coefficient used to control the amount of smoothing; Fennema and Chaudhry (1986) reported typical values in the range of 0.5 to 3, however for simulations performed within the scope of this research values of $5(10^{-3})$ to $5(10^{-4})$ are most effective. Numerical tests have shown that ε values can take on a much wider range of values depending on Δx and Δt, as ξ is a function of both. The numerical approach implemented here incorporates an additional smoothing parameter ε_3 for the y direction allowing different discretization in the x and y directions.

5.2.2. Infiltration

5.2.2.1. Governing Equations

The governing equation for one-dimensional flow of water in soil can be written in the form

$$\frac{\partial}{\partial z_g}\left(K(\psi)\frac{\partial \psi}{\partial z_g}\right)+\frac{\partial K(\psi)}{\partial z_g}=\frac{\partial \theta(\psi)}{\partial t} \qquad \textbf{5.24}$$

a second order cubic partial differential equation commonly referred to as the Richards equation, where ψ is the soil water pressure head, $\theta(\psi)$ is the soil volumetric water content, $K(\psi)$ is the hydraulic conductivity and z_g denotes a length scale directed parallel with the gravity vector. Richards equation is derived by combining conservation of mass written as

$$\frac{\partial}{\partial z_g}\left(q_{z_g}\right)=-\frac{\partial \theta}{\partial t} \qquad \textbf{5.25}$$

where q_{zg} is a volumetric flux of water, with Darcy's law

$$q_{z_g}=-K(\psi)\frac{\partial h_T}{\partial z_g} \qquad \textbf{5.26}$$

where h_T is total head = $\psi + z_g$. Combining equations **5.25** and **5.26** results in

$$\frac{\partial}{\partial z_g}\left(K(\psi)\frac{\partial}{\partial z_g}\left(\psi+z_g\right)\right)=\frac{\partial \theta}{\partial t}. \qquad \textbf{5.27}$$

Simplifying equation **5.27** results in

$$\frac{\partial}{\partial z_g}\left(K(\psi)\frac{\partial \psi}{\partial z_g}+K(\psi)\right)=\frac{\partial \theta}{\partial t} \qquad \textbf{5.28}$$

which can also be written in the form of equation **5.24**. Equation **5.24** is referred to as the mixed form of Richards equation because it contains gradients of θ and ψ. Two other common forms of Richards equation are the head-based and the theta-based forms, where all the gradients are of ψ and θ, respectively.

Table 5.1: Forms of Richards Equation

Head based	$\frac{\partial}{\partial z_g}\left(D(\theta)\frac{\partial\theta}{\partial z_g}\right)+\frac{\partial K(\theta)}{\partial z_g}=\frac{\partial\theta}{\partial t}$
Theta based	$\frac{\partial}{\partial z_g}\left(K(\psi)\frac{\partial\psi}{\partial z_g}\right)+\frac{\partial K(\psi)}{\partial z_g}=C(\psi)\frac{\partial\psi}{\partial t}$
Mixed form	$\frac{\partial}{\partial z_g}\left(K(\psi)\frac{\partial\psi}{\partial z_g}\right)+\frac{\partial K(\psi)}{\partial z_g}=\frac{\partial\theta(\psi)}{\partial t}$

where $D(\theta)$ is the unsaturated diffusivity, $D(\theta) = \left(\frac{\partial\theta}{\partial\psi}\right)$, and $C(\psi)$ is the specific moisture capacity, $C(\psi) = \left(\frac{\partial\theta}{\partial\psi}\right)$. While each of these forms has been used extensively throughout the literature (*e.g.*, Celia et al. 1990, Paniconi et al. 1991, Rathfelder and Abriola 1994) the mixed form has been chosen for implementation here because its numerical implementation has been shown to be perfectly mass conservative (Celia et al. 1990). As seen above, knowledge of soil water properties, specifically hydraulic conductivity and volumetric water content, as a function of head, ψ, is required. The van Genuchten equations are the most commonly used to relate hydraulic conductivity and volumetric water content to pressure head. The van Genuchten equations for $\theta(\psi)$ and $K(\psi)$can be written as

$$\theta(\psi) = \theta_r + \frac{(\theta_s - \theta_r)}{(1+\beta)^m} \qquad \psi \le 0 \qquad \textbf{5.29}$$

$$\theta(\psi) = \theta_s \qquad \psi > 0$$

and

$$K_r(\psi) = \frac{\left[(1+\beta)^m - \beta^m\right]^2}{(1+\beta)^{\frac{5m}{2}}} \qquad \psi \le 0 \qquad \textbf{5.30}$$

$$K_r(\psi) = 1 \qquad \psi > 0$$

where $\beta = \left(\frac{\psi}{\psi_s}\right)^n$, n is a constant that can be viewed as the pore size distribution index, and m is a constant related to n by $m = 1 - 1/n$ or $mn = n - 1$ (van Genuchten and Nielsen 1985). Because of its complex non-linear nature, there is no known general analytical solution to the Richards equation for water flow in an unsaturated soil column. Therefore it is necessary to use numerical methods.

5.2.2.2. Numerical Methods

Numerical solutions to the mixed form of Richards equation can be shown to be perfectly mass conservative where as solutions based on the head or theta based forms generally yield poor results specifically due to large mass balance errors (Celia et al. 1990). Following the work of Celia et al., (1990), a fully implicit finite difference scheme coupled with a simple one-step Euler time-marching algorithm is used to solve Richards equation. The solution uses the Picard method for the iteration procedure of the linearized system of non-linear equations that result from discretizing Richards equation.

The following development follows that of Celia et al. (1990) and is presented here for completeness. The backward Euler approximation of equation **5.24** is

$$\frac{\theta^{n+1}-\theta^{n}}{\Delta t}-\frac{\partial}{\partial z_g}\left(K^{n+1,m}\frac{\partial \psi^{n+1,m+1}}{\partial z_g}\right)-\frac{\partial K^{n+1,m}}{\partial z_g}=0 \qquad \textbf{5.31}$$

where superscripts n and m denote time and iteration level, respectively. The mass balance accuracy of the numerical solution of the mixed form of Richards equation comes from the expansion of $\theta^{n+1,m+1}$ in a truncated Taylor series with respect to ψ, about the expansion point $\psi^{n+1,m}$

$$\theta^{n+1,m+1}=\theta^{n+1,m}+\left.\frac{d\theta}{d\psi}\right|^{n+1,m}\left(\psi^{n+1,m+1}-\psi^{n+1,m}\right)+O\left(\delta^{2}\right) \qquad \textbf{5.32}$$

Substituting equation **5.32** into equation **5.31** and an iteration increment $\delta^{m} = \psi^{n+1,m+1} - \psi^{n+1,m}$ results in

$$\left(\frac{1}{\Delta t}C^{n+1,m}\right)\delta^{m}-\frac{\partial}{\partial z_g}\left(K^{n+1,m}\frac{\partial \delta^{m}}{\partial z_g}\right)=\frac{\partial}{\partial z_g}\left(K^{n+1,m}\frac{\partial \psi^{n+1,m}}{\partial z_g}\right)+\frac{\partial K^{n+1,m}}{\Delta z_g}-\frac{\theta^{n+1,m}-\theta^{n}}{\Delta t} \qquad \textbf{5.33}$$

Equation **5.33** has been called the general mixed-form Picard approximation by Celia et al. (1987) and by Zarba (1988). Using finite differences results in the final discrete form of the approximation

$$\begin{aligned} &C_i^{n+1,m}\frac{\delta_i^{m}}{\Delta t}-\frac{1}{\left(\Delta z_g^{\,2}\right)}\left[K_{i+1/2}^{n+1,m}\left(\delta_{i+1}^{m}-\delta_i^{m}\right)-K_{i-1/2}^{n+1,m}\left(\delta_i^{m}-\delta_{i-1}^{m}\right)\right]= \\ &\frac{1}{\Delta z_g^{\,2}}\left[K_{i+1/2}^{n+1,m}\left(\psi_{i+1}^{n+1,m}-\psi_i^{n+1,m}\right)-K_{i-1/2}^{n+1,m}\left(\psi_i^{n+1,m}-\psi_{i-1}^{n+1,m}\right)\right]+\frac{K_{i+1/2}^{n+1,m}-K_{i-1/2}^{n+1,m}}{\Delta z_g}-\frac{\theta_i^{n+1,m}-\theta_i^{n}}{\Delta t}=\left(R_i^{n+1,m}\right) \end{aligned} \qquad \textbf{5.34}$$

where $R_i^{n+1,m}$ is a measure of the error associated with the current iteration level and approaches zero along with all values of δ^{m} as the solution converges. Equation **5.34** is appropriate for all interior nodes. Boundary conditions must be specified at $i = 0$ and N -

1 where N is the number of nodes. Boundary conditions can be one of two types, fixed head and flux type. With fixed head boundary conditions there are N - 2 equations with N - 2 unknown values of δ^m. The form of these N - 2 equations can be put into a matrix equation with a dominant tri-diagonal matrix

$$\begin{bmatrix} b_1 & c_1 & 0 & \dots & & & \\ a_2 & b_2 & c_2 & \dots & & & \\ & & & \dots & & & \\ & & & \dots & a_{N_n-1} & b_{N_n-1} & c_{N_n-1} \\ & & & \dots & 0 & a_{N_n} & b_{N_n} \end{bmatrix} \cdot \begin{bmatrix} u_1 \\ u_2 \\ \dots \\ u_{N_n-1} \\ u_{N_n} \end{bmatrix} = \begin{bmatrix} r_1 \\ r_2 \\ \dots \\ r_{N_n-1} \\ r_{N_n} \end{bmatrix} \qquad 5.35$$

where $N_n = N - 2$, and from expanding equation **5.34**

$$a_i = -\frac{1}{\Delta z_g^{\,2}} K_{i+1/2}^{n+1,m} \qquad 5.36$$

$$b_i = C_i^{n+1,m} \frac{1}{\Delta t} + K_{i-1/2}^{n+1,m} \frac{1}{\Delta z_g^{\,2}} + K_{i+1/2}^{n+1,m} \frac{1}{\Delta z_g^{\,2}} \qquad 5.37$$

$$c_i = -\frac{1}{\Delta z_g^{\,2}} K_{i-1/2}^{n+1,m} \qquad 5.38$$

$$u_i = \delta_i^m \qquad 5.39$$

$$r_i = \frac{1}{\Delta z_g^{\,2}} \left[K_{i+1/2}^{n+1,m} \left(\psi_{i+1}^{n+1,m} - \psi_i^{n+1,m} \right) - K_{i-1/2}^{n+1,m} \left(\psi_i^{n+1,m} - \psi_{i-1}^{n+1,m} \right) \right] + \frac{K_{i+1/2}^{n+1,m} - K_{i-1/2}^{n+1,m}}{\Delta z_g} - \frac{\theta_i^{n+1,m} - \theta_i^n}{\Delta t} \qquad 5.40$$

This matrix system can be solved where equation **5.35** is of the form

$$\mathbf{L} \cdot \mathbf{U} = \mathbf{A} \qquad 5.41$$

by decomposing equation **5.41** into the form

$$\mathbf{A}\cdot\mathbf{x} = (\mathbf{L}\cdot\mathbf{U})\cdot\mathbf{x} = \mathbf{L}\cdot(\mathbf{U}\cdot\mathbf{x}) = \mathbf{b} \qquad \textbf{5.42}$$

and solving for $\mathbf{y}$ such that

$$\mathbf{L}\cdot\mathbf{y} = \mathbf{b} \qquad \textbf{5.43}$$

and then solving for $\mathbf{x}$ such that (Press et al. 1986)

$$\mathbf{U}\cdot\mathbf{x} = \mathbf{y}. \qquad \textbf{5.44}$$

This form of a solution is termed **LU** decomposition. In the case where **L** is a tri-diagonal matrix, as is the case here, the solution can be performed in a very straightforward manner of backward and forward substitution; a specific solution can be found in (Press et al. 1986).

For a flux boundary condition at $i = 0$ there are N - 1 equations and N - 1 values of δ^m where the interior nodes are described by equation **5.34** and the boundary at $i = 0$ is described by Darcy's Law, equation **5.25**. This set of equations can be solved exactly as above where $N_n = N - 1$ and a_1 is described through Darcy's Law.

In order to couple the above infiltration model to the overland flow description, the solution approach of Celia et al. (1990) requires two modifications. First, because of erosion and sediment transport processes, surface elevations are not constant in general, and, therefore the soil column is not generally static. Thus, new node vectors must be defined at each time step. Redefining the node vector is accomplished by changing Δz_g while maintaining the same number of nodes in each soil column. Values of ψ at each node at the beginning of each time step are computed by linear interpolation from the

previous time steps values. The second modification to Celia et al.'s (1990) approach incorporates the ability to switch boundary conditions. When rainfall starts, the boundary condition is a flux type equal to the rainfall rate and the flow onto each cell from adjacent cells. When the head value in the uppermost node becomes greater than the saturated head, ponding occurs and the boundary condition at that cell switches to a fixed head type with the head equal to the saturated head value.

5.2.3. Sediment Detachment and Transport

5.2.3.1. Governing Equations

The development of the sediment detachment and transport algorithm is after Julien (1994) where not otherwise noted. Conservation of mass for a three dimensional control volume applied to sediment continuity gives

$$\frac{\partial C_s}{\partial t} + \frac{\partial \hat{q}_{sx}}{\partial x} + \frac{\partial \hat{q}_{sy}}{\partial y} + \frac{\partial \hat{q}_{sz}}{\partial z} = \dot{C}_s \qquad \textbf{5.45}$$

where C_s is the spatial averaged sediment concentration, $\hat{q}_{sx}$, $\hat{q}_{sy}$ and $\hat{q}_{sz}$ are the mass fluxes through the faces of the control volume and $\dot{C}_s$ is the rate of sediment per unit volume supplied by an external source. The units of concentration are unimportant as long as $\hat{q}_s$ and $\dot{C}_s$ have the same units. Assuming no sediment source and a time invariant supply of sediment, $\frac{\partial C_s}{\partial t} = 0$, equation **5.45** reduces to

$$\frac{\partial \hat{q}_{sx}}{\partial x} + \frac{\partial \hat{q}_{sy}}{\partial y} + \frac{\partial \hat{q}_{sz}}{\partial z} = 0 \qquad \textbf{5.46}$$

The flux through the face $\hat{q}_{xx}$ can be expanded to include both advective flux and diffusive and mixing flux as

$$\hat{q}_{xx} = \overbrace{vC_s}^{\text{advective flux}} \overbrace{-(D+\varepsilon_x)\frac{\partial C_s}{\partial x}}^{\text{diffusive and mixing flux}}. \qquad \textbf{5.47}$$

The advective flux describes the movement of sediment particles by velocity currents where v in equation **5.47** is the velocity of the flow in the x direction. The other two fluxes are directly proportional to the concentration gradient and are molecular diffusion and diffusion due to turbulent fluid motion. The constant D is the proportionality constant due to molecular diffusion and ε_x is the turbulent mixing coefficient. The negative sign in equation **5.47** represents a mass flux in the direction of decreasing concentration. A similar equation for $\hat{q}_{sy}$ and $\hat{q}_{sz}$, analogous to equation **5.47**, may be written. Assuming that the diffusive and mixing fluxes are very small compared to advective fluxes and that settling velocity, ω_s, is the dominant advective flux in the z direction then equation **5.47** can be written as

$$\frac{\partial vC_s}{\partial x} + \frac{\partial uC_s}{\partial y} - \frac{\partial \omega C_s}{\partial z} = 0. \qquad \textbf{5.48}$$

Making further assumptions that the flow is gradually varied, constant fall velocity and $\frac{\partial C_s}{\partial z} = \frac{C_s}{h}$, equation **5.48** becomes

$$v\frac{\partial C_s}{\partial x} + u\frac{\partial C_s}{\partial y} + \frac{\omega C_s}{h} = 0. \qquad \textbf{5.49}$$

C_s in one dimension as a function of inflowing concentration, Cs_0, can therefore be written as

$$C_s = C_{s0x} e^{\frac{-X\omega_s}{hv}} . \qquad \textbf{5.50}$$

The percentage of sediment that settles over a given distance X is defined as the transport efficiency and can be written from equation **5.50** as

$$T_E = \frac{C_{s0} - C_s}{C_{s0}} = 1 - e^{\frac{-X\omega_s}{hv}} \qquad \textbf{5.51}$$

The settling sediment flux in the z direction causes a change in bed elevation, z. With porosity, p_o, defined as 1 - C_v, where C_v is volumetric concentration [L^3/L^3] we can integrate equation **5.36** over the flow depth, h and rearrange to get the governing equation for two-dimensional erosion and sediment transport

$$\frac{\partial z}{\partial t} = -\frac{T_E}{(1-p_o)}\left(\frac{\partial q_{sx}}{\partial x} + \frac{\partial q_{sy}}{\partial y}\right) \qquad \textbf{5.52}$$

modified to two-dimensions from the one-dimensional form in Julien (1994), q_{sx} and q_{sy} are unit sediment discharges in the x and y directions respectively [L^2/T]. In its current implementation the model utilizes only one size class of sediment and p_o is determined by the specific weight of the sediment as

$$p_o = 1 - \frac{\gamma_{md}}{\gamma_s}, \qquad \textbf{5.53}$$

where γ_{md} is the average dry specific weight of the water-sediment mixture, defined here as the dry weight of sediment per unit total volume, and γ_s is the specific weight of the sediment (Julien 1994). The unit sediment transport capacity in the x direction is determined by

$$q_{s_x} = a\left[pS_{0x} - (pS_0)_{crit}\right]^b, \qquad \textbf{5.54}$$

where S_{ox} is the bed slope in the x direction of flow and $(qS_0)_{crit}$ is a minimum value below which no sediment is transported and is implemented as a constant in the x and y directions. The unit sediment transport in the y direction is determined in an analogous manner. The value for the constant, a, is a measure of the soils' erosivity properties and the exponent b should be approximately 1.5 – 1.8 (Kilinc and Richardson 1972). Utilizing equations **5.52** and **5.54** separates the processes of detachment and transport as suggested by Meyer and Wischmeier (1969).

5.2.3.2. Numerical Methods

These equations are solved using a finite difference method, centered in space, forward in time. Through experimentation it was determined that in solving these equations, the coupling of the erosion and sedimentation algorithm to the overland flow equations can cause steep gradients in flow conditions as well as bed slope which can lead to discretization errors. A control is then added through a simple Gaussian low pass filter applied to the bed elevation after each time the sediment detachment and transport algorithm is implemented. The Gaussian distribution in 2-D is given by

$$G(x,y)=\frac{1}{2\pi\sigma^2}e^{\frac{-(x^2+y^2)}{2\sigma^2}} \quad . \qquad \textbf{5.55}$$

The distribution gives a "point-spread" function where each cell's new elevation is determined by its own value as well as the values of the cells within a neighborhood of dimensions specified in the input. This filter is applied to every cell in the domain to determine the bed elevation values for the next time step. The variance of the distribution, σ^2, determines the relative convolution weight in determining elevation values and it is assumed constant in the x and y directions.

Implementation of the erosion algorithm can also cause oscillations that are self-propagating within the overland flow algorithm. To control these oscillations, a time step adjustment has proven to be very successful. Operating the erosion algorithm at a time step, $\Delta t_e > 3\Delta t_o$ (time step for overland flow algorithm) provides stability under most applications. Thus, for every time sediment is detached and transported three or more operations to determine depth and discharges are done and stability controls within the overland flow algorithm control minor oscillations.

5.3. Model Component Verification

5.3.1. Overland Flow

The overland flow component of HYDROR was extensively tested when originally presented by Fiedler and Ramírez (2000) and it is retested because the Green-Ampt component has been replaced by Richards equation. The first test is a comparison of the hydrodynamic model with a kinematic wave analytical solution to overland flow depth and discharge on a wide plane. The input characteristics as well as the solution are given in Chow (1988) pg. 157 and are restated here.

Table 5.2: Input parameters for the steady state kinematic wave comparison

Lateral Inflow (rainfall intensity)	25.4 [mm / hr]
Length of plane	30.48 [m]
Bed slope	5 %
K_o	60

The model was set up with ten cells in the x-direction having an arbitrary length of 1 [m] and 20 cells in the y-direction having a length of 1.524 [m]. Other parameters were $\varepsilon_1 = 2$, $\varepsilon_2 = \varepsilon_3 = 0$ for this example.

Table 5.3: Steady-state kinematic wave comparison results

	Depth [cm]	Discharge [cm^2/sec]
Kinematic Wave	.146	2.151
Hydrodynamic Model	.147	2.037
Percent Difference	.68	5.3

The second test is similar to a one-dimensional dam break problem originally reported in Stoker (1957) and later simulated by Jha et al. (1995). A vertical face of water (a dam) is released at $x = 0.5$ [m] on a 1 [m] long plane and a shock wave develops. The ground surface is horizontal, the stage above $x = 0.5$ [m] is 1 [m] and the stage below is 0.5 [m]. Model parameterization is $\Delta y = 2$ [mm], $\Delta t = 0.0002$ [s], and $\varepsilon_1 = \varepsilon_2 = \varepsilon_3 = 0$. A comparison between the analytical solution and the numerical solution can be seen in Figure 5.1. It is determined visually that this theoretical model does an excellent job of simulating the dam break.

5.3.2. Infiltration

5.3.2.1. Numerical Accuracy

To test the numerical accuracy of the model implementation, model results are compared to a quasi-analytical solution to Richards equation for the condition of a homogeneous soil column with a fixed head boundary condition presented by Philip (1969). Two different scenarios are tested, a clay and a sand soil column. The soil properties for these two soils are defined as follows (Haverkamp et al. 1977):

Yolo Light Clay:

$$K = K_s \frac{A}{A + |\psi|^{\beta}}\ ;\ K_s = 4.428(10^{-2})\ \text{cm/h},\ A = 124.6,\ \beta = 1.77 \qquad \textbf{5.56}$$

$$\theta = \frac{\alpha(\theta_s - \theta_r)}{\alpha + (\ln|\psi|)^{\beta}} + \theta_r\ ;\ \theta_s = 0.495,\ \theta_r = 0.124,\ \alpha = 739,\ \beta = 4$$

Sand:

$$K = K_s \frac{A}{A + |\psi|^{\beta}}; K_s = 34 \text{ cm/h}, A = 1.175(10^6), \beta = 4.74 \qquad 5.57$$

$$\theta = \frac{\alpha(\theta_s - \theta_r)}{\alpha + |\psi|^{\beta}} + \theta_r; \theta_s = 0.287, \theta_r = 0.075, \alpha = 1.611(10^6), \beta = 3.96$$

Figures 5.2 and 5.3 show the comparison between the theoretical and analytical solution to fixed head infiltration into a soil column for the two soils above. As can be seen the numerical implementation of Richards equation does an excellent job of predicting the distribution of water in the soil column.

5.3.2.2. Mass Balance

The mass balance ratio (MB) at any point in time is defined as the ratio of the total additional mass in the domain to the total net flux into the domain, written as

$$\text{MB} = \frac{\sum_{i=1}^{E-1} \left(\theta_i^{j+1} - \theta_i^{0}\right)(\Delta z)}{\sum_{j=1}^{n+1} \left[K^j_{N-\frac{1}{2}} \left(\frac{H_N^j - H_{N-1}^j}{\Delta z} + 1 \right) - K^j_{\frac{1}{2}} \left(\frac{H_1^j - H_0^j}{\Delta z} + 1 \right) \right] (\Delta t)} \qquad 5.58$$

where $N = E + 1$ nodes $\{z_0, z_1, z_2, \ldots z_E\}$, and constant nodal spacing Δz is assumed; H is the pressure head and K is the unsaturated hydraulic conductivity. The specific head based implementation used here leads to perfect mass balance, implying a value of MB of unity.

In both numerical experiments as presented in Figures 5.2 and 5.3 the MB is unity. This is a result of the utilization of the mixed form of Richards equation and the numerical implementation used here as it has been shown to be perfectly mass conservative (Celia et al. 1990).

5.3.3. Sediment Detachment and Transport

Since there is no known analytical solution to coupled erosion and overland flow algorithms as is being implemented here, it is impossible to perform an analytical verification of this component. However, an empirical verification is feasible. Qualitatively, the solution should provide a realistic longitudinal profile for a 10 [m] long plane with initial 8% slope and constant rainfall rate of 105 [mm/hr].

Figure 4 shows the landform progression through time to a near equilibrium condition with a longitudinal profile that is best described using an exponential function with a negative exponent. The shape of the steady state solution is largely determined by the constant lateral inflow as well as the constant and exponent chosen in equation **5.54**. This is a realistic result for the conditions presented.

5.3.4. Physical / Theoretical Model Comparison

A physical experiment was conducted in the rainfall facility described in Chapter 4 to test the theoretical model's ability to model a real world rainfall event. The experiment consists of a 1 [m] X 0.5 [m] plot subjected to rainfall at a spatially homogeneous rate of 65 [mm/hr] applied in two 25-minute pulses separated by a 5-minute time period of no rain. Measurements of volumetric water flux [L^3/T] are made at 120 [s] intervals. The plot was rained on 1 day before the experiment for a period of one-hour. The soil within

the physical model has the following soil moisture characteristics $\theta_s = 0.42$, $\theta_r = 0.04$, $\alpha = 0.0436$ [cm-1], $n = 1.34$, $l = 0.5$, $K_s = 0.0004$ [cm/s] for the van Genuchten functions:

$$K(h) = K_s S_e^l \left[1 - \left(1 - S_e^{\frac{1}{m}} \right)^m \right]^2 \qquad 5.59$$

$$S_e = \frac{\theta(h) - \theta_r}{\theta_s - \theta_r} = \frac{1}{\left[1 + |\alpha h|^n \right]^{\left(1 - \frac{1}{n}\right)}} \qquad 5.60$$

The theoretical model is parameterized with the above van Genuchten functions and the initial soil moisture condition is assumed to be ψ = -10 [cm] everywhere in the domain, a number consistent with the volumetric water content after 1 day of drying (Chapter 4 Figure 4). The model was discretized with $d_x = d_y = 50$ [mm] and a time step of 0.02 [s] was utilized. The model was run continuously for a period of 3600 [s] with a spatially homogenous rainfall field of 65 [mm/hr] and a storm as conducted physically. A comparison of hydrographs can be seen in Figure 5.5. The theoretical model does a reasonable job of reproducing the rising and falling limbs of both pulses of rain. This is an advantage of implementing Richards equation because using another infiltration equation such as Green-Ampt requires additional parameterization for a multi-storm event. The theoretical model also does a reasonable job of reproducing the mean value of volumetric water flux at other times during the simulation although large scale oscillations, which can be of the same order as the signal, seen in the physical experiment are not reproduced in the theoretical model. During the physical experiment mass-wasting events dam the outflow until the water behind the dam becomes deep enough to over top the dam and move the sediment. A pulsed outflow is observed due to this dam and release process and can be seen in the physical results. There is no mass-wasting

mechanism within the theoretical model and therefore this pulsed outflow type of event cannot be reproduced exactly.

5.4. Discussion

Two examples are presented here for HYDROR illustrating the model's capability of capturing the fine scale processes that lead to hillslope drainage network development and also its ability to model the interactions between overland flow, infiltration, and erosion. The two cases model a 3 x 10 [m^2] slope void of vegetation at 9° degree slope. The implementations have cell dimensions of 0.0625 [m] in the x and y directions for a total of 7,889 cells. The two examples differ in their antecedent moisture conditions as well as the rainfall rate. Example 1 is subjected to 105 [mm/hr] rainfall for 4 hours and Example 2 is subjected to 95 [mm/hr] rainfall for 2 hours. The initial soil moisture conditions are specified by a self-similar distribution in space. The self-similar distribution of soil moisture is created using HYDRO_GEN (Rubin and Bellin, 1997) with a mean, variance, and fractal dimension equal to -550 [mm], 1100 [mm], and 2.25 respectively for Example 1 and –550 [mm], 2730 [mm], and 2.25 for Example 2. These characteristics are determined through a power law semi-variogram (Rubin and Bellin, 1997). The soil moisture is assumed to be constant initially in the vertical direction. Example 1 (Figure 5.6) shows the model's ability to develop concentrated flow paths. It is this development of concentrated flow paths that leads to drainage network development. The areas of most erosion are also the areas where discharge began the earliest. Due to this initial discharge the area erodes and causes further accumulation of water as neighboring areas develop overland flow. Hypothetically drainage network development occurs through the process described above in different areas and at

different length scales, and through interactions, which would eventually lead to an end equilibrium state.

Example 2 (Figure 5.7) illustrates the model's ability to simulate discontinuous flows over the spatial domain and spatially distributed erosion. Only in very small areas does the rainfall rate exceed the infiltration capacity of the soil leading to Hortonian overland flow. In these areas of flow, erosion is occurring leading to a channel development largely in the down-slope direction. The numerical implementation of this scenario has steep gradients in overland flow depth and sediment concentrations, which can be difficult to model. As can be seen in Figure 5.7, HYDROR is capable of simulating this scenario although there are some small-scale oscillations occurring near the up-slope boundary.

5.5. Conclusions

This paper presents the mathematical development of a distributed physically based mechanistic hillslope hydrology model. The model consists of three components which each perform accurately when compared to analytical solutions. The development of this model utilizes the most stable and accurate approaches developed for each algorithm individually, and implements some new stability controls on the coupled algorithm as a whole.

Two examples are presented to qualitatively assess the ability of the model to capture interactions between overland flow, infiltration and erosion. These examples show how the spatial distribution of initial soil moisture, which leads to spatially distributed ponding time and overland flow depths and velocities, interacts with channel development and spatially distributed erosion. In Chapter 6 a study is presented which

measures model performance and its ability to capture some of the spatially distributed characteristics of erosion on a hillslope, namely channel formation and energy expenditure.

5.6. References

Celia MA, Bouloutas ET, Zarba RL. 1990. A General Mass-Conservative Numerical Solution for the Unsaturated Flow Equation, *Water Resources Research* **26**(7): 1483-1496.

Chow VT, Maidment DR, Mays LW. 1988. Applied Hydrology. McGraw-Hill Inc.

Emmett WW. 1970. The hydraulics of overland flow on hillslopes, *United States Geological Survey Professional Paper* 662-A.

Fennema RJ, Chaudhry MH. 1986. Explicit numerical schemes for unsteady free-surface flows with shocks, *Water Resources Research* **22**(13): 1923-1930.

Fiedler F. 1997. Hydrodynamic simulation of overland flow with spatially variable infiltration and microtopography, *Ph.D. dissertation*, Colorado State University.

Fiedler F, Ramírez JA. 2000. A numerical method for simulating discontinuous shallow flow over an infiltrating surface, *International Journal for Numerical Methods in Fluids* **32**: 219-240.

Foster GR. 1982. Modeling the erosion process, In: *Hydrologic modeling of small watersheds*, ed. Haan CT, Johnson HP, Brakensiek DL, ASAE, New York.

van Genuchten MT, Nielsen DR. 1985. On describing and predicting the hydraulic properties of unsaturated soils, Ann. *Geophys.* **3**(5): 615-628.

Green WH, Ampt GA. Studies on soil physics, part I, the flow of air and water through soils. *J. Agric. Sci.* **4**(1): 1-24.

Haverkamp R, Vauclin M, Touma J, Wierenga PJ, Vachaud G. 1977. A Comparison of Numerical Simulation Models For One-Dimensional Infiltration, *Soil Sci. Soc. Am. J.* **41**: 285-294.

Jameson A, Schmidt W, Turkel E. 1989. Numerical solution of the Euler equations by finite-volume methods using Runge-Kutta time-stepping schemes, *AIAA Paper 81-1259.*

Jha AK, Akiyama J, Ura M. 1995. First- and Second-Order Flux Difference Splitting Schemes for Dam-Break Problem, *Journal of Hydraulic Engineering* **121**(12): 877-884.

Julien PY. 1994. *Erosion and Sedimentation*, Cambridge University Press, New York, NY.

Kilinc M, Richardson EV. 1972. Mechanics of soil erosion from overland flow generated by simulated rainfall. *Hydrology Papers No. 63*, Colorado State University.

Meyer LD, Wishmeier WH. 1969. Mathematical simulation of the process of soil erosion by water, *Trans. ASAE* **12**(6): 754-762.

Paniconi C, Aldama AA, Wood EF. 1991. Numerical Evaluation of Iterative and Noniterative Methods for the Solution of the Nonlinear Richards Equation, *Water Resources Research* **27**(6): 1147-1163.

Philip JR. 1957. Theory of infiltration, Adv. Hydrosci. **5**: 215-305. Academic Press, NY.

Playan E. 1992. Two-dimensional hydrodynamic simulation of basin irrigation: analysis of shape effects on irrigation performance, *Ph.D. dissertation*, Utah State University.

Press WH, Teukolsky SA, Vetterling WT, Flannery BP. 1986. Numerical Recipes in Fortran 77. Press Syndicate of the University of Cambridge, New York.

Rathfelder K, Abriola LM. 1994. Mass conservative numerical solutions of the head-based Richards equation, *Water Resources Research* **30**(9): 2579-2586.

Richardson JR, Julien PY. 1994. Suitability of simplified overland flow equations, *Water Resources Research* **30**(3): 665-671.

Rubin Y, Bellin A. 1997. Conditional simulation of geologic media with evolving scales of heterogeneity, In: *Scale Dependence and Scale Invariance in Hydrology*, ed. Sposito G, Cambridge University Press.

Stoker JJ. 1957. *Water waves*. John Wiley & Sons, Inc., New York, N.Y.

Woolhiser DA. 1975. Simulation of unsteady overland flow, In: *Unsteady Flow in Open Channels, Volume 2*, eds. Mahmood K, Yevjevich V. Water Resources Publications, Ft. Collins, CO.

Zarba RL. 1988. A numerical investigation of unsaturated flow, *M.S. thesis*, Dep. of Civ. Eng., M.I.T. Cambridge.

Figure 5.1: Theoretical and analytical solution to dam break problem

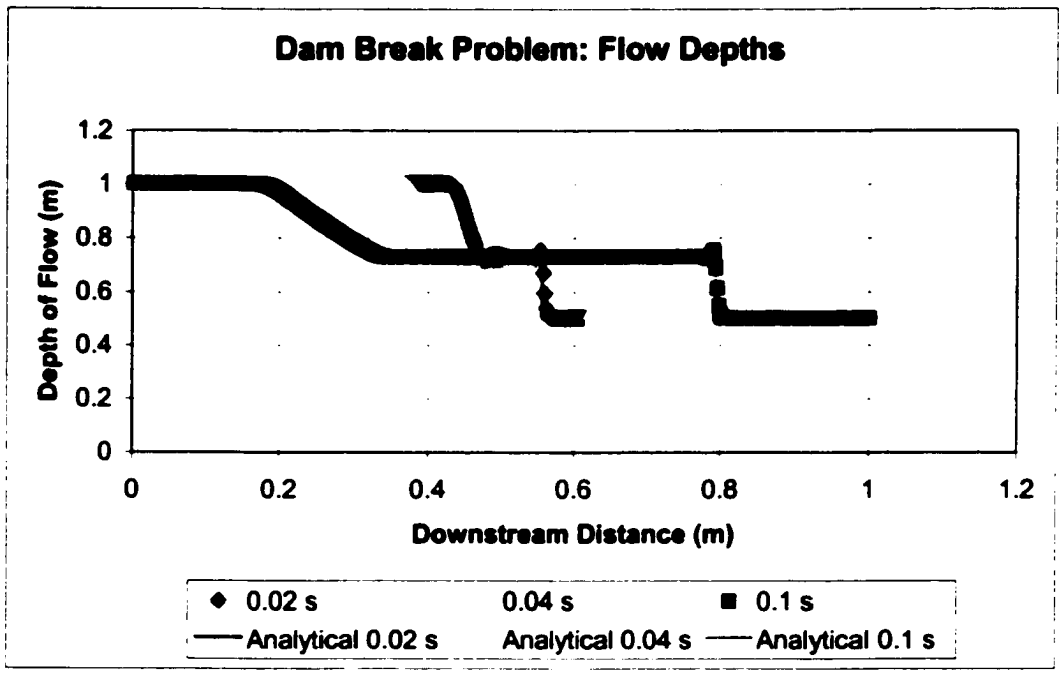

Figure 5.2: Theoretical and analytical solution for infiltration into yolo light clay

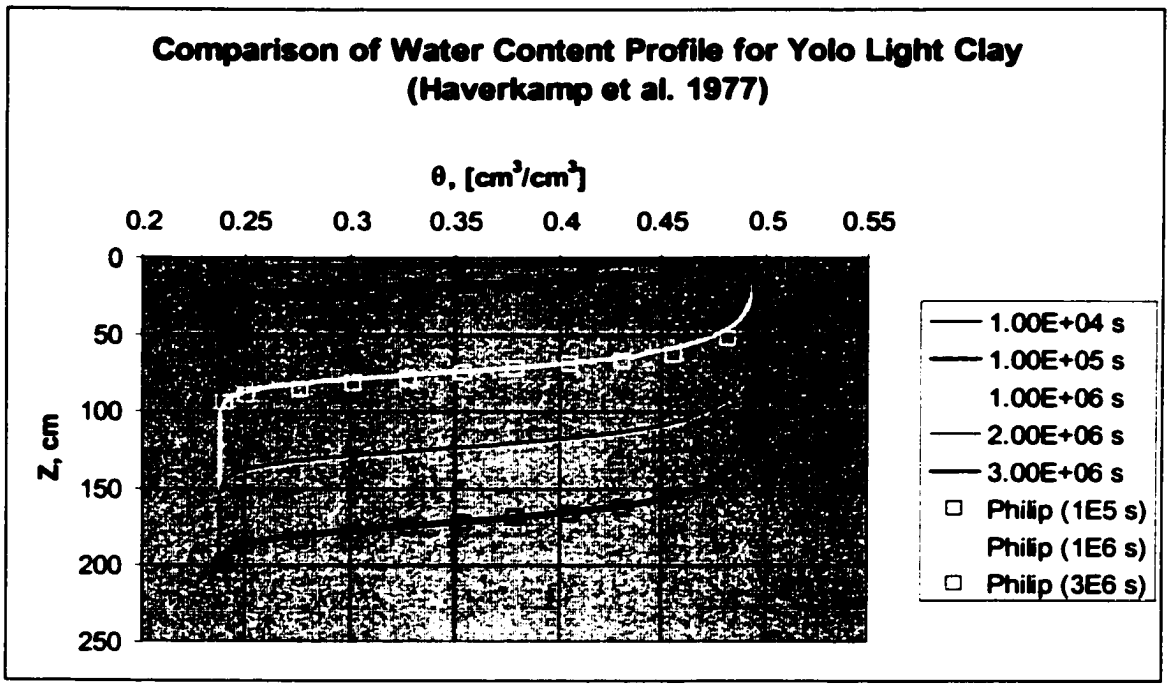

Figure 5.3: Theoretical and analytical solution for infiltration into sand

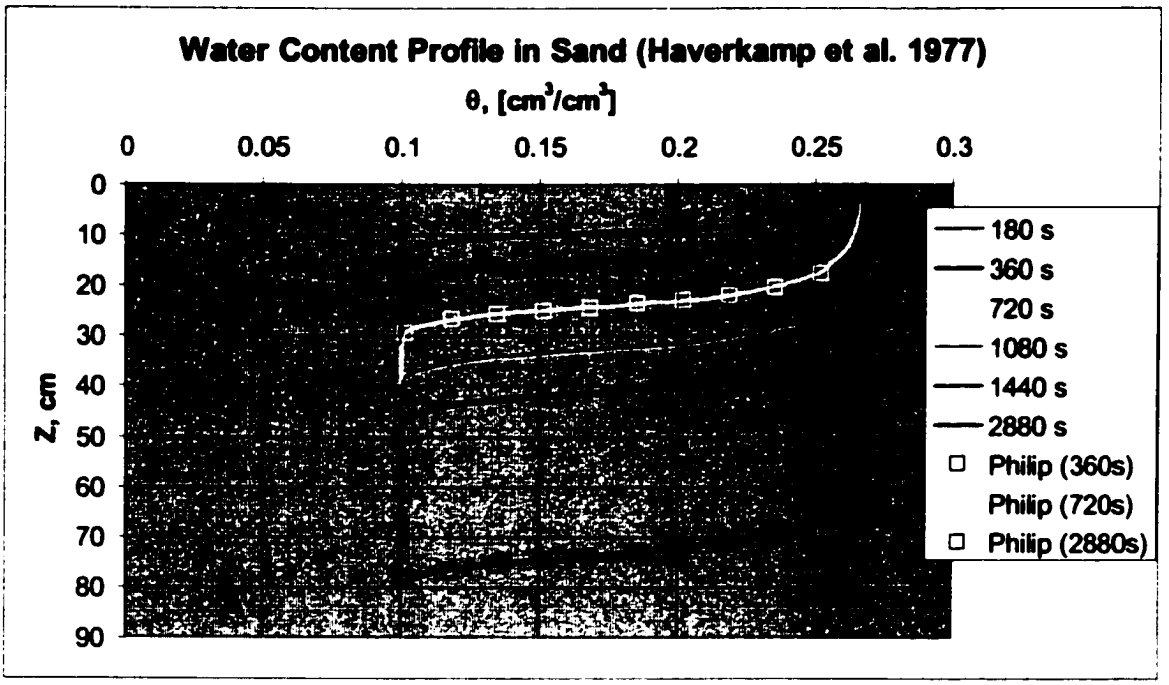

Figure 5.4: Theoretical longitudinal profile development

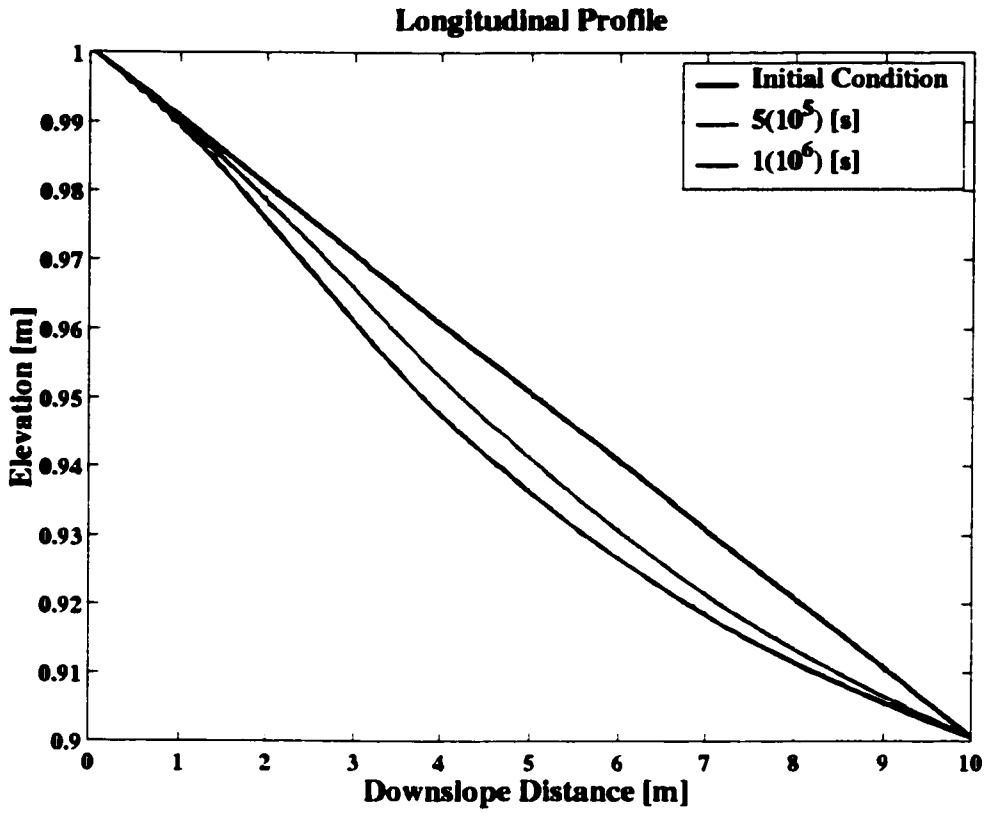

Figure 5.5: Model verification with physical experiment

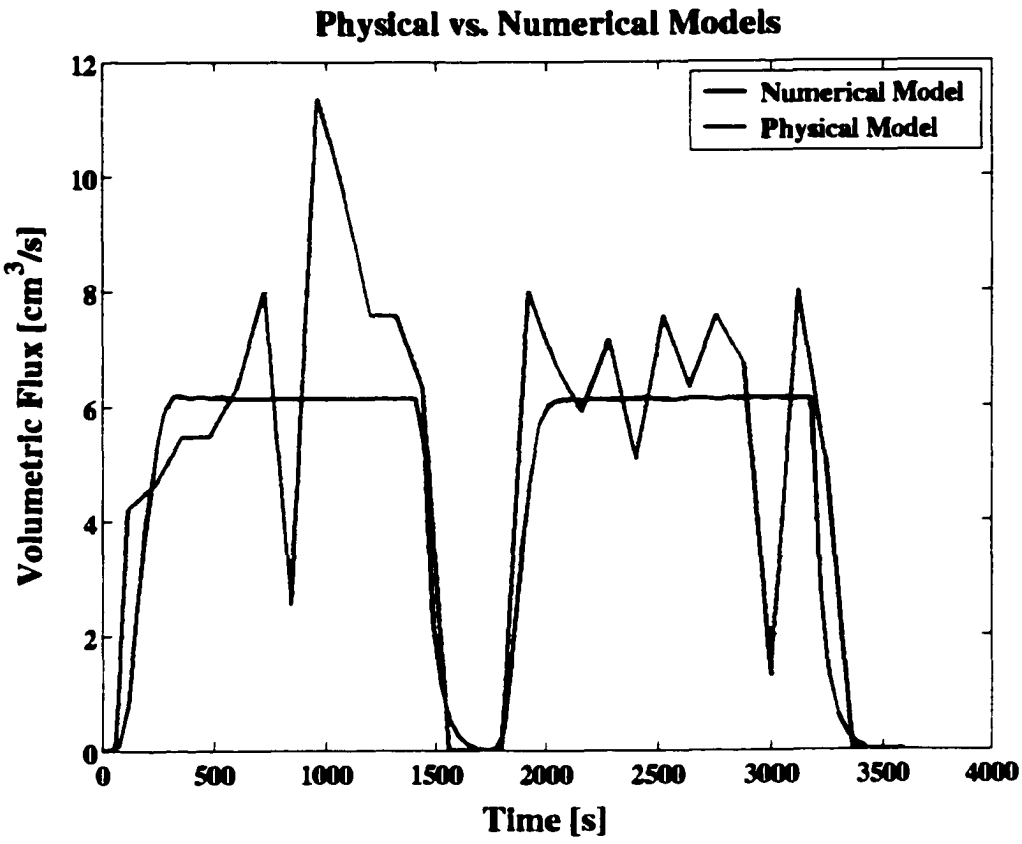

Figure 5.6: HYDROR Example 1

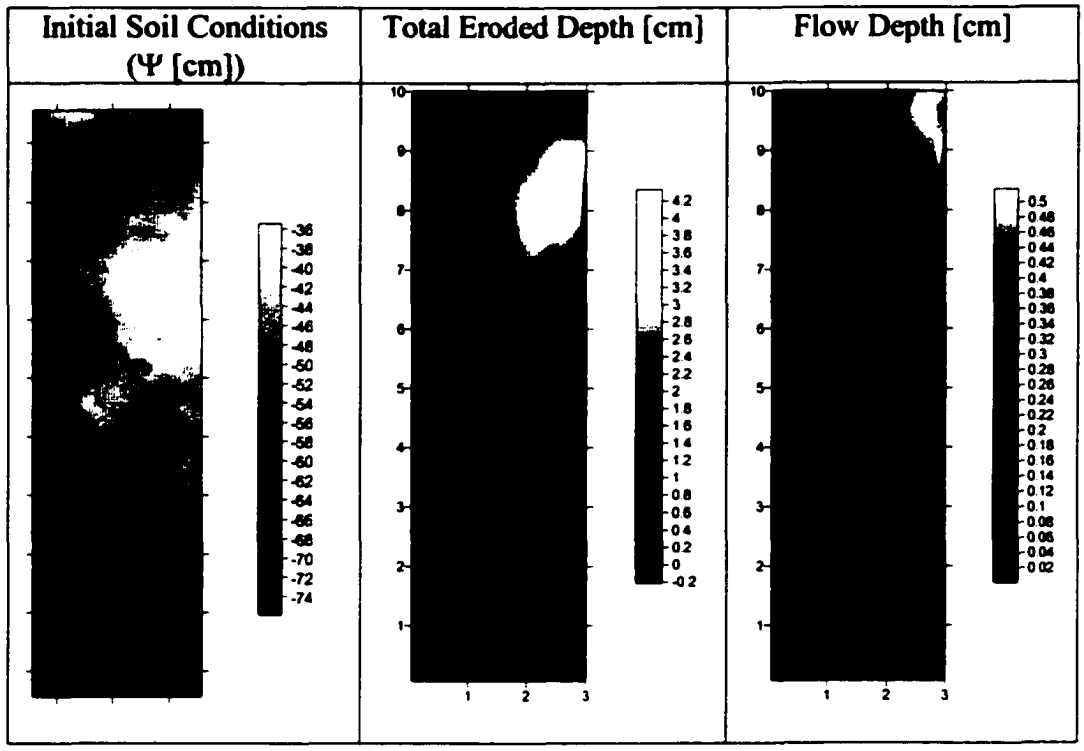

Figure 5.7: HYDROR Example 2

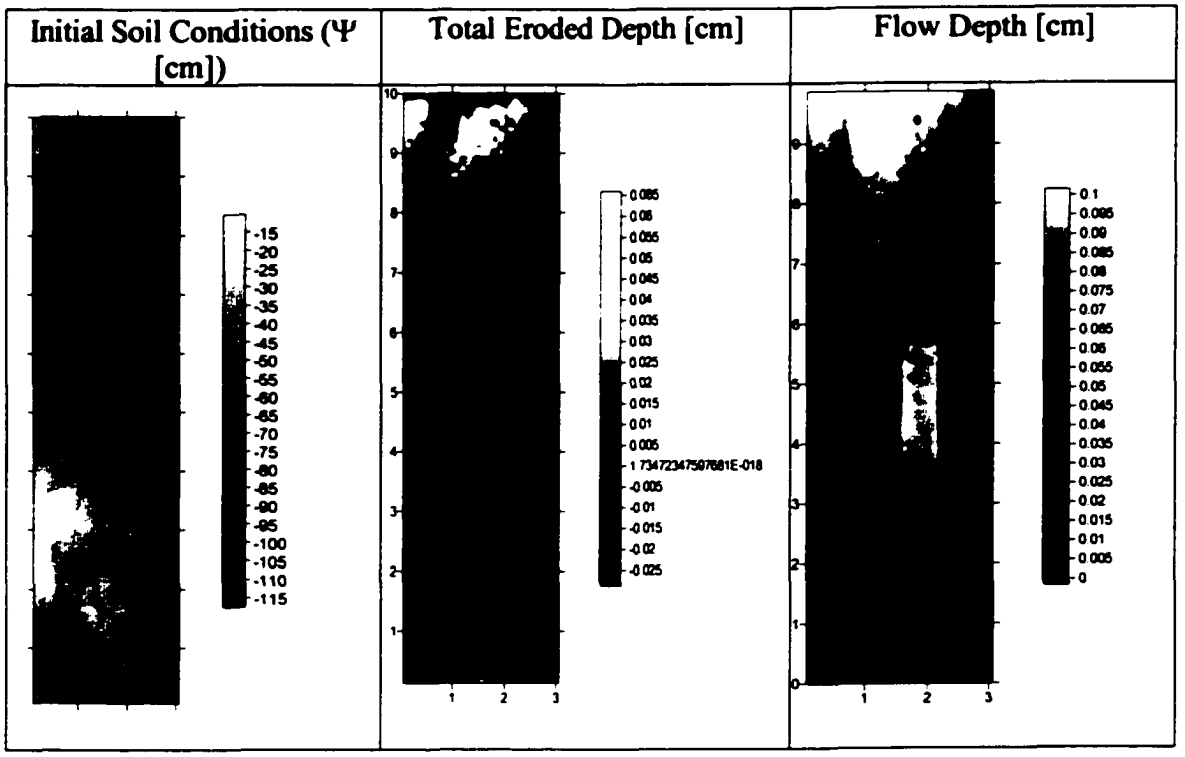

Chapter 6: Theoretical Hillslope Evolution

Abstract

This Chapter presents an examination of the evolution of hillslopes modeled within the framework of a physical, process-based hillslope hydrology model. The model couples the full two-dimensional hydrodynamic equations for overland flow to a sediment detachment and transport model in two dimensions and an infiltration model in one dimension. The evolution of hillslopes is analyzed with respect to energy expenditure characteristics. Analyses are carried out for one-dimensional and two-dimensional systems. Results indicate that, for the one-dimensional system, Hortonian overland flow produces a slope-discharge relationship and energy expenditure characteristics that approach those predicted by global and local hypotheses of optimal energy expenditure. The time that it takes hillslopes to approach optimality is related to the rainfall rate and the rate at which sediment is being transported. In two dimensions, the trends in energy expenditure characteristics depend critically on the threshold of flow rate [L^3/T] demarking the initiation of an organized flow path, or channel. Two-dimensional hillslopes subject to spatially variable lateral inflow (*e.g.*, rainfall – infiltration) appear to approach a minimum in the total global rate of energy expenditure and stream power (*i.e.*, optimality) but the distribution of these energies and the total unit stream power are highly influenced by

what is delineated as a concentrated flow. Two-dimensional systems also possess simple scaling defined by slope-discharge relationship.

6.1. Introduction

In Chapter 5 a mathematical model of hillslope hydrology is introduced that couples the two-dimensional hydrodynamic equations for overland flow with equations describing two-dimensional erosion and transport processes and a one-dimensional implementation of Richards equation for infiltration. In this chapter I examine how this model simulates hillslope evolution. The idea that hillslope evolution may tend towards a state at which optimality in energy expenditure is achieved is essentially a predictive tool that can be used to estimate hillslope erosional response. However, it is not known whether at any given point in time and space the hillslope system is progressing towards a dynamic equilibrium state, defined by relatively stable characteristics, and to which it will return after a disturbance (Renwick 1992). Current models of hillslope hydrology and hillslope erosion (*e.g.*, WEPP) separate processes defined by form (*e.g.*, rills and inter-rill areas) (Flanagan et al. 2001). If a hillslope is indeed a system progressing towards equilibrium then the rill and inter-rill areas must be intricately tied through the energy expenditure characteristics of the system as a whole as are hillslopes and rivers. As Knighton (1998) notes, there is a need to relate the "activity of fluvial processes and the forms that develop to the physical concept of work."

Let us note the similarity between rill networks on hillslopes and river networks, which have been observed qualitatively for nearly a half-century (Leopold et al. 1964). From this let us assume that river networks and rill networks evolve under similar

processes and mechanisms. Indeed it has been shown that water pathways on hillslopes, defined using elevation maps, have many of the same fractal and scaling characteristics as river networks (*e.g.*, bifurcation and length ratios and fractal dimension D_f) (Ogunlela et al. 1989, Wilson and Storm 1993) and that channel development on hillslopes occurs through processes of mass wasting and hydraulic erosion (Schumm et al. 1987) as do rivers. Mass wasting is defined as the downslope movement of soil, rock, and regolith under the influence of gravity. At the hillslope-scale, mass wasting occurs through the movement of cohesive blocks of sediment under the influence of gravity. There have been many theories that may explain the structure of river networks and relate them to the work being done within the system. Noting some hydraulic variables, v is velocity [L/T], Q is volumetric water flux [L^3/T], Q_s is volumetric sediment flux [L^3/T] and S is slope [L/L], Yang (1971) proposed a theory that rivers adjust their geometrical characteristics as to obtain a minimum unit stream power ($vS \rightarrow$ minimum), the equivalent of the rate of potential energy expenditure per unit mass along its course. Chang (1980) makes an argument that a natural stream adjusts its course and cross-sectional geometry as to obtain the minimum stream power ($\gamma QS \rightarrow$ minimum). Rodríguez-Iturbe et al. (1992) hypothesized that river networks tend towards a state of optimality in energy dissipation both globally and locally and showed that these hypotheses predict river networks that share many characteristics with natural river systems. River networks that comply with the minimum energy expenditure hypotheses are dubbed optimal channel networks (OCNs). Applications of these theories have been used to explain different characteristics of river systems including river longitudinal profiles, river meanders, and downstream hydraulic geometry components, a good summary of which can be found in

Rodríguez-Iturbe and Rinaldo (1997) and Knighton (1998). One particular downstream hydraulic relationship that is intricately tied to energy expenditure characteristics is the slope-discharge relationship ($S \propto Q^z$). In previous chapters an analogous form has been used ($S \propto A^z$) where drainage area, A is a surrogate for Q. Theoretically it has been shown that $z = -0.5$ for optimality in energy dissipation when the scaling exponents of the hydraulic geometry relationships for width and depth are held equal to each other (Rodríguez-Iturbe et al., 1992).

The model presented here accurately describes the dominant processes driving landscape evolution under the assumption of Hortonian overland flow and therefore constitutes an adequate tool to study the energy characteristics of an evolving hillslope. Mechanisms for channel initiation other than by Hortonian overland flow are not included in this model and it is acknowledged that shallow land sliding, the mass movement of a shallow layer of the soil surface often in a rotational manner may play a significant role in hillslope evolution.

In essence HYDROR is an evolutionary model where the rate of change in elevation at a point is

$$\frac{\partial z}{\partial t} = -\frac{T_E}{(1-p_o)}\left(\frac{\partial q_{sx}}{\partial x} + \frac{\partial q_{sy}}{\partial y}\right) \qquad \textbf{6.1}$$

where q_{sx} and q_{sy} are the sediment fluxes in the x and y directions respectively, T_E is the trap efficiency and p_o is the porosity which is similar to other sediment transport relationships proposed in the literature (Foster 1982, Kilinc and Richardson 1972)

$$\frac{\partial z}{\partial t} = \alpha f(\tau - \tau_{crit})^n \qquad \textbf{6.2}$$

and

$$\frac{\partial z}{\partial t} = \alpha f(Q^m S^n) \qquad 6.3$$

where τ is shear stress and τ_{crit} is a shear stress below which there is no sediment transport. Models based on equation **6.2** have been shown to reproduce the fractal characteristics of river basins (Rigon et al. 1994). In one dimension, Kirkby (1971) showed that equation **6.3** produces longitudinal profiles that are highly dependent on m and n but have exponents of z that are very near –0.5 for m and n representative of rivers. Hillslope evolution is fundamentally a multidimensional process and therefore modeling two-dimensional systems is much more informative. Implementing equation **6.2** into a two-dimensional landscape evolution model with a diffusion term ($\frac{\partial z}{\partial t} = f(S)$), Rodríguez-Iturbe (1997) showed that the landforms produced possess simple scaling defined by a slope-area relationship ($S \propto A^z$) where z is often very close to -0.5. They present evidence that only in the case of spatially variable erosional processes does multi-scaling occur. In the case of HYDROR there is no diffusion term of the form $\frac{\partial z}{\partial t} = f(S)$ and it is yet unknown whether the model will produce landforms that possess simple scaling and progress towards a state of optimality in energy dissipation in one- and/or two-dimensions.

6.2. Methods

To study the evolution of hillslopes under the governing equations of overland flow and hydraulic erosion and sedimentation, a series of mathematical simulations are presented and analyzed with respect to their energy characteristics. The analysis consists in determining how the total unit stream power, the total stream power, and the rate of

global and local energy expenditure adjust through time in areas of concentrated flow. Areas of concentrated flow are defined with respect to a threshold of discharge, $Q > Q_T$ [L^3/T]. Two kinds of simulations are carried out, one- and two-dimensional. One-dimensional simulations allow flow and system properties to vary only in the longitudinal direction, which is parallel to the gradient of the terrain elevation. Two-dimensional simulations allow flow and system properties to vary in two directions. For the purposes of discussion, let y denote the direction of initial slope (down-slope) and x denote the direction of initially no slope (cross-slope).

Unit stream power is defined as (Yang 1971)

$$\omega = vS. \tag{6.4}$$

Application to these simulations where the flow domain may be continuous across the entire hillslope requires unit stream power at a point i, j to be defined as

$$\omega_{i,j} = v_{i,j} S_{i,j} \tag{6.5}$$

and the total unit stream power in the system as,

$$\omega_T = \sum_{i=1}^{Nx} \sum_{j=1}^{Ny} v_{i,j} S_{i,j}, \tag{6.6}$$

where $i \in (1{:}Nx)$ and $j \in (1{:}Ny)$ and Nx and Ny are the number of grid cells in the x and y directions respectively. Stream power per unit length is defined as (Chang 1980)

$$\Omega = \gamma Q S. \tag{6.7}$$

Again defined here for a continuous domain, stream power at a point i, j is

$$\Omega_{i,j} = \gamma_{mi,j} Q_{i,j} S_{i,j} \tag{6.8}$$

where $\gamma_{mi,j}$ is the specific weight of the sediment water mixture and can be calculated as

$$\gamma_{mi,j} = \gamma(1 + C_v(G-1)) \tag{6.9}$$

where G is the specific gravity of the sediment and C_v is the concentration of sediment by volume. Here, for simplicity in calculations, it is assumed that $\gamma_{mi,j}$ is a constant in space and time and it is acknowledged that this assumption can lead to underestimation of stream power by as much as 15% where the concentration of sediment approaches 50% and the specific gravity of sediment is near 2.65. However, by setting a threshold for Q at which calculations are conducted such that only one order of magnitude in flow rates is considered, the error associated with this assumption affects the overall magnitude of stream power but has little influence on the distribution of stream powers within the domain in space or with time. In addition, concentrations rarely exceed 10 - 20% by volume, which corresponds to an error of less than 8%. The total stream power in the system is thus

$$\Omega_T = \gamma \sum_{i=1}^{Nx} \sum_{j=1}^{Ny} Q_{i,j} S_{i,j} . \qquad \textbf{6.10}$$

The global rate of energy expenditure is defined for a river network as (*e.g.*, Rodríguez - Iturbe et al. 1992)

$$P = k \sum_{i}^{N} Q_i S_i L_i \qquad \textbf{6.11}$$

where k is a constant throughout the network, i is a summation index from 1 to N, the number of channels in the network, Q_i, S_i and L_i are the volumetric water flux, slope and length of the individual link i. The local rate of energy expenditure per unit area is

$$P_l = \frac{QS}{w + 2d} \qquad \textbf{6.12}$$

for a rectangular channel of width, w, and depth, d. For a continuous flow domain the global rate of energy expenditure is defined here as

$$P_T = \sum_{i}^{Nx} \sum_{j}^{Ny} Q_{i,j} S_{i,j} L_{i,j} \qquad 6.13$$

where Q is the volumetric water flux through a cell of bottom area $d_x d_y$, S_{ij} is the slope in the direction of Q_{ij}, and L_{ij} is the length of the cell in the direction of Q either d_x, d_y or $\sqrt{d_x^2 + d_y^2}$, summed over the entire domain. The local rate of energy expenditure per unit flow area is computed at each cell as

$$P_l = \frac{QS}{2h + d_x} \qquad 6.14$$

where h is flow depth at that cell and d_x is the cell dimension along the direction of flow. Equation **6.14** assumes that the flow is directed in the x direction, but analogous equations may be written regardless of the direction of flow. The coefficient of variation of P_l across the entire domain is computed as

$$CV_{Pl} = \frac{\sigma(P_l)}{\mu(P_l)} \qquad 6.15$$

where σ and μ are the standard deviation and mean of P_l across the entire flow domain.

6.2.1. One-dimensional simulations

One-dimensional overland flow tests are conducted to examine the rates of energy expenditure as a function of time and the longitudinal hillslope profile created from an initially smooth hillslope subject to rainfall of constant intensity. The 1-D simulations utilize a grid of 6 X 160 cells with dimensions 6.25 [mm] in both the x and y directions for a domain 375 [mm] X 10(10^3) [mm]. A series of experiments is presented where an initially smooth hillslope at a 9% grade is subjected to arbitrarily chosen rainfall at a rate 65, 75, 95 and 105 [mm/hr] for a time period of 10^6 [s] each at model time steps of 0.1 [s]. No infiltration is simulated for these tests. The resistance parameter, $K_0 = fR_e$, is set

to 3500, corresponding approximately to the roughness associated with a sparsely vegetated surface (Woolhiser 1975). If infiltration were to be simulated in a spatially homogenous manner, the resultant discharges would still reflect a homogenous effective rainfall field of rate equal to the difference between gross rainfall and infiltration. If infiltration were considered spatially variable the result would be two-dimensional. The initial transport capacity is set to $q_s = (Sq)^{1.8}$, a transport capacity consistent with the literature (*e.g.*, Kilinc and Richardson 1972) where q is the unit discharge in the down-slope direction and q_s is the unit sediment discharge. For the 95 and 105 [mm/hr] rates, a second experiment is conducted in which $q_s = (Sq)^{1.5}$ (see Table 6.1).

Table 6.1: 1D experimental summary

Experiment ID	Rainfall rate [mm/hr]	b value $q_s = (Sq)^b$
E1	65	1.8
E2	75	1.8
E3	95	1.8
E4	105	1.8
E5	95	1.5
E6	105	1.5

The values ω_T, Ω_T, P_T, and CV_{PI} are determined at time intervals of 400 [s] throughout the simulation. At every 400 [s] the longitudinal profile is also fit with a power function $S = gQ^z$.

6.2.2. Two-dimensional simulations

One of the advantages of the mathematical model developed and implemented here is that physical characteristics of the hillslope may be explicitly defined at each grid cell, namely rainfall rates, elevation, soil infiltration characteristics (*e.g.*, saturated hydraulic conductivity), soil erodability, etc. In order to study how the governing equations affect

hillslope evolution with respect to energy characteristics a couple of assumptions are made. Initial soil moisture distribution and erodability are assumed constant throughout the domain. The hillslope is initially completely smooth. Variability into the system is introduced by spatially variable rainfall rate. Three experiments are presented which vary in the spatial dimensions of the simulated domain and the distribution of rainfall rates. The first two two-dimensional tests have cell dimensions $d_x = d_y = 6.25$ [mm] and 48 X 160 cells over all which simulated a 3 X 10 [m^2] plot, the same dimensions as the physical model referred to in Chapter 4. The third test is conducted on a model domain 96 X 320 cells with $d_x = d_y = 3.125$ [mm] and also has a total projected area of 30 [m^2]. At time intervals on the $O(10^2)$ seconds the energy expenditure characteristics of the systems are analyzed with respect to P_T, CV_{PI}, ω_T and Ω_T. A threshold is set as to delineate areas of concentrated flows where these energy characteristics are analyzed. Two thresholds for each of the three two-dimensional experiments are presented here. The two thresholds are set from analysis of the slope-discharge relationships presented in Figures 6.11, 6.14 and 6.17 determined at the end of the simulation. The thresholds are constant in time and reflect magnitudes of discharge at the end of the simulation. This threshold is set as a function of total volumetric water flux and the two selections represent a) a lower magnitude which includes flows that are still in development at the end of the simulation and b) a higher magnitude which only includes those flows which have a slope-discharge relationship with $z \approx -0.5$.

Model parameters are set to resemble the physical rainfall facility described in Chapter 4. . A median grain size of 0.12 [mm] is selected to correspond with the physical model (see Chapter 4, Figure 3). Initial slope angle is 9° as are half the physical model

tests. The sediment transport capacity is parameterized as to allow for rapid sediment transport. It is acknowledged that the maximum value selected (50% sediment concentration by volume) is an unrealistic value when compared to observations made during a physical experiment. However, it was found during model experimentation, that at hydraulic erosion rates corresponding to low sediment concentrations elevation changes do not occur over any reasonable time scale. Model stability requires that a time step be selected such that the Courant condition be met and that the change in elevation at a cell at any time step is not greater than 5% of the flow depth. Time steps are of $O(10^{-3})$ [s].

A summary of the three simulations presented here can be seen in Table 6.2. As mentioned before, initial conditions were set by a spatially variable rainfall rate.

Table 6.2: 2 Dimensional Simulations IDs

Experiment ID	Mean Rainfall rate [mm/hr]	Standard Deviation Rainfall rate	d_x / d_y [mm]	N_x / N_y	Rainfall Distribution
DD1	85	22	6.25 / 6.25	48 / 160	Self-Similar (Figure 6.6)
DD2	56	4	6.25 / 6.25	48 / 160	Gaussian (Figure 6.7)
DD3	59	5	3.125 / 3.125	96 / 320	Gaussian (Figure 6.8)

DD1 has an initial condition defined by a self-similar distribution of rainfall rates where the mean is 85 [mm/hr] and has a variance of 496 $[mm/hr]^2$. The distribution is specified by a power function semi-variogram ($g = ar^{\beta}$) where g is half the variance between points located distance r apart. For this distribution a is set to 1 and β is set to 1.5, which yields a fractal dimension of 2.25. The initial rainfall distribution for DD2 is Gaussian, the mean value is 56 [mm/hr], the variance is 16 $[mm/hr]^2$ and the correlation length scales in

both the x and y directions are 200 [mm]. DD3 has a Gaussian initial rainfall distribution whose mean is 59 [mm/hr], the variance is 25 [mm/hr]^2, and the correlation length scale in the x-direction is 600 [mm] and 800 [mm] in the y-direction.

As with all numerical solutions of hyperbolic partial differential equations, this model is prone to oscillations and instabilities. Simulations are carried out for as long as model stability allows, a function of the sediment transport capacity relationship, the spatial variability introduced both initially, and computationally, the grid size and the time step chosen.

6.3. Results and Discussion

6.3.1. One-dimensional simulations

Results from the 1-D simulations indicate that the energy expenditure characteristics on an evolving hillslope are highly dependent on the energy input into the system and the sediment transport properties of the system. In all cases ω_T, Ω_T, P_T, and CV_{PI} appear to approach a minimum for the case of Hortonian overland flow.

Figures 6.1 and 6.2 show P_T and CV_{PI} for E1-6. No system reaches a steady state in 10^6 [s] although the rate of change decreases exponentially with time. The global rate of energy expenditure, P_T, decreases with time for all rainfall rates as a function of the rate of potential energy input by rainfall into the system and the sediment transport capacity (Figures 6.1 - 6.2, Tables 6.2 – 6.3). The energy characteristics are described through power functions,

$$E = mt^n, \qquad 6.16$$

where E can be any of the energy measurements (*e.g.*, P_T, ω_T) and t is time in [s]. Transport capacities where

$$q_s = q^b \quad 6.17$$

defined with b = 1.5 decrease much more rapidly with time as compared to b = 1.8 and appear to be approaching an overall lower rate of global energy expenditure (Figure 6.1, Table 6.2 - 6.3).

Table 6.3: Fit of $P_T = mt^n$ where t has units of [s]

Experiment	*m*	*n*
E1	9.48	$-3.2(10^{-8})$
E2	9.54	$-4.3(10^{-8})$
E3	9.64	$-6.9(10^{-8})$
E4	9.68	$-8.4(10^{-8})$
E5	9.63	$-1.7(10^{-7})$
E6	9.67	$-2.0(10^{-7})$

Table 6.4: Fit of $CV_H = mt^n$ where t has unit of [s]

Experiment	*m*	*n*
E1	-0.25	$-8.7(10^{-8})$
E2	-0.26	$-1.1(10^{-7})$
E3	-0.27	$-1.6(10^{-7})$
E4	-0.28	$-1.9(10^{-7})$
E5	-0.31	$-3.1(10^{-7})$
E6	-0.33	$-3.4(10^{-7})$

The total unit stream power and total stream power also approach a minimum value with time and again the magnitude of the minimum is determined by the energy input (rainfall rate) into the system and the efficiency of sediment transport (Figure 6.3). Under Yang's (1971) hypothesis this channel should develop towards a state at which unit stream power is minimized. Indeed, Figure 6.3 shows that ω_T does approach a minimum value regardless of the rainfall intensity and sediment transport capacity. The actual minimum and rate at which this minimum is achieved depends on the rainfall rate and sediment transport capacity (Table 6.4).

Table 6.5: Fit of $\omega_T = mt^n$ where t has units of [s].

Experiment	*m*	*n*
E1	2.85	$-2.9(10^{-8})$
E2	2.89	$-3.8(10^{-8})$
E3	2.96	$-5.9(10^{-8})$
E4	2.98	$-7.2(10^{-8})$
E5	2.94	$-1.4(10^{-7})$
E6	2.97	$-1.7(10^{-7})$

According to Chang (1980), a channel develops towards a state at which total stream power is minimized. For the conditions simulated here, the numerically simulated hillslopes exhibit a stream power function that decreases monotonically as a function of time and appear to approach a minimum as predicted (Figure 6.4). The actual minimum and the rate at which the total stream power approaches this minimum are again determined by the energy input into the system through rainfall and the efficiency of the water to transport sediment (Table 6.5).

Table 6.6: Fit of $\Omega_T = mt^n$ where t has units of [s].

Experiment	*m*	*n*
E1	8.40	$-5.8(10^{-8})$
E2	8.53	$-7.8(10^{-8})$
E3	8.72	$-1.2(10^{-7})$
E4	8.81	$-1.4(10^{-7})$
E5	8.70	$-2.6(10^{-7})$
E6	8.77	$-2.9(10^{-7})$

These results are physically expected. A hillslope governed by the mathematical laws stipulated within the model, adjusts itself as to obtain continuity in sediment discharge. As there is always more water flowing as the outlet is approached and a sediment transport relationship of the form of equation **6.17**, local slope is in constant adjustment as to obtain Q_s out = Q_s in. Therefore, there should be an overall decrease in slope where

there is more water, and an increase in slope where there is less. As local energy per unit flow area is a function of q and S, it is necessary that CV_{PI} should progress towards 0 with time as it is also a function of q and S. As a result, if not fundamental, the global rate of energy expenditure also decreases as a state in which local energy approaches a minimum (Rodríguez-Iturbe and Rinaldo 1997). Holding the sediment transport capacity relationship constant, the exponential decrease of any of the energy characteristics decreases (Tables 6.3 – 6.6), $n < 0$, is directly related to the rainfall rate:

$$n \propto r \qquad 6.18$$

where r is rainfall rate, for P_T, CV_{PI}, Ω_T, ω_T (Table 6.7).

Table 6.7: Fits of $n = mr + b$ for P_T, CV_{PI}, Ω_T and ω_T

Energy Characteristic	m	b	r^2
P_T	$-1(10^{-9})$	$8(10^{-8})$	.998
CV_{PI}	$-3(10^{-9})$	$5(10^{-8})$	.998
Ω_T	$-2(10^{-9})$	$8(10^{-8})$	1
ω_T	$-1(10^{-9})$	$4(10^{-8})$	.996

This says that all other things being equal, the rate at which hillslope slope adjusts to a rainstorm is exponentially related to the rainfall rate. This is a physically realistic result given the sediment transport capacity relationship. The slope can only adjust as fast as the water flowing on the surface is able to transport sediment. As the sediment transport capacity relationship changes so should the rate of hillslope slope adjustment as the work being done by the same discharge increases exponentially. This exponential increase in the amount of work being done by a given discharge is the explanation for equation **6.18**. Clearly, the rate at which this system approaches optimality (*i.e.*, a minimum) in energy

dissipation is closely tied to the rate of change in elevation $\left(\frac{\partial z}{\partial t}\right)$ and therefore this result is consistent with that of Kirkby (1971).

The implications of optimality in energy dissipation for a system such as this are that the longitudinal profile can be described using a downstream hydraulic geometry relationship of the form $S = gQ^z$, and that this relationship has z values approaching –0.5 (*e.g.*, Rodríguez-Iturbe and Rinaldo 1997, Knighton, 1998). As Figures 6.9 and 6.10 show, these hillslopes do in fact have longitudinal profiles that can be described with the above relationship having z values that approach –0.5. The coefficient of determination (*i.e.*, the r^2 value) for the $S = gQ^z$ fit varied over a range of less than 0.5 to greater than 0.8, always increasing with time. The rate of adjustment is closely tied with the rate at which the energy dissipation is approaching a minimum and is therefore tied to the rate at which potential energy is input into the system through rainfall and the efficiency of the water to move sediment.

6.3.2. Two-dimensional simulations

Results from two-dimensional simulations on an initially smooth slope subject to spatially variable rainfall rates are very complex. The scales at which the system is in adjustment vary in both space and time. Some sample flow domain plots can be seen in Figures 6.9, 6.12 and 6.15. Under the initial and boundary conditions specified for these three examples (see Table 6.2), it is clear that the down slope component of discharge is initially dominant in all three cases; however, with time, the cross-slope component of discharge can become of equal magnitude (Figures 6.9, 6.12 and 6.15). There is definite two-dimensional organization with time. The two-dimensional development should,

under any of the extremal hypotheses, approach optimality throughout hillslope evolution.

The values and trends in energy expenditure characteristics are highly variable, subject to the threshold set for delineating concentrated flow areas. As discussed in the methods section, two different thresholds of volumetric water flux are considered for each of the three two-dimensional examples. The lower threshold encompasses flows that are still in active landform development determined by the slope-discharge relationships shown in Figures 6.11, 6.14 and 6.17. The higher threshold only includes those flows at which the slope-discharge relationship ($S \propto Q^z$) where z is very close to – 0.5. While the trends in global rate of energy expenditure and stream power appear not to be affected by changes in threshold, the coefficient of variation of the local rate of energy expenditure per unit area and the total unit stream power vary dramatically.

Physically there is less overall energy being expended within the system throughout time and this is due to the distributed erosional work being done throughout the domain decreasing slope overall ($\frac{\partial z}{\partial t} < 0$). This can be seen by the generally decreasing trend in total stream power and global energy expenditure. The amount of work that can be done given any time interval is related exponentially to the discharge and slope during that time. Thus, different areas are varying at different rates as can be seen in the CV_{PI} plots as function of the local slope and local discharge. As the system approaches equilibrium CV_{PI} should begin to approach an overall minimum in accordance to optimality in energy expenditure. The implication being that networks not in equilibrium do not always have trends in local energy expenditure approaching optimality.

Studies of channel networks based on digital elevation data where a critical drainage area criterion is used for delineating channel networks will be highly dependent on the area selected and how far the network is from the equilibrium state. The relationship between energy expenditure and network adjustment has been noted by Molnár and Ramírez (1998 a, b) who generalized the global and local energy expenditure hypothesis of Rodríguez-Iturbe et al. (1992) in order to study real world systems and identified areas within river networks which are in active adjustment as because they have local rates of energy dissipation per unit flow area that are very different from the rest of the network.

Figures 6.11, 6.14 and 6.17 show the slope-discharge relationship at the end of each of the three sample simulations. The line in yellow is proportional to $Q^{-0.5}$ and the proportionality factor is selected to fit the data with a minimum sum of square errors. As can be seen, the slope of the fit is very close to the slope of the data at high discharges and deviates at low discharge values. This is consistent with DEM data for river networks (Tarboton et al. 1989) where $S \propto A^z$. In their analysis Tarboton et al. (1989) associated the change in fit with a transition from hillslopes to channels. The transition can be applied to the hillslope regime if it is considered in general to be a difference in time scales related with the work being done by the surface water. In these simulations the low flows are not able to do enough work to create a continuous slope-discharge relationship in the time of simulation. For river networks, the time that water is present on the hillslopes and the work done by that water compared to geologic uplift, vegetation response, and the rate at which the water within channels is able to move sediment are operating at very different time scales thus producing various slope-area relationships. Given enough time and any threshold value for initiation of erosion, $(QS)_{crit}$, the slope-

discharge relationship will extend to the point at which the local value of $QS < (QS)_{crit}$. Clearly the slope-discharge of the form $S \propto Q^z$ where $z < 0$ cannot extend infinitely as this would require and infinite slope where $Q = 0$. This simple scaling of the type shown in Figures 6.11, 6.14 and 6.17 has been used to choose the critical area threshold for digital elevation model (DEM) analysis (Tarboton et al. 1989). Indeed, when the threshold chosen in Figures 6.10, 6.13 and 6.16 is compared to the slope-discharge relationships in Figures 6.11, 6.14 and 6.17 this appears to be an appropriate method.

Throughout these two-dimensional simulations, spatially heterogeneous flows do occur and develop with time and have been shown to possess many of the characteristics as expected of systems following optimality hypotheses, however these simulations do not produce an organized network of rills, at least not in any reasonable simulation time interval. Physical experiments conducted on artificial hillslopes, as described in Chapter 4, develop equilibrium rill networks in a matter of hours, usually less than 5 hours, but the time required for these rill networks to develop depends on the characteristics of the substrate, the rainfall rate, and the hillslope-scale slope. Numerical simulations run for well over twice this time still show no rill network. One possible explanation is a lack of mass wasting mechanisms within the model for channel initiation. Mass wasting, specifically shallow landsliding causes abrupt variations in the flow domain and topography (nick points) and leads to active rill development through upslope migration of the rill heads as observed during physical experiments and noted in the literature (*e.g.*, Schumm et al. 1987). Also, distributions in soil infiltration characteristics as well as erodability, along with the distribution of rainfall on a much more discrete spatial domain should add increased variability into the system and encourage two-dimensional

heterogeneity and were not considered here due to limitations of current computer technology as implementation of these scenarios are very computationally expensive. Only variability in rainfall rates is considered here and a suggestion for future research is studying the interactions between distributions of initial soil moisture content, hydraulic conductivity, and soil erodability and what impacts these have for hillslope development and overall rates of erosion.

6.4. Conclusion

Hillslope evolution driven by shallow Hortonian overland flow has been modeled with a new two-dimensional overland flow model based on the full hydrodynamic equations, Richards equation for infiltration and a physically based equations describing erosion and sediment transport processes. Results indicate that for a one-dimensional system these equations lead to hillslope longitudinal profiles that minimize the global rate of energy expenditure, the coefficient of variation of the local rate of energy expenditure per unit area, the total unit stream power, and the total stream power. The longitudinal profiles developed for the one-dimensional case have slope-area relationships that approach global and local optimality. The rates at which the energy characteristics are minimized is exponentially related to the rainfall input to the system because the work that can be done by a flow is exponentially related to that input.

In two-dimensional cases, the model shows that the total global rate of energy expenditure and the total stream power approach a minimum throughout hillslope evolution but unit stream power and the distribution of local energy expenditure per unit area are highly variable and depend critically upon the threshold at which the concentrated flow paths are delineated. The landform development exhibits

minimization in global energy expenditure and the distribution of energy expenditure per unit flow area approaches a minimum when a critical discharge threshold is set to encompass all the areas that are in active development. This is attributed to the interdependence in flow regions on an actively developing hillslope.

6.5. References

Chang HH. 1980. Geometry of gravel streams, *Journal of the Hydraulics Division ASCE* **106**, HY9: 1443-1456.

Flanagan DC, Frankenberger JR, Renschler CS, Laflen JM, Engel BA. 2001. Simulating small watersheds with Water Erosion Prediction Project (Ascough II JC, Flanagan DC eds.): Proc. Soil Erosion Research for the 21st Century, 3-5 Jan. 2001, Honolulu, HI, Amer. Soc. Agric. Engrs. St. Joseph MI. pp. 363-366.

Foster GR. 1982. Modeling the erosion process. *Hydrologic modeling of small watersheds* (Haan CT, Johnson HP, Brakensiek DL eds.). ASAE, New York. pp. 295-380

Kilinc M, Richardson EV. 1972. Mechanics of soil erosion from overland flow generated by simulated rainfall. *Hydrology Papers No. 63*, Colorado State University.

Kirkby MJ. 1971. Hillslope process-response models based on continuity equation. In Slopes: *Form and Process*, ed. Kirkby MJ. Special Publication, 3, institute of British Geographers, London, pg 15-30.

Knighton D. 1998. Fluvial forms and processes: a new perspective, Arnold, London.

Leopold LB, Wolman MG, Miller JP. 1964. Fluvial Processes in Geomorphology, W.H. Freeman, New York.

Molnár P, Ramírez JA. 1998 a. Energy dissipation theories and optimal characteristics of river networks. *Water Resources Research* **34**(7): 1809-1818.

Molnár P, Ramírez JA. 1998 b. An analysis of energy expenditure in Goodwin Creek. *Water Resources Research* **34**(7): 1819-1829.

Ogunlela A, Wilson BN, Rice CT, Couger G. 1989. Rill network development and analysis under simulated rainfall, ASAE Paper No. 89-2112, ASAE, St. Joseph, Michigan.

Renwick WH. 1992. Equilibrium, disequilibrium, and nonequilibrium landforms in the landscape, *Geomorphology* **5**: 265-276.

Rodríguez -Iturbe I, Rinaldo A, Rigon R, Bras RL, Marani A, Ijjaz-Vaquez E. 1992. Energy dissipation, runoff production, and the three-dimensional structure of river basins, Water Resources Research **28**(4): 1095-1103.

Rodríguez-Iturbe I, Rinaldo A. 1997. *Fractal River Basins*. Cambridge University Press, New York, NY.

Schumm SA, Mosley MP, Weaver WE. 1987. *Experimental Fluvial Geomorphology*, New York, New York, Wiley-Interscience.

Tarboton DG, Bras RL, Rodriguez-Iturbe I. 1989. Scaling and elevation in river networks, *Water Resources Research* **25**(9): 2037 – 2051.

Wilson BN, Storm DE. 1993. Fractal analysis of surface drainage networks for small upland areas, *Trans. ASAE* **36**(5): 1319-1326.

Yang CT. 1971. Potential energy and stream morphology, *Water Resources Research* **7**(2): 311-323.

Figure 6.1: Total global rate of energy expenditure, P_T

a) Varying rainfall rate ($q_s = q^{1.8}$)

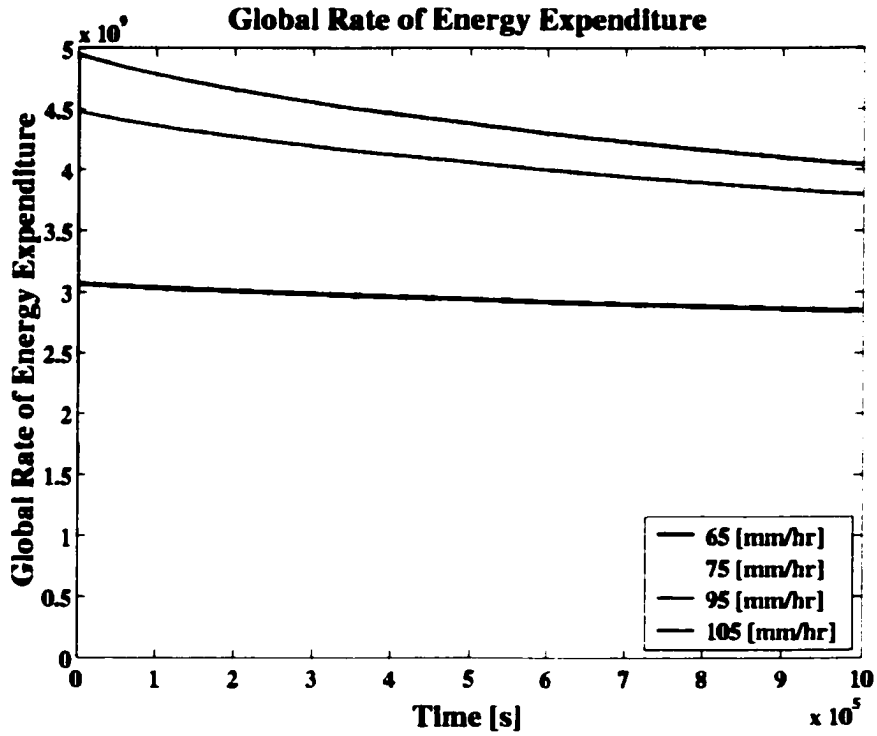

b) Varying Transport capacity ($q_s = q^b$)

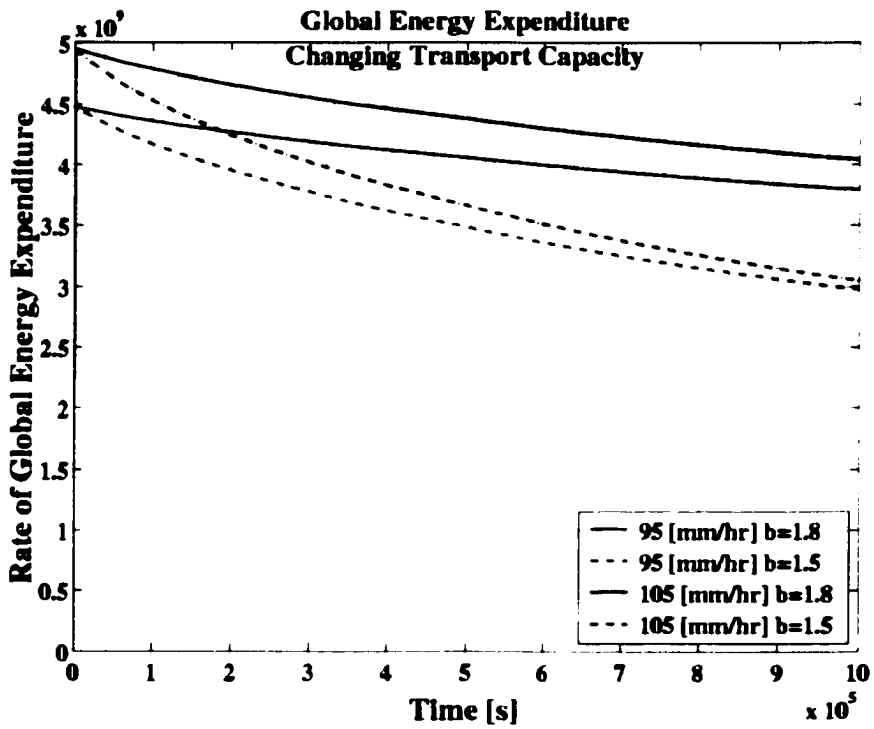

Figure 6.2: Coefficient of variation of the local energy expenditure per unit area, CV_{PI}

a) Varying rainfall rate ($q_s = q^{1.8}$)

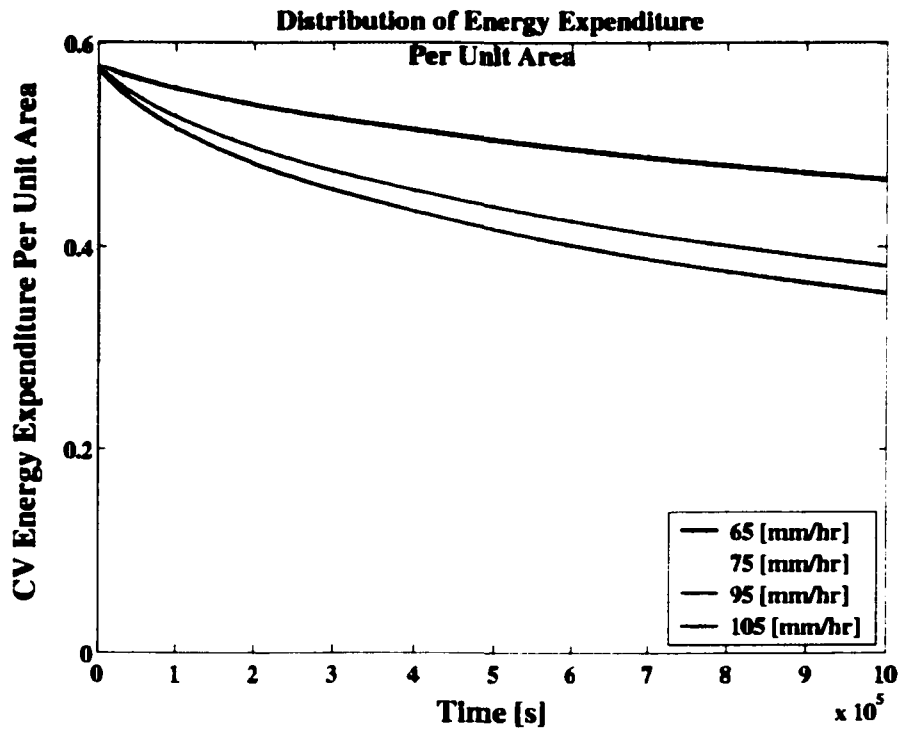

b) Varying Transport capacity ($q_s = q^b$)

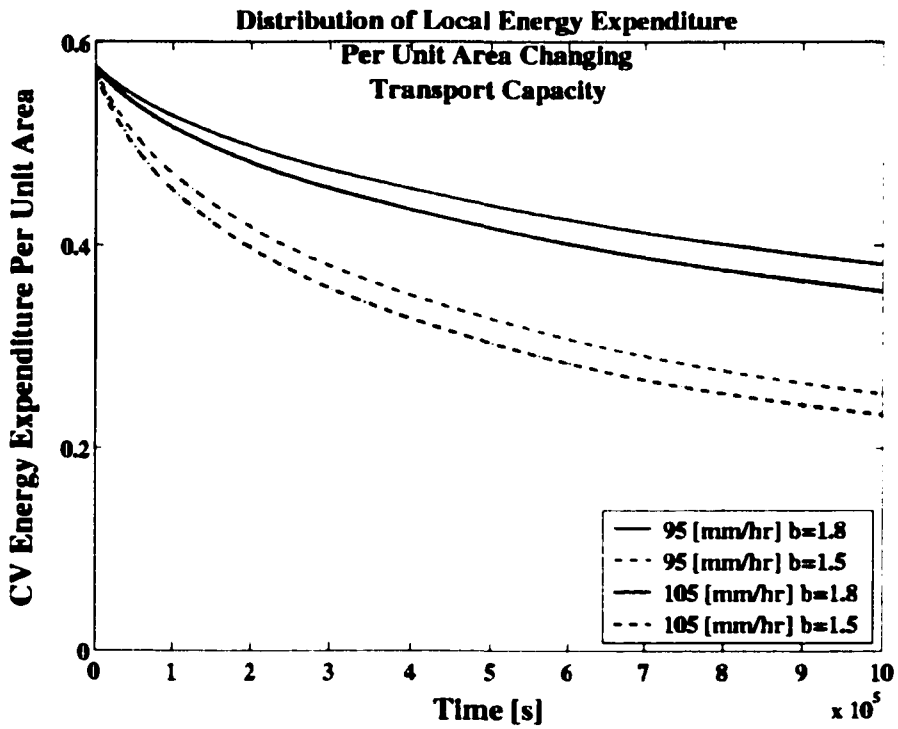

Figure 6.3: Total unit stream power, ω_T

a) Varying rainfall rate ($q_s = q^{1.8}$)

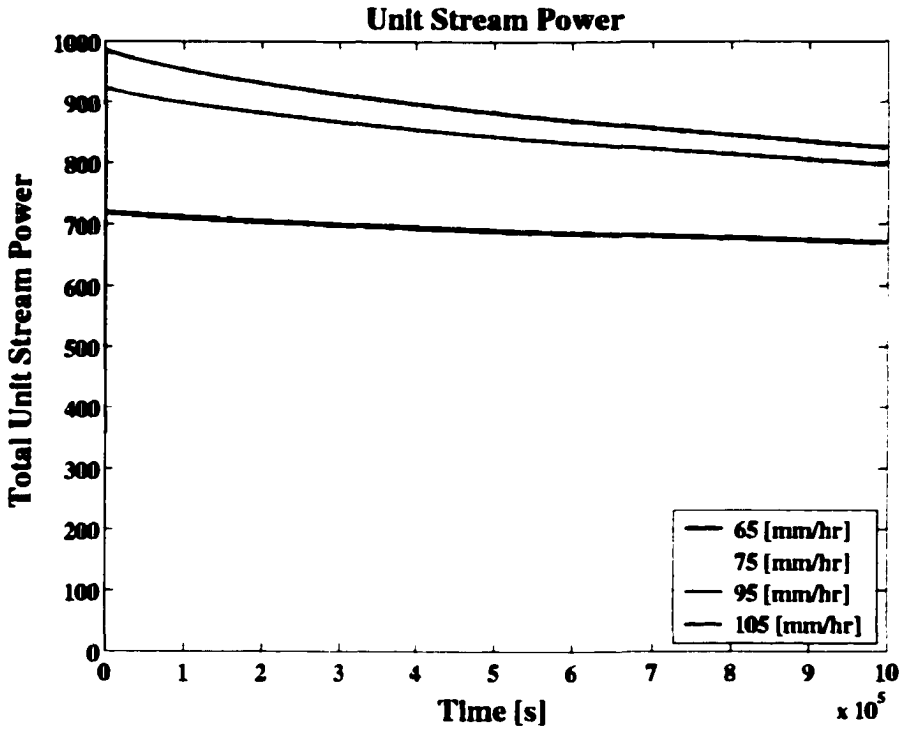

b) Varying Transport capacity ($q_s = q^b$)

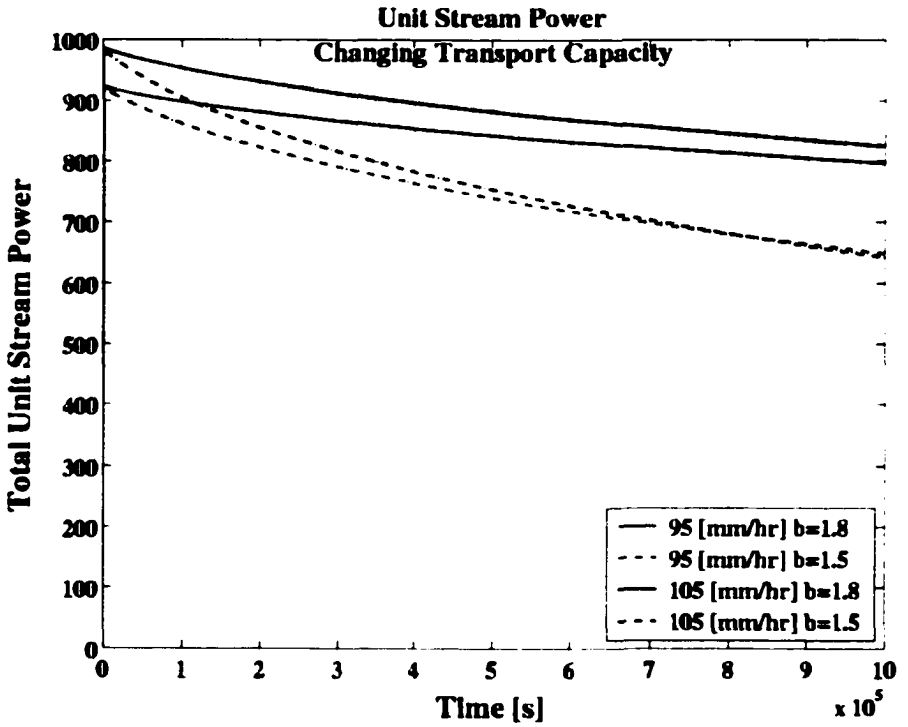

Figure 6.4: Total stream power, Ω_T

a) Varying rainfall rate ($q_s = q^{1.8}$)

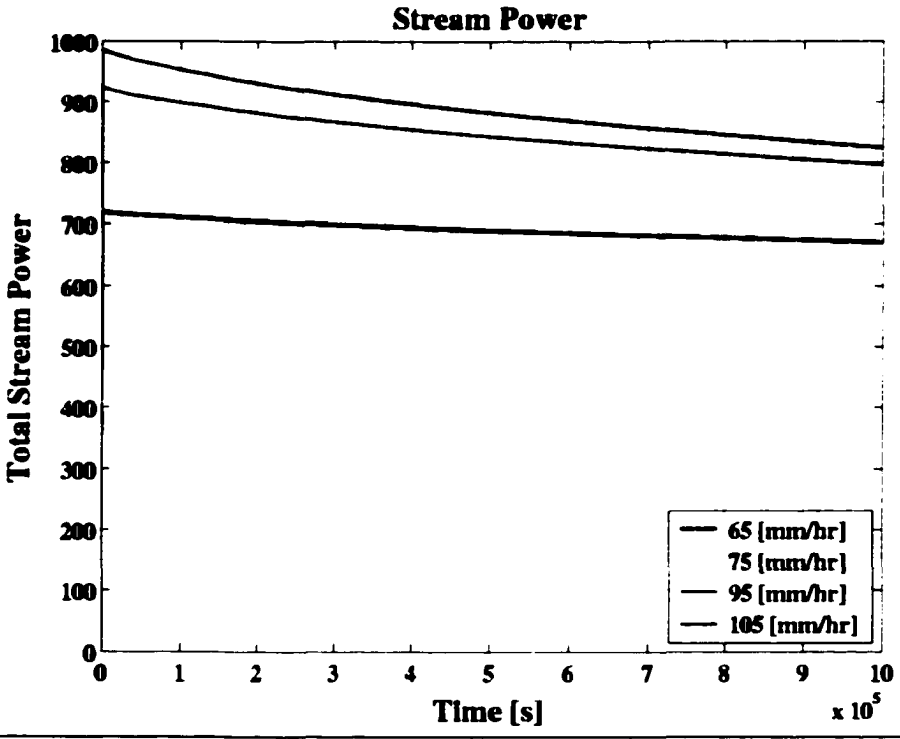

b) Varying Transport capacity ($q_s = q^b$)

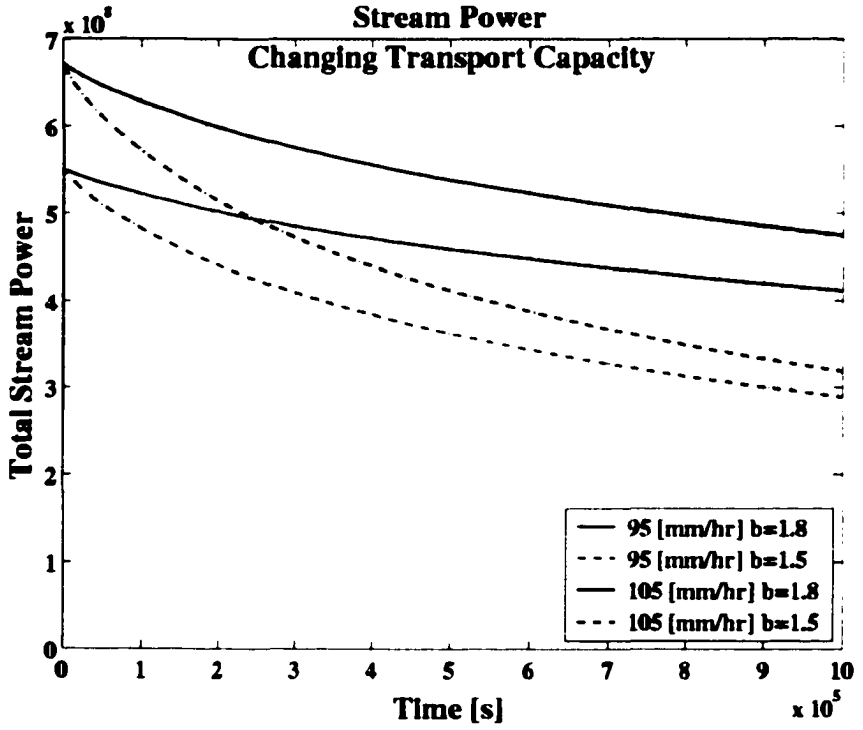

Figure 6.5: Values of z from equation $S = gA^z$

a) Varying rainfall rate ($q_s = q^{1.8}$)

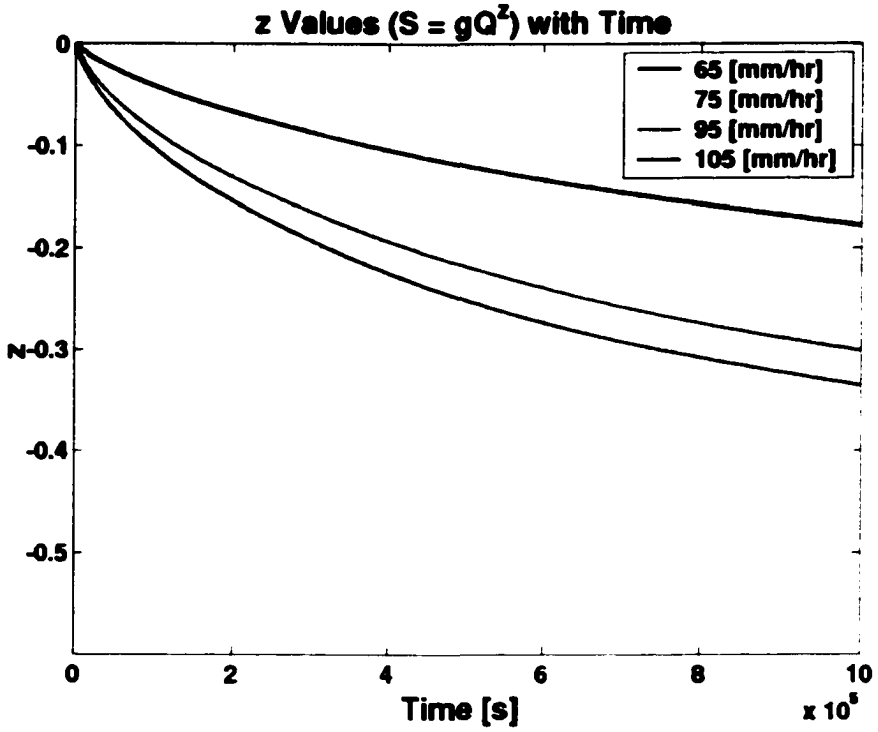

b) Varying Transport capacity ($q_s = q^b$)

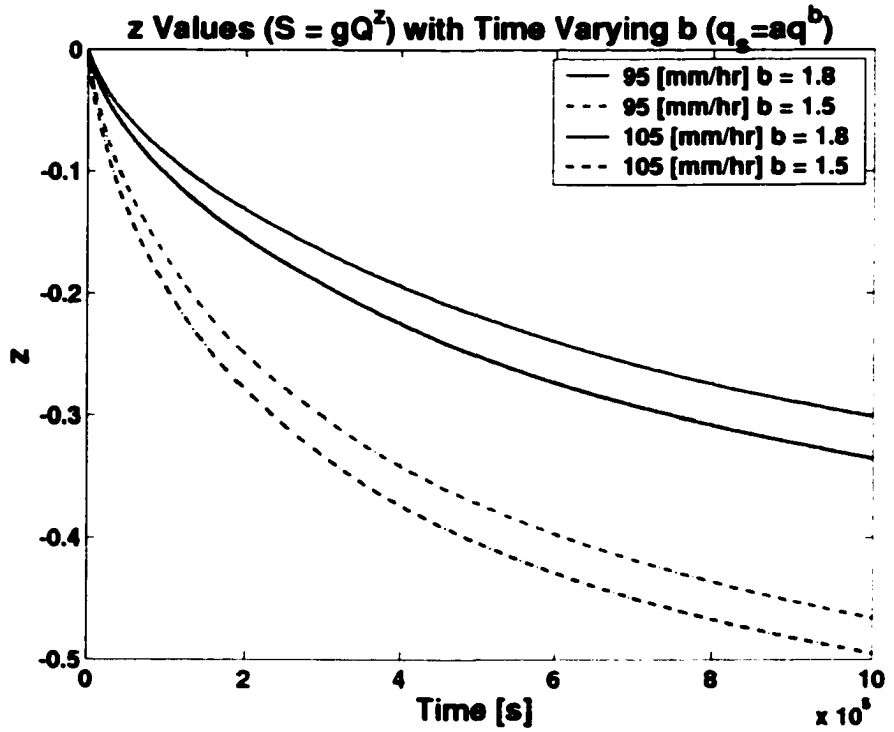

Figure 6.6: Self-similar rainfall rate distribution for simulation DD1

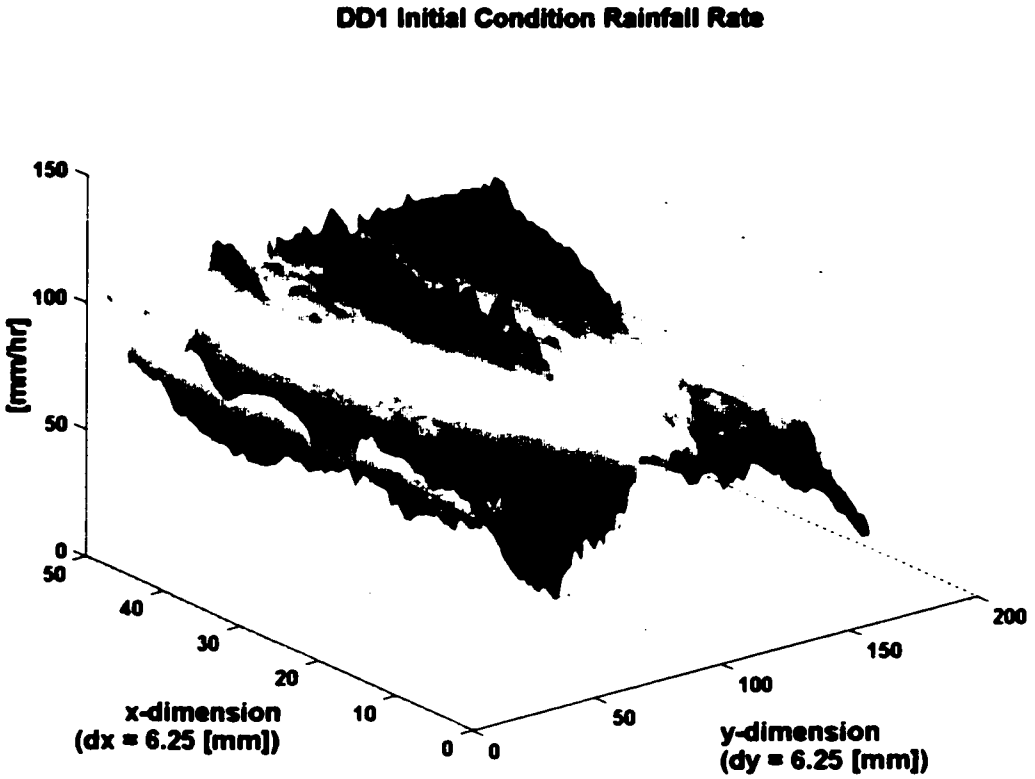

Figure 6.7: Gaussian rainfall rate distribution for simulation DD2

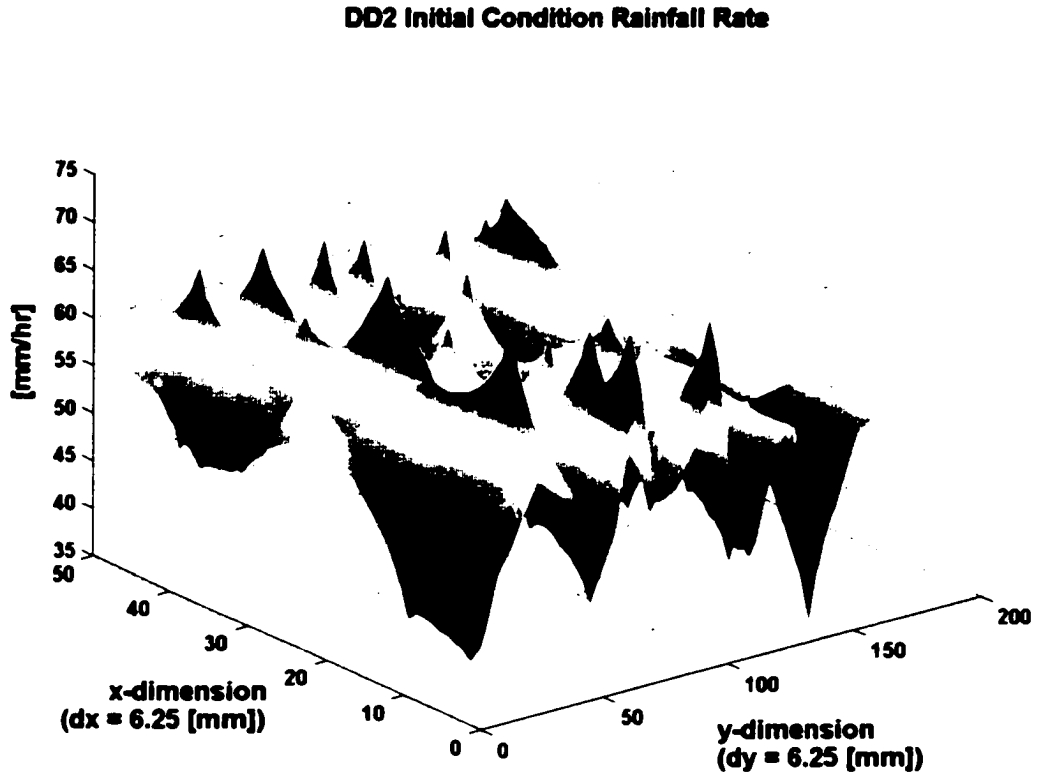

Figure 6.8: Gaussian rainfall rate distribution for simulation DD3

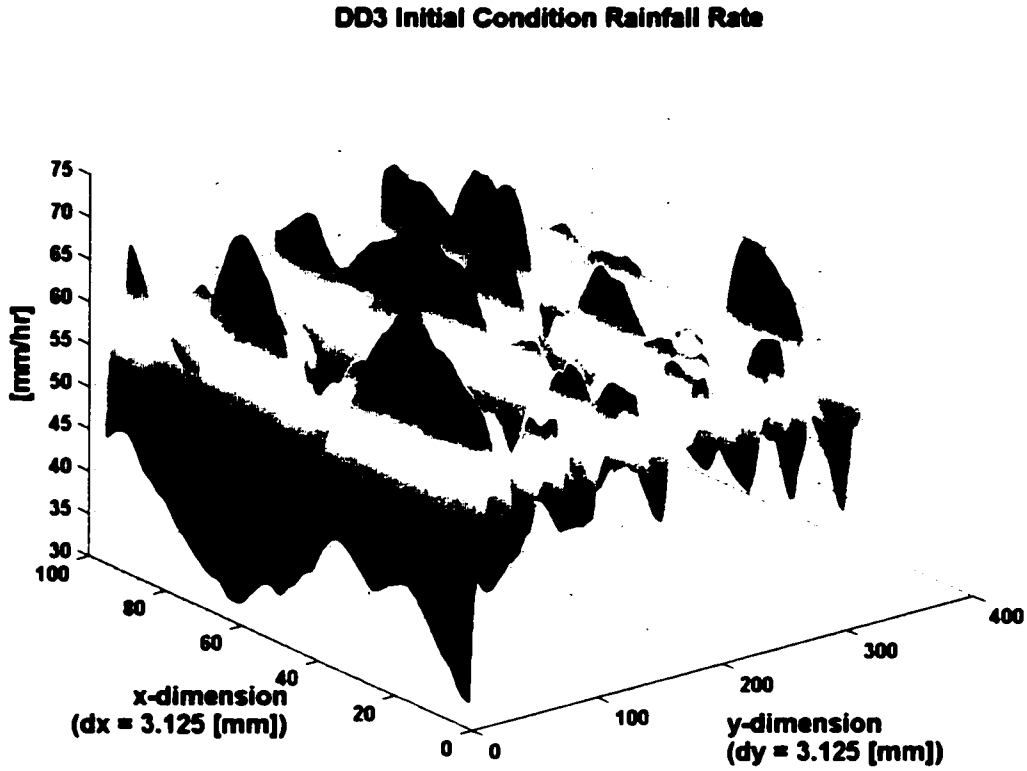

Figure 6.9: Sample Flow Domain (DD1)

Time = 3001 [s]

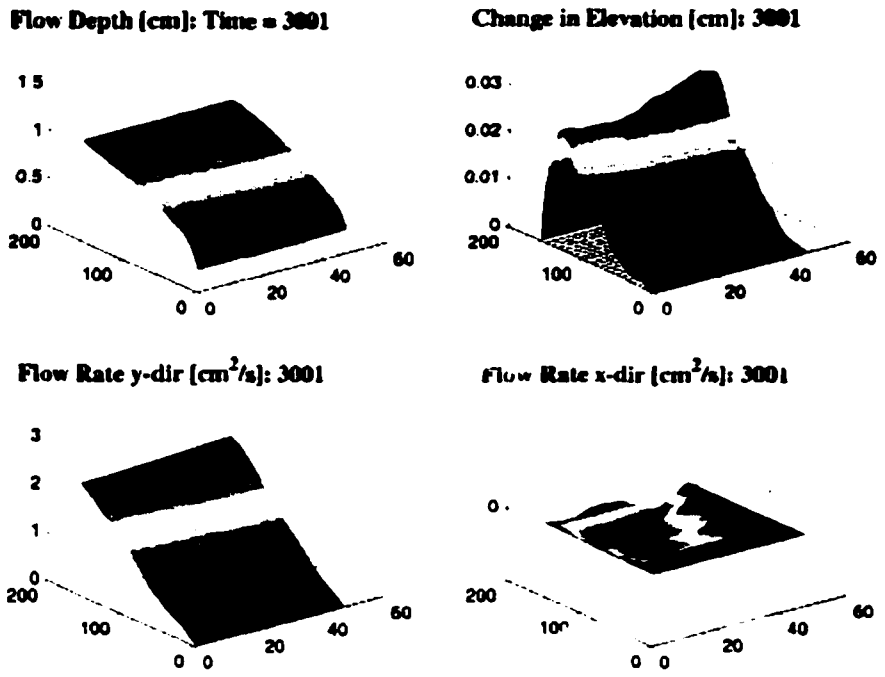

Time = 210,000 [s]

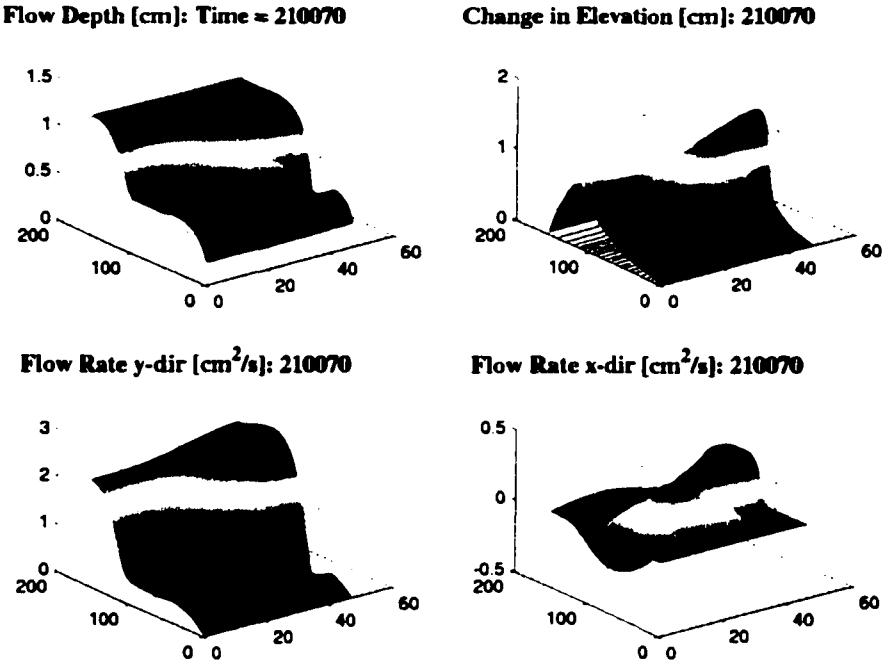

Figure 6.10: Energy Characteristics (DD1)

a) Threshold at Q = 0.2 [cm^3/s]

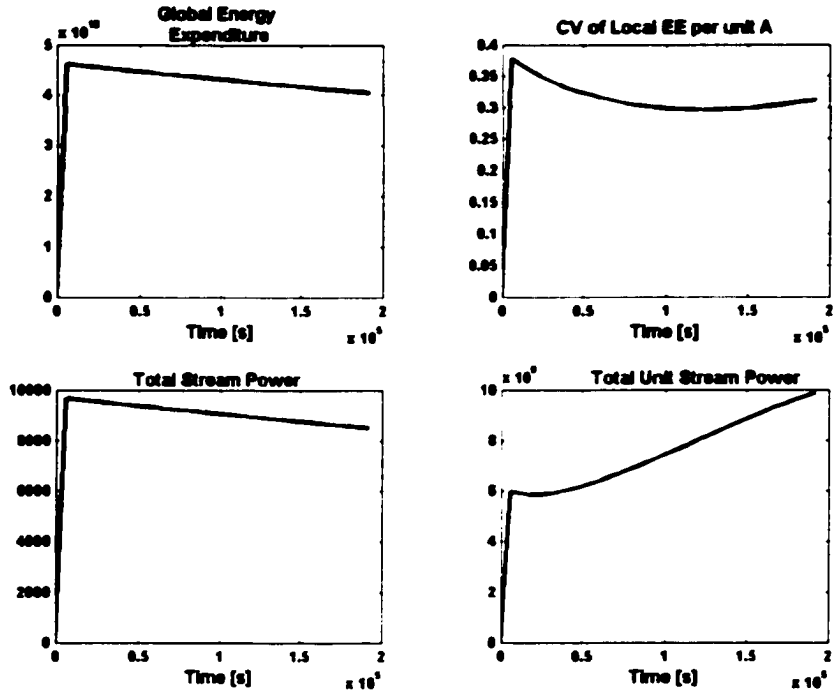

b) Threshold at Q = 1.0 [cm^3/s]

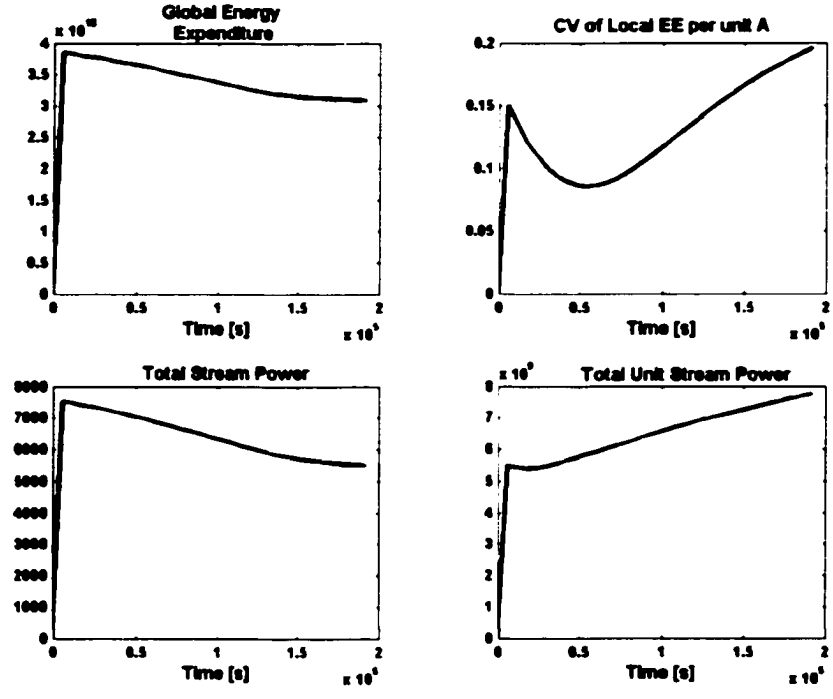

Figure 6.11: DD1 Slope – Discharge Relationship Fit is $S \propto Q^{-0.5}$

Green data are raw slope discharge. Yellow is best fit of $S \propto Q^{-0.5}$. Red and blue are thresholds for Figure 6.10.

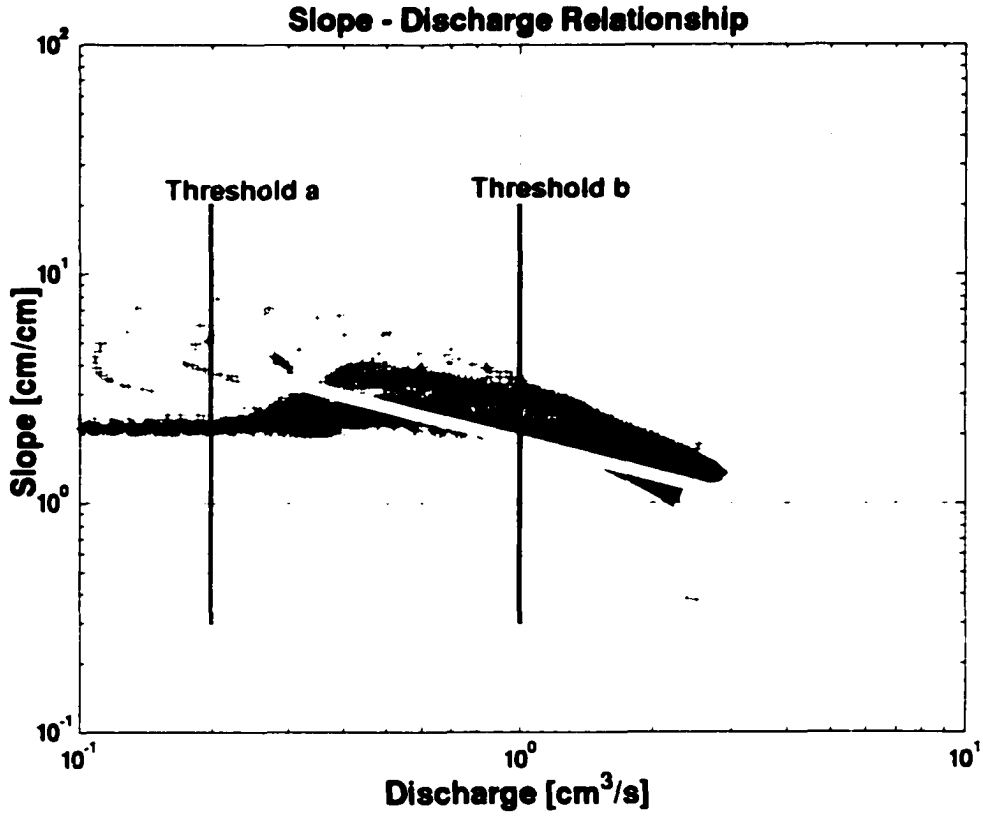

Figure 6.12 Sample Flow Domains (DD2)

Time = 1000 [s]

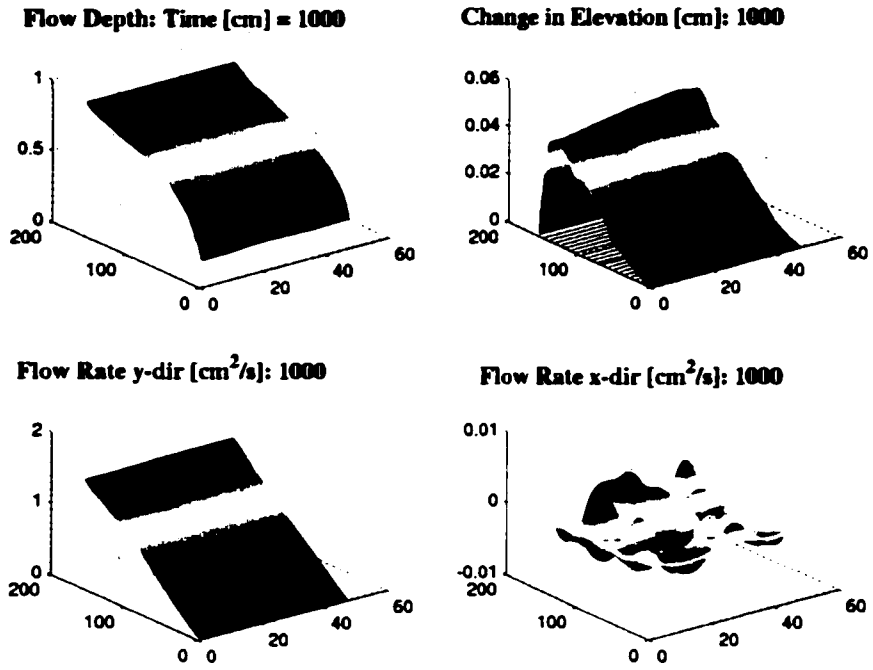

Time = 97,019 [s]

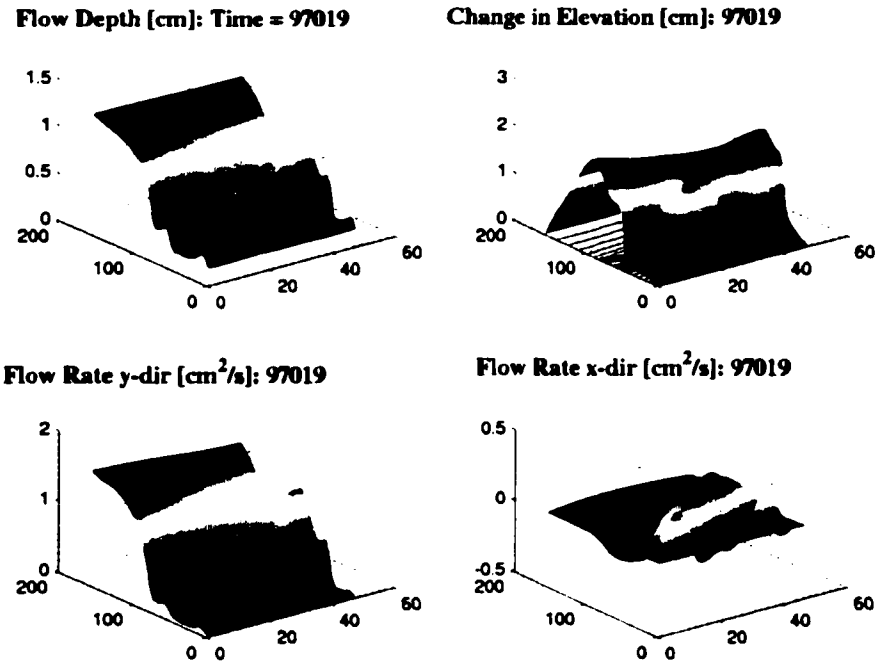

Figure 6.13 Energy Characteristics (DD2)

a) Threshold at Q = 0.1 [cm^3/s]

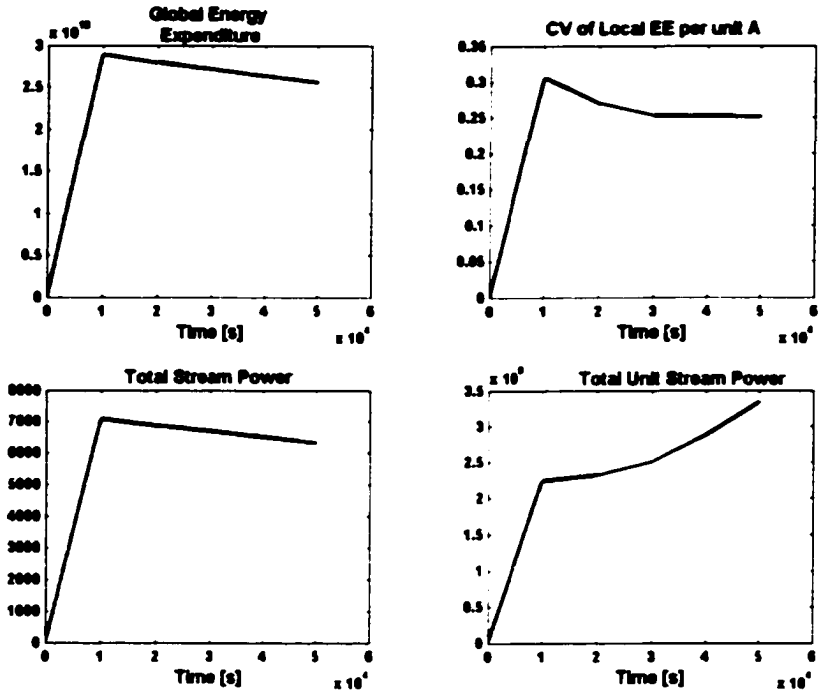

b) Threshold at Q = 0.5 [cm^3/s]

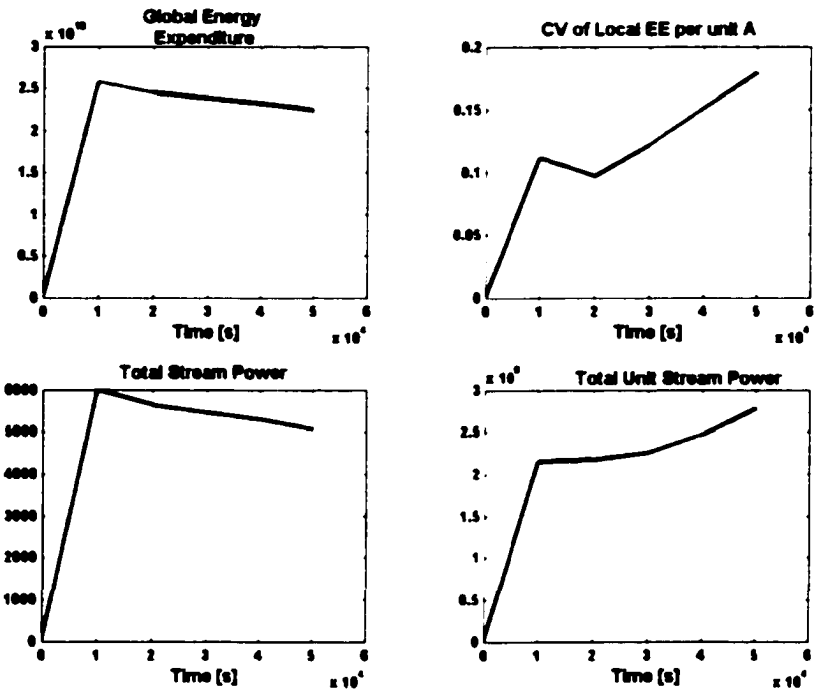

Figure 6.14: DD2 Slope – Discharge Relationship Fit is $S \propto Q^{-0.5}$

Green data are raw slope discharge. Yellow is best fit of $S \propto Q^{-0.5}$. Red and blue are thresholds for Figure 6.13.

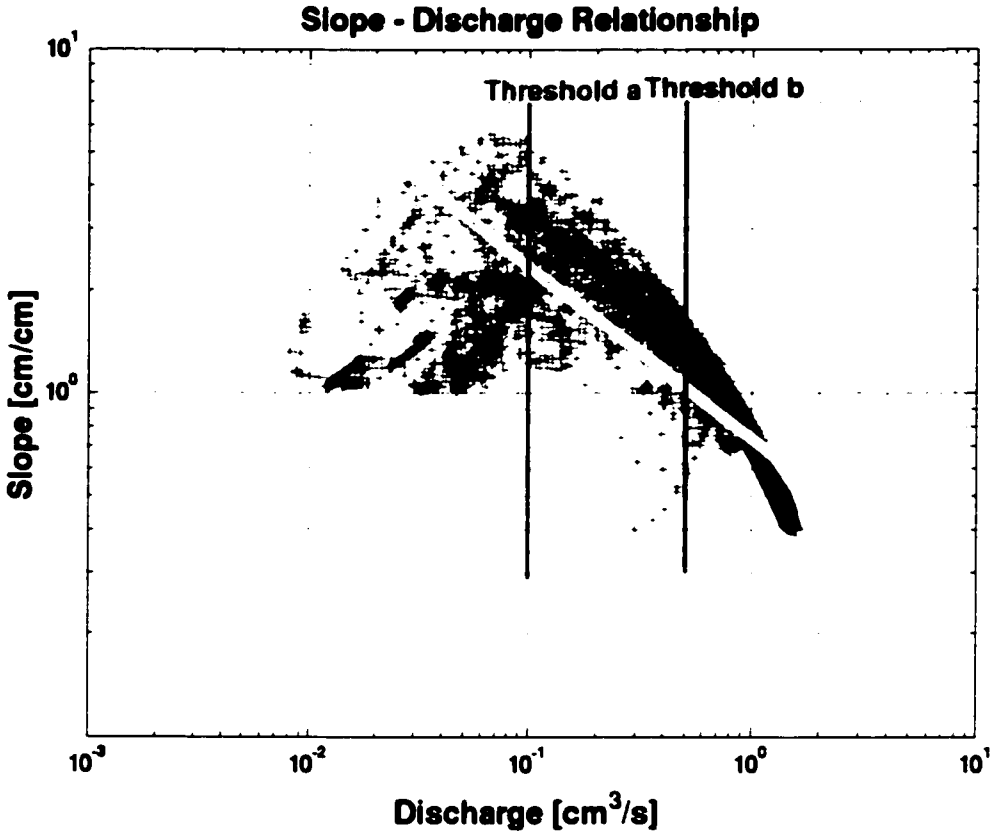

Figure 6.15: Sample Flow Domain (DD3)

Time = 402 [s]

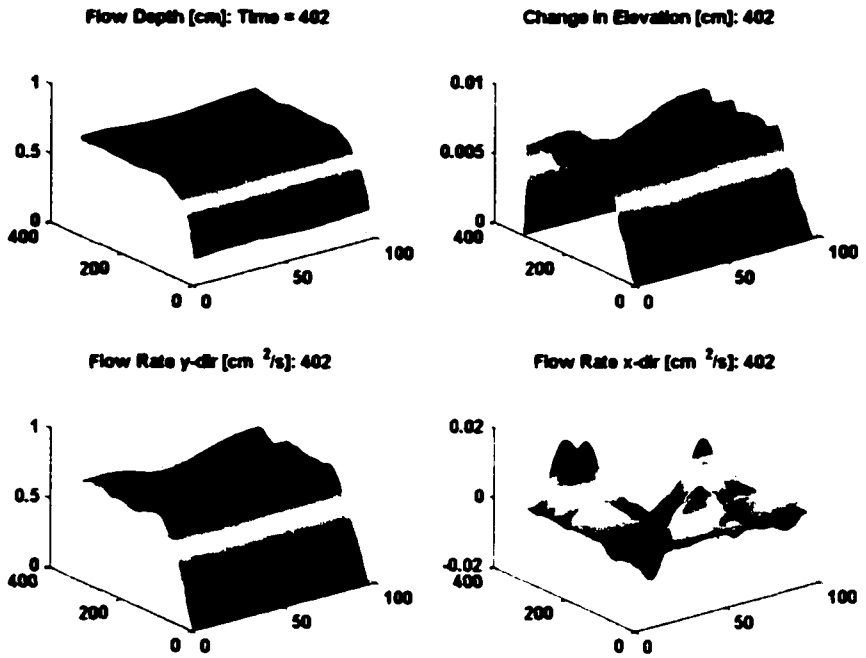

Time = 7598 [s]

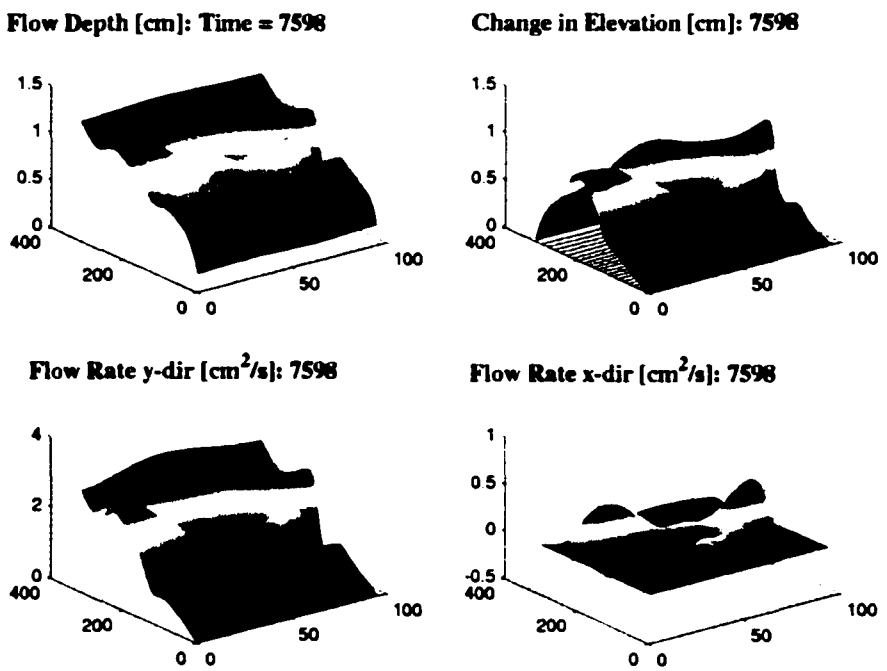

Figure 6.16: Energy Characteristics (DD3)

a) Threshold at Q = 1.0 [cm^3/s])

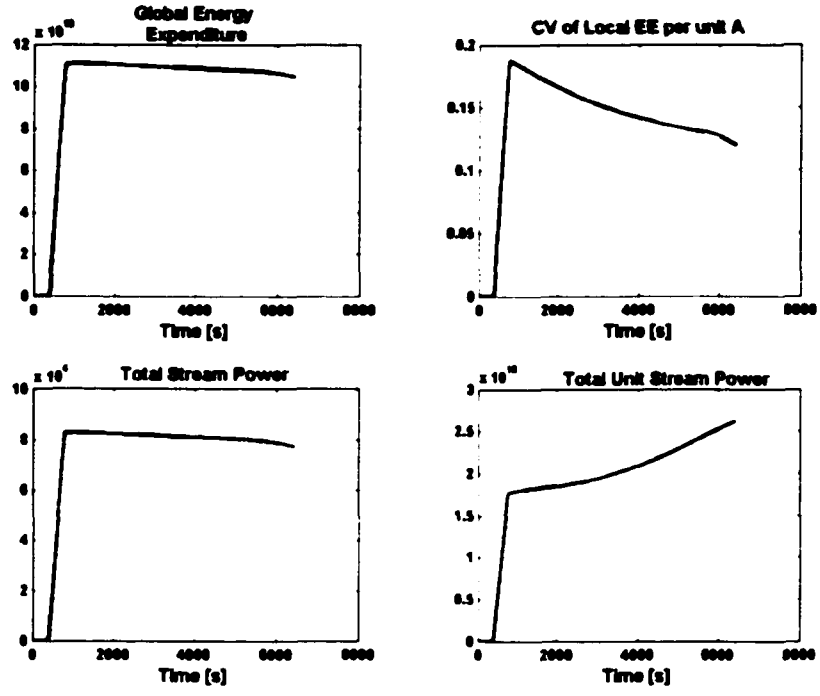

b) Threshold at Q = 2.0 [cm^3/s]

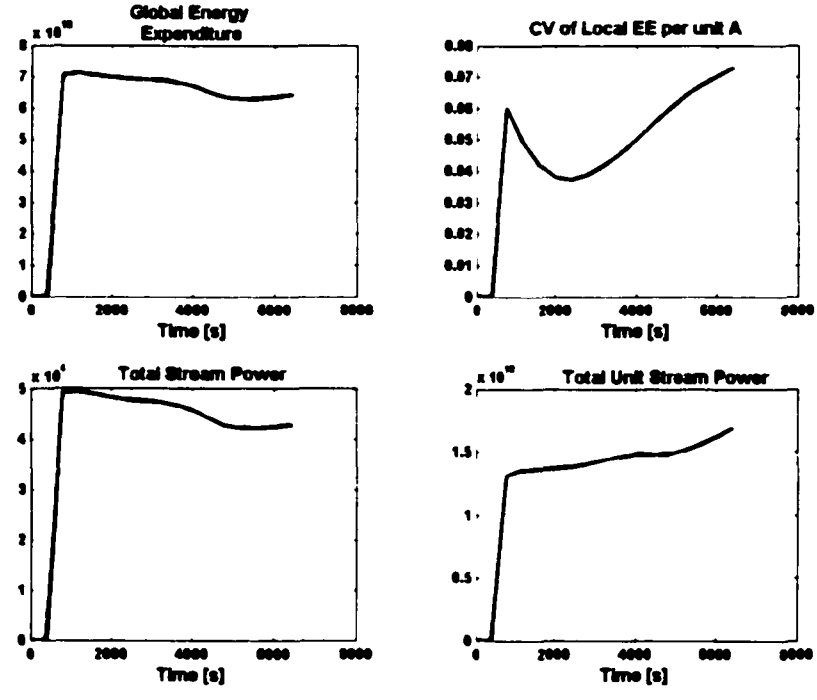

Figure 6.17: DD3 Slope – Discharge Relationship Fit is $S \propto Q^{-0.5}$

Green data are raw slope discharge. Yellow is best fit of $S \propto Q^{-0.5}$. Red and blue are thresholds for Figure 6.16.

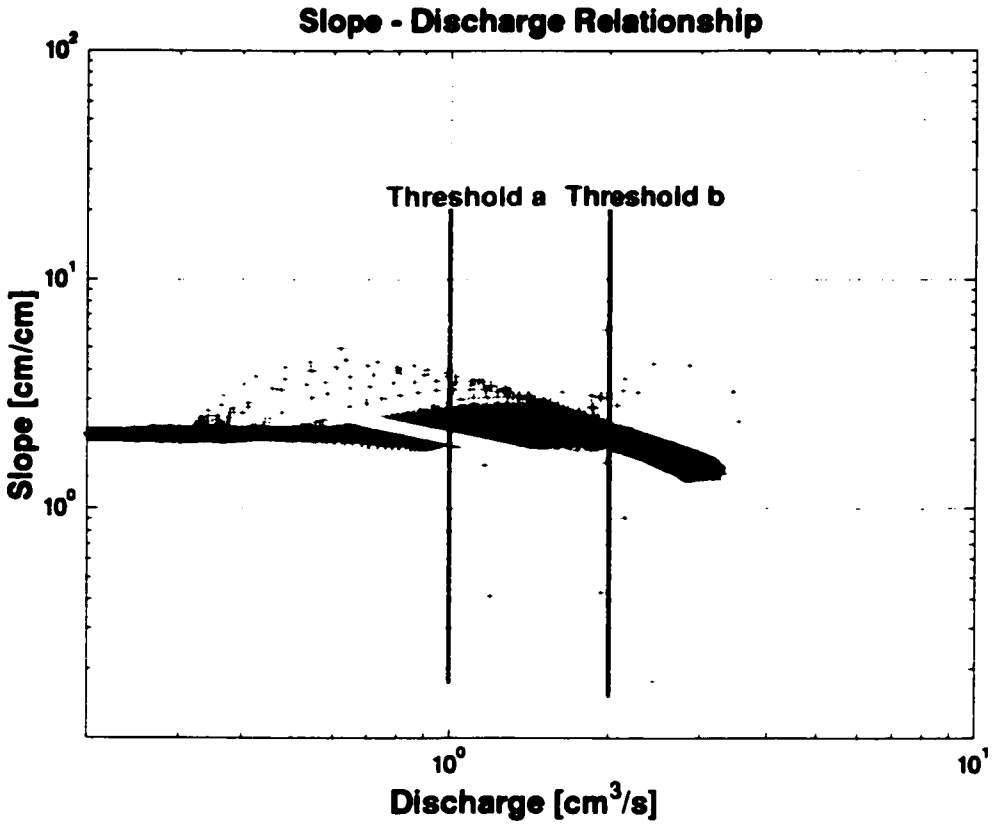

Chapter 7: Conclusions

7.1. Summary

The main goal of this dissertation is to define and describe some of the driving factors for drainage network evolution and to study hillslope evolution with respect to drainage network development. In order to accomplish this overall goal four individual papers are presented. These papers present both theoretical and physical experiments that study both optimal drainage networks and those which physically develop on a hillslope void of vegetation.

In Chapter 3 a numerical, conceptual simulation experiment is presented that considers the variability in the distribution of flows that can occur in a river network, and the relative effectiveness of these flows to transport sediment and shape the longitudinal profile of the individual links. An equal distribution of energy expenditure per unit flow area is considered the goal of network development and comparisons are presented between theoretical results and empirical data.

In Chapter 4 a physical simulation experiment is presented that studies channel network development on an experimental hillslope void of vegetation. The rate of channel network development is studied with respect to hillslope scale slope through its fractal dimension and width function. The geometric characteristics of channels within the network are also studied with respect to hillslope scale slope.

In Chapter 5 a mathematical model of hillslope hydrology is presented which couples physical process based algorithms for overland flow, infiltration and sediment

detachment and transport. The performance of the model is compared to analytical solutions, and to a multi-storm physical experiment conducted on an artificial hillslope. In Chapter 6 the model is used to simulate the evolution of hillslopes , which are studied with respect to hillslope evolution and energy dissipation. One- and two-dimensional cases are presented with respect to global energy dissipation and the distribution of local energy dissipation per unit flow area.

7.2. General Conclusions

In this dissertation four individual papers have been presented from which the following conclusions are drawn:

- The variability in longitudinal profiles of a river networks expressed as variability in the exponent of a slope-area relationship can be explained by optimality in energy expenditure, variations in discharge distribution and flow effectiveness.
- The rate at which a drainage network fills space on a hillslope subject to rainfall is dependent on the hillslope scale slope. Equilibrium networks on hillslopes are statistically similar to river networks. Individual erosion channel widths and depths are influenced by hillslope scale slope.
- A new physically based hillslope hydrology model, HYDROR, that couples a series of hyperbolic and parabolic differential equations describing overland flow, infiltration and erosion and sediment transport is developed. Its numerical solution is possible utilizing some existing numerical techniques and some additional stability controls. The model is numerically accurate when compared to analytical solutions and an empirical experiment.

- The interactions between the hillslope hydrology algorithms within HYDROR produce longitudinal profiles in one dimension that tend toward optimality in energy expenditure. In two dimensions energy characteristics are highly dependent on the scale at which concentrated flow paths are defined but tend towards optimality globally. The scale at which the concentrated flow paths occur is tied to the simple scaling of the slope-discharge relationship.

7.3. Recommendations

While the specific findings of this research are presented above, this dissertation research has led to many additional questions, which will hopefully be studied in the future. Specifically, the findings in Chapter 3 suggest that the distribution and effectiveness of flows influence the slope-area relationship for a river network. The model presented assumes lognormal distributions and it would be useful to study other distributions, as lognormal may not always be the best description of channel discharges. Also a including a more advanced model in terms of routing flows rather than assuming simple mass conservation, as well as including over bank flows may reduce the distribution of results and be more physically realistic. In addition, only channel adjustment with respect to slope is considered in the present research while it is acknowledged that channel adjustment can occur through width, depth and slope changes and an additional experiment is warranted to study these interactions.

In Chapter 4 a physical experiment is presented which concludes that the space filling tendency of networks on a hillslope void of vegetation is influenced by hillslope scale slope. Only two slopes are considered here and a study of a larger distribution of slopes is warranted to characterize the actual difference in rates of development and of

steady state geometrical properties of the channels within the networks. It would also be beneficial to have a denser data set, which can be accomplished using some modern laser topography measurement techniques. One of the findings from the work in Chapters 5 and 6 is that mass wasting may be a specific mechanism that leads to drainage network development on a hillslope. Quantitative measurements of such mechanisms made on a physical experiment would lead to better models of hillslope evolution although no specific recommendations are presented here with respect to this goal.

The numerical algorithms within HYDROR can be improved with respect to stability and accuracy. Proposed additions to the model are mass wasting mechanisms, multiple sediment size classes and different sediment transport algorithms for bed and suspended sediment. In order to model mass wasting mechanisms a different grid scheme will probably be necessary, the most appropriate being a finite element scheme and would require a much more complex time stepping routine. Also, unconditional stability is guaranteed with a totally implicit approach and is suggested for further study. Of course, these changes require exponentially more computational time and therefore may not be feasible for the near future until computing power is increased. With a model capable of simulating the fine scale processes affecting hillslope evolution, a detailed analysis should be performed with the goal of identifying the different length and time scales necessary to simulate rill network development.